

RESEARCH ARTICLE

Open Access



Geology and stratigraphy of the Neogene section along the Oued Beth between Dar bel Hamri and El Kansera (Rharb Basin, northwestern Morocco) and its otolith-based fish fauna: a faunal inventory for the Early Pliocene remigration into the Mediterranean

Werner Schwarzthans^{1,2*} 

Abstract

The coquina on the banks of the Oued Beth in the Rharb Basin in northwestern Morocco has long been known to be exceptionally rich in fossils. The stratigraphic position ranging from the Late Miocene to the Pliocene has been controversial, however. In the course of my master's degree field work in 1975/76, I mapped the right bank of the Oued Beth from Dar bel Hamri to El Kansera. Following multiple recent studies in the general region, I here review my results and present an updated comprehensive stratigraphic and geologic frame for the first time. The coquina near Dar bel Hamri is interpreted to be of Early Pliocene age, possibly containing some reworking of Late Miocene fossils. The coquina and other locations along the Oued Beth have yielded a rich otolith assemblage, which is described in this article. It represents the first fossil otolith-based fish fauna described from Northwest Africa and contains 96 species, 16 of which are new. The new species in the order of their description are *Diaphus maghrebensis* n. sp., *Ophidion tuseti* n. sp., *Centroberyx vonderhochti* n. sp., *Myripristis ouarredi* n. sp., *Deltentosteus planus* n. sp., *Caranx rharbensis* n. sp., *Trachurus insectus* n. sp., *Parapristipoma bethensis* n. sp., *Pomadasys zemmourensis* n. sp., *Cepola lombartei* n. sp., *Trachinus maroccanus* n. sp., *Trachinus wernlii* n. sp., *Uranoscopus hoedemakersi* n. sp., *Uranoscopus vanhinsberghi* n. sp., *Spondylisoma tingitana* n. sp., and *Opsodentex mordax* n. sp. In addition, a new species is described from the Tortonian and Zanclean of Italy: *Rhynchoconger carnevalei* n. sp. Some additional otoliths are described from another Northwest Moroccan location of Early Pliocene age near Asilah, 50 km south of the Strait of Gibraltar. The Early Pliocene fish fauna from Dar bel Hamri in the Rharb Basin is also of interest, because it constitutes the nearest Atlantic fauna of the time of the reconnection of the Mediterranean with the Atlantic and may have acted as a hosting area for the remigration of fishes into the Mediterranean. Indeed, the correlation is high between the Northwest Moroccan and the well-known time-equivalent Mediterranean fish fauna, but the Moroccan fauna also contains a good proportion of putative endemic taxa and taxa with tropical West African affinities that apparently did not migrate into the

Editorial handling: Lionel Cavin

*Correspondence:

Werner Schwarzthans
wswschwarz@aol.com

Full list of author information is available at the end of the article



© The Author(s) 2023. **Open Access** This article is licensed under a Creative Commons Attribution 4.0 International License, which permits use, sharing, adaptation, distribution and reproduction in any medium or format, as long as you give appropriate credit to the original author(s) and the source, provide a link to the Creative Commons licence, and indicate if changes were made. The images or other third party material in this article are included in the article's Creative Commons licence, unless indicated otherwise in a credit line to the material. If material is not included in the article's Creative Commons licence and your intended use is not permitted by statutory regulation or exceeds the permitted use, you will need to obtain permission directly from the copyright holder. To view a copy of this licence, visit <http://creativecommons.org/licenses/by/4.0/>.

Mediterranean. Thus, the Early Pliocene fish fauna from the Rharb Basin represents a unique assemblage for which I propose the biogeographic term “Maghrebian bioprovince.”

Keywords Fish otoliths, Morocco, Rharb Basin, Pliocene, Maghrebian bioprovince, Stratigraphy

Introduction

The fossil-rich coquina (*lumachelle* in French) of Dar bel Hamri in northwestern Morocco was discovered by Lecointre in 1916. The outcrop is located about 1.5 km south of Dar bel Hamri along the right river banks of the Oued Beth. It belongs to a sequence of sediments deposited along the southern margin of the funnel-shaped Neogene Rharb Embayment that opened to the Atlantic and connected eastward through the Prerifian strait to the Mediterranean prior to its closure during the terminal Miocene (Fig. 1). Lecointre considered the coquina at Dar bel Hamri to be of Early Pliocene age. Molluscs found there were the subject of extensive research that led to controversial views in respect to the stratigraphic position of the deposits ranging from the Tortonian (Gignoux, 1950) to the Sahelian (Late Miocene equivalent) by Deperet and Gentil (1917), Bourcart et al. (1940),

and Chavan (1944) and to the Early Pliocene. Lecointre always maintained the view that the Lagerstätte was of Early Pliocene age (1944, 1952, 1963), culminating in an article with the title “La faune de Dar bel Hamri (Maroc) est d’âge pliocène” by Lecointre and Roger (1943). All these studies were based primarily on the rich mollusc fauna from Dar bel Hamri and did not take into account other fossil groups or outcrops along the Oued Beth.

These controversial views, and the information supplied by my colleague F. von der Hocht (Kerpen), who found abundant otoliths in the coquina during a sampling expedition in 1974, triggered my desire to undertake a more regional stratigraphic study in the course of my master’s thesis at the Freie Universität Berlin. The Oued Beth cuts through a Neogene sedimentary section that is particularly well and nearly continuously exposed along its right bank over a distance of about

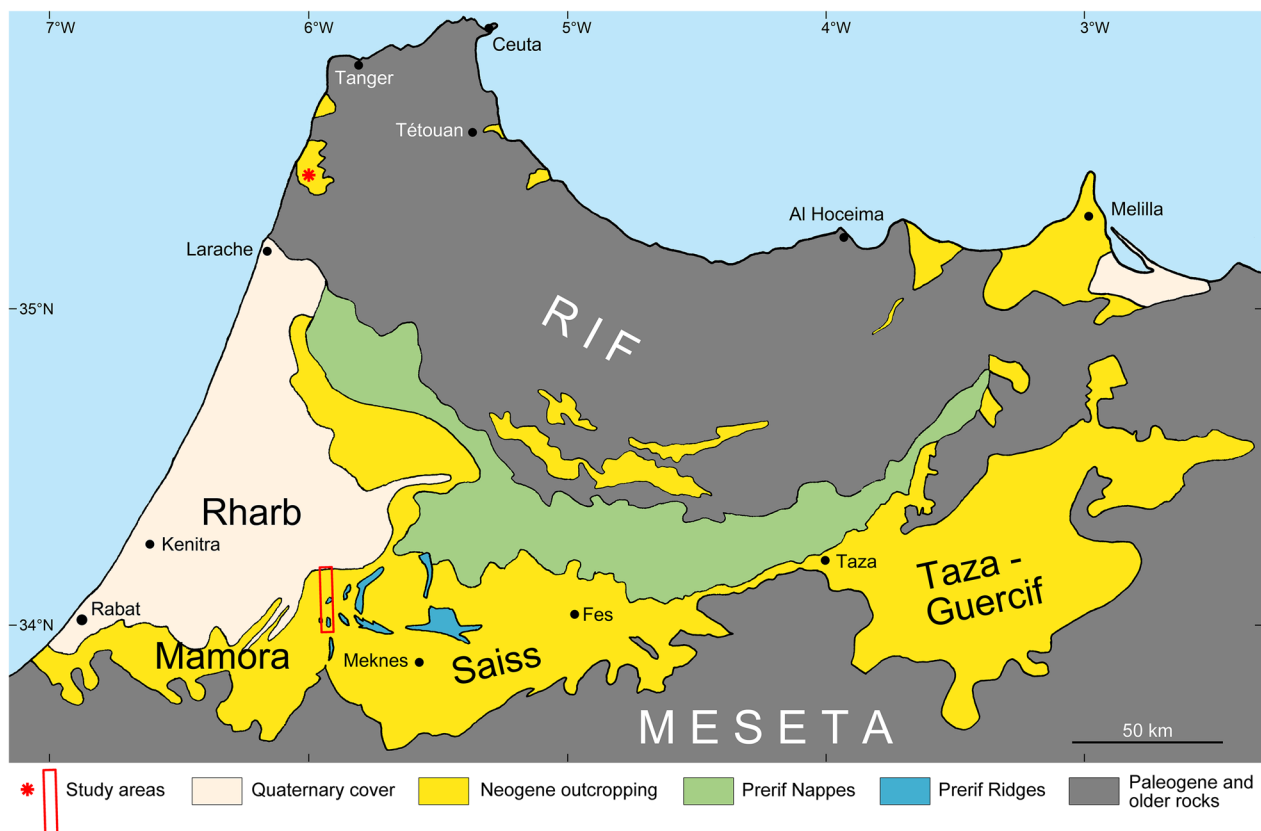


Fig. 1 Regional map of northern Morocco outlining distribution of Neogene sediments. Schematized and simplified after the detailed map published by Saadi et al. (1980). The study areas highlighted are the Oued Beth outcrop section (red rectangle) and the Asilah outcrop (red asterisk)

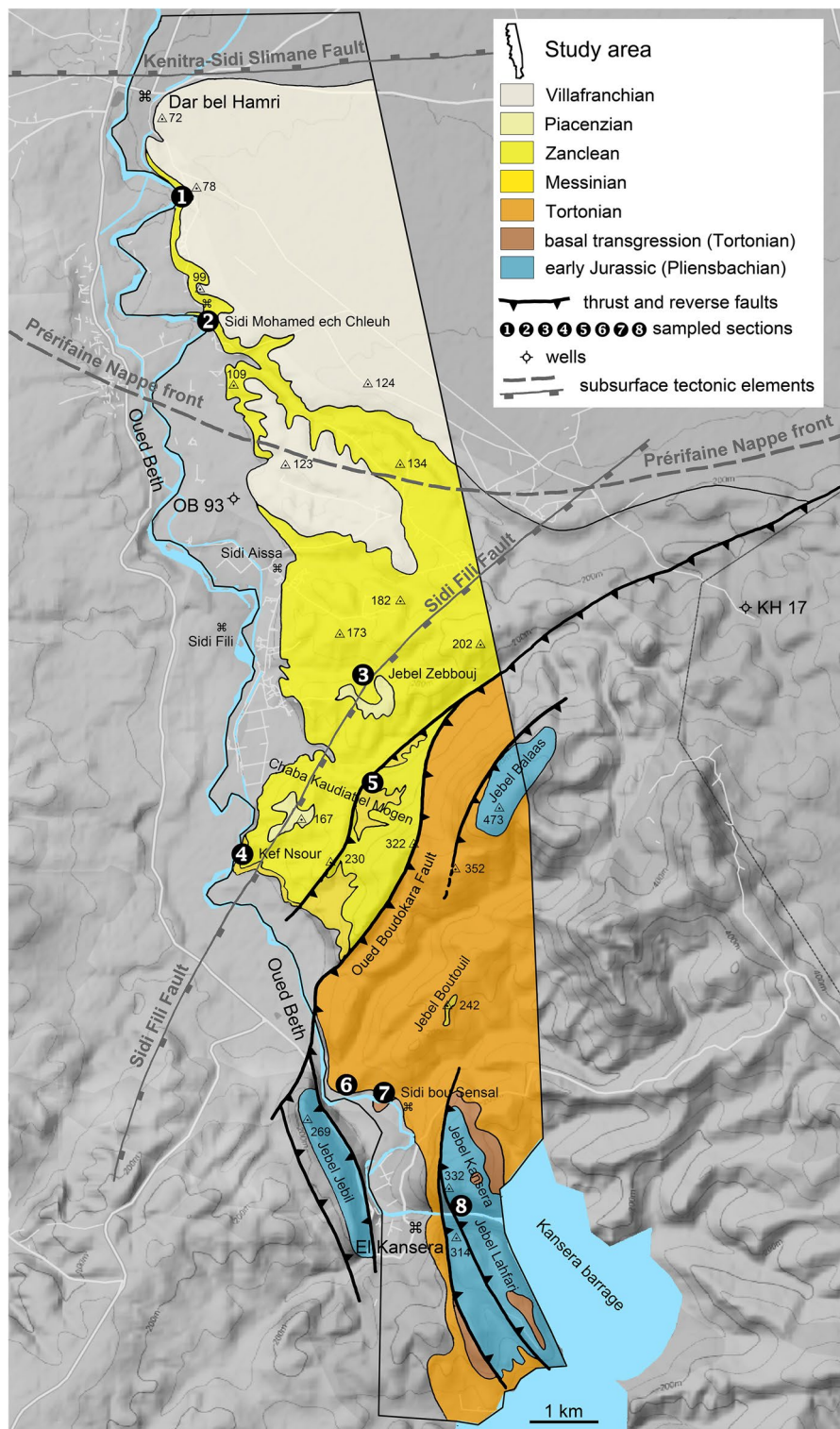


Fig. 2 Geological map of the studied area from Dar bel Hamri to El Kansera resulting from a review of my master thesis (1977), and highlighting sections sampled. The location of the subsurface Sidi Fili fault and Nappe Prérifaine front are extrapolated from Tilloy (1952) and the postulated extension of the Kenitra-Sidi Slimane fault is from Zouhri et al. (2002)

25 km north to south between Dar bel Hamri and El Kansera (Fig. 2). The idea was to apply the then still fairly newly established biostratigraphic zonation with planktonic foraminifera to these sediments. Field work was undertaken in 1974, 1975 and 1976. During this time, I had the most pleasant experience with Moroccan hospitality and was invited to stay at the home of Abdslam Ouarred and his family, who became a good friend. The thesis was completed in 1977. It was among the first studies using planktonic foraminifera in the region along with Feinberg (1976, 1978), Feinberg and Lorenz (1970, 1971), and Wernli (1978). A large, supra-regional biostratigraphic study of post-nappe ("Nappe Prerifaine") Neogene strata in Morocco was performed by Wernli (1988) and has remained the standard reference to date. All these planktonic foraminifer studies concluded that the coquina of Dar bel Hamri is of Early Pliocene age, thereby confirming Lecointre's view.

More recently, the Neogene sedimentary sequence south of the Rif Mountain chain in northern Morocco has triggered renewed interest, as it is considered to represent the last marine strait between the Northeast Atlantic and the Mediterranean prior to the Messinian Salinity Crisis in the Mediterranean. Many detailed geological and biostratigraphic studies have been conducted on the Atlantic side at the iconic Bou Regreg section near Rabat further to the west of the study area (Barbieri & Ori, 1997; Barhoun et al., 1999; Benson & Rakic-El Bied, 1991; Gebhardt, 1993; Hilgen et al., 2000; Hodell et al., 1994; Krijgsman et al., 2004; Rakic-El Bied & Benson, 1996), in the Saiss region further to the east of the study area (Capella et al., 2017, 2018a, 2018b; Tulbure et al., 2017), and in samples from wells in the Rharb Basin (Daya et al., 2005; Yousfi et al., 2013). The Oued Beth section does not seem to have been comprehensively studied.

A number of samples from my field work in 1974/75/76 and the otoliths that F. von der Hocht (Kerpen) and I then collected are still preserved. Here, I review the results of my unpublished master's thesis and update them in the light of newer biostratigraphic research. Only a few otolith-based species have so far been described from there (Schwarzzhans, 1981, 1993, 1999). Therefore, the second, larger part of the current article deals with the description of the otoliths mostly collected from the classical locality at Dar bel Hamri plus a few other localities along the Oued Beth section and from Asilah further north in Morocco. One of the main aims is to compare the Early Pliocene fish fauna reconstructed from otoliths from the Atlantic realms of Morocco with those found in many well-studied coeval localities around the Mediterranean (e.g., Nolf & Cappetta, 1988; Nolf & Girone, 2006; Nolf & Martinell, 1980; Nolf et al., 1998; Schwarzzhans, 1978a, 1986; van Hinsbergh & Hoedemakers, 2022).

Regional geology

Along its course in the North, the level of the Oued Beth falls from about 60 m AMSL near El Kansera to about 40 m at Dar bel Hamri. The summit plane level rises from about 78 m ASML due south of Dar bel Hamri to 230 m near Kef Nsour and 332 m at the top of the Jebel Kansera (Fig. 2). The summit plane is also distinctly tilted westward; for instance, from 230 m near Kef Nsour to about 150 m on the distant western bank. In consequence, the Neogene outcrop situation is particularly well exposed along the right river banks and specifically at certain eroding banks that have been selected as main geological sections (Fig. 3). These are the eroding banks about 1.5 km south of Dar bel Hamri with the famous coquina exposed at river level (section 1; see Fig. 7 in Tilloy, 1952), low banks at Sidi Mohamed ech Chleuh (section 2; Figs. 2, 3a), the high cliff of Kef Nsour (section 4; Figs. 2, 3b,c), exposures near Sidi bou Sensal (sections 6 and 7; Figs. 2, 3d–e), and local outcrops in cross-cutting ravines of small streams below the Jebel Zebouj (section 3; Fig. 2) and in the Chaba Koudiat el Mogen (section 5; Fig. 2).

The terrain southward from Dar bel Hamri is relatively flat lying away from the river for about 5 to 6 km rising from about 70 to 120 m, and to the North of Dar bel Hamri grades into the Rharb Plain between 30 and 40 m. The flat lying terrain south of Dar bel Hamri is topped by terrestrial to fluvial Early Pleistocene deposits, the Villafranchian, and in the Rharb Plain by fertile Quaternary soil. South of Sidi Aissa (Fig. 2), the morphology becomes hilly due to erosion exposing Neogene sediments at the surface, although rarely well exposed due to agricultural activity except in the eroding river banks. Westward of El Kansera, the Oued Beth has cut a deep gorge through a Prerif Ridge with beautifully exposed upthrust Early Jurassic limestones (section 8; Figs. 2, 3f). The Oued Beth is dammed at the entry to the gorge, forming the Kansera barrage lake (Fig. 2).

Stratigraphy

The identification of the observed planktonic foraminifera is mainly based on Wernli (1988), with a few cases not covered in Wernli being identified from mikrotax.org (Young et al., 2022) and other literature sources. Absolute range charts vary to some extent in the literature. I have followed mikrotax.org (Young et al., 2022) and Aze et al. (2011) for the main part and Maniscalco and Brunner (1998) for the *Globorotalia margaritae* plexus. Occurrences in studied sections and related regional biostratigraphic events follow Wernli (1988), Barhoun and Bachiri Taoufiq (2008), and Yousfi et al. (2013).

The Neogene sedimentary sequence in the study area commences with a conglomerate with carbonatic

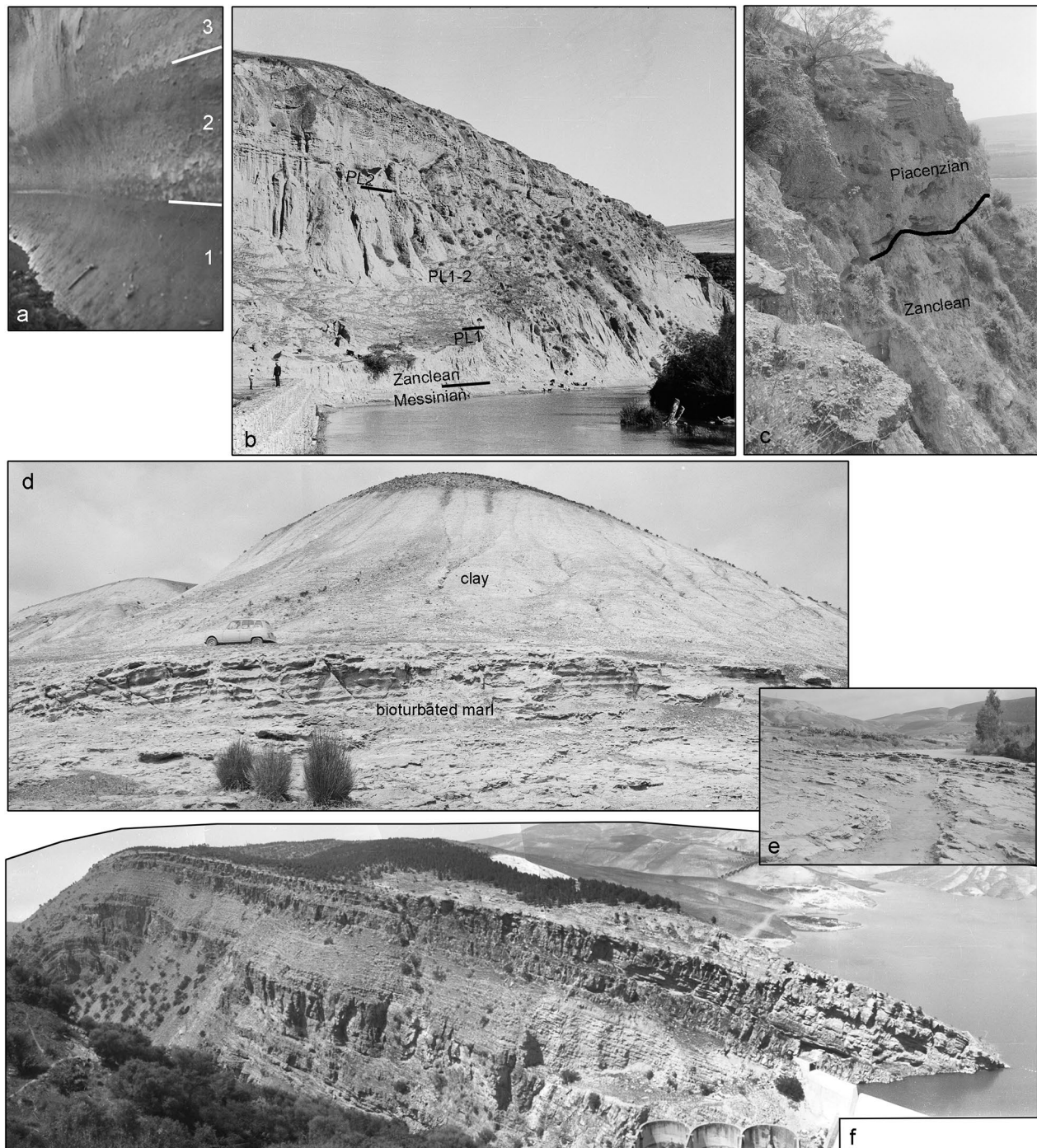


Fig. 3 Photographs of selected section locations. **a** Base of section 2 at Sidi Mohamed ech Chleuh above river level. **b, c** Kef Nsour cliff (section 4); **b** panoramic view; **c** view of cliff top with Piacenzian sediments exposed. **d, e** Tortonian outcrop sequence near Sidi bou Sensal (section 7, and section 6 to the left in **d**); **d** panoramic view; **e** eroded basal Tortonian bioturbated mudstones at section 7 in the Oued Beth river bed; **f** panoramic view of upthrust Jurassic rocks of the Jebel Kansera along the Oued Beth gorge

matrix preserved in small pockets on the Jebel Kansera and Jebel Lahfari and an overlying unit of banked silty marl and marlstone with abundant bioturbation found

along the back-limb of the upthrust Jebel Kansera-Lahfari complex and in a shallow anticline exposed in the Oued Beth riverbed and right bank near Sidi Bou Sensal

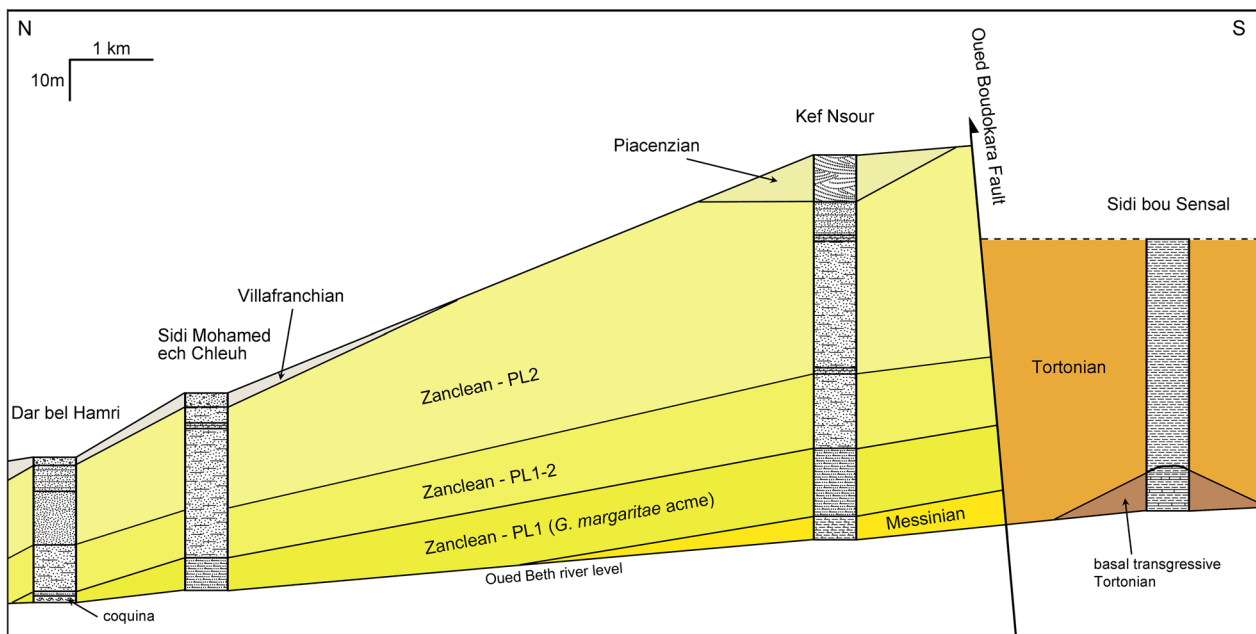


Fig. 4 Schematized outcrop-section along the Oued Beth right river bank based on studied sections

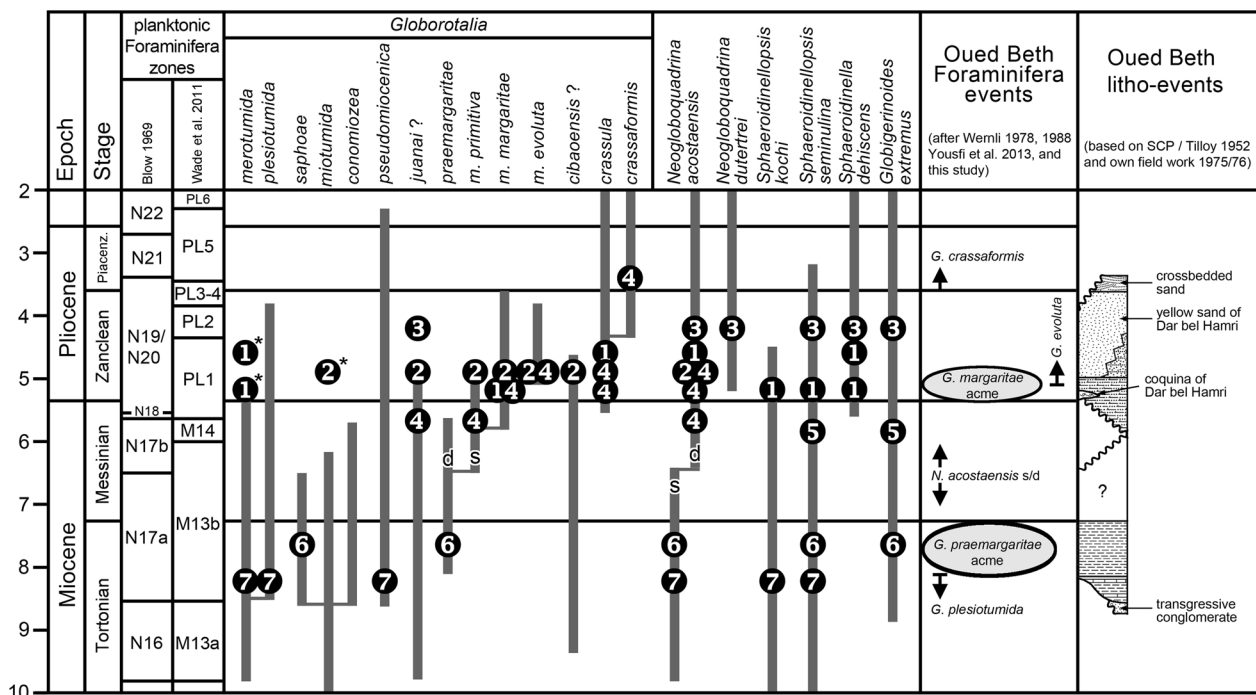


Fig. 5 Range chart of selected planktonic foraminifera observed in the study area. Ranges after mikrotax.org (2022) and Aze et al. (2011) and Maniscalco and Brunner (1998) for the *Globorotalia margaritae* plexus. Occurrences in studied sections and related regional biostratigraphic events mainly after Wernli (1988), Barhoun and Bachiri Taoufiq (2008) and Yousfi et al. (2013). Numbers refer to the sampled sections shown in Fig. 2

(section 7; Figs. 2, 3d,e, 4, 5). No fossils were found in the conglomerate and the sediments on the flanks of the Jebels. Samples taken from the outcrop at Sidi bou

Sensal, the highest part of this unit, which may not be much thicker than 10–20 m in total, contained planktonic foraminifera, most commonly *Sphaeroidinellopsis*

seminulina and *Trilobatus trilobus*, but also a few specimens of *Globorotalia plesiotumida* (Figs. 5, 6l) and *G. merotumida* and *Neogloboquadrina acostaensis* (sinistral; Fig. 5). The biostratigraphic position is interpreted

as early late Tortonian (base of planktonic foraminifera zone N17a / M13b), but the lower, seemingly barren, part of the section could be older.

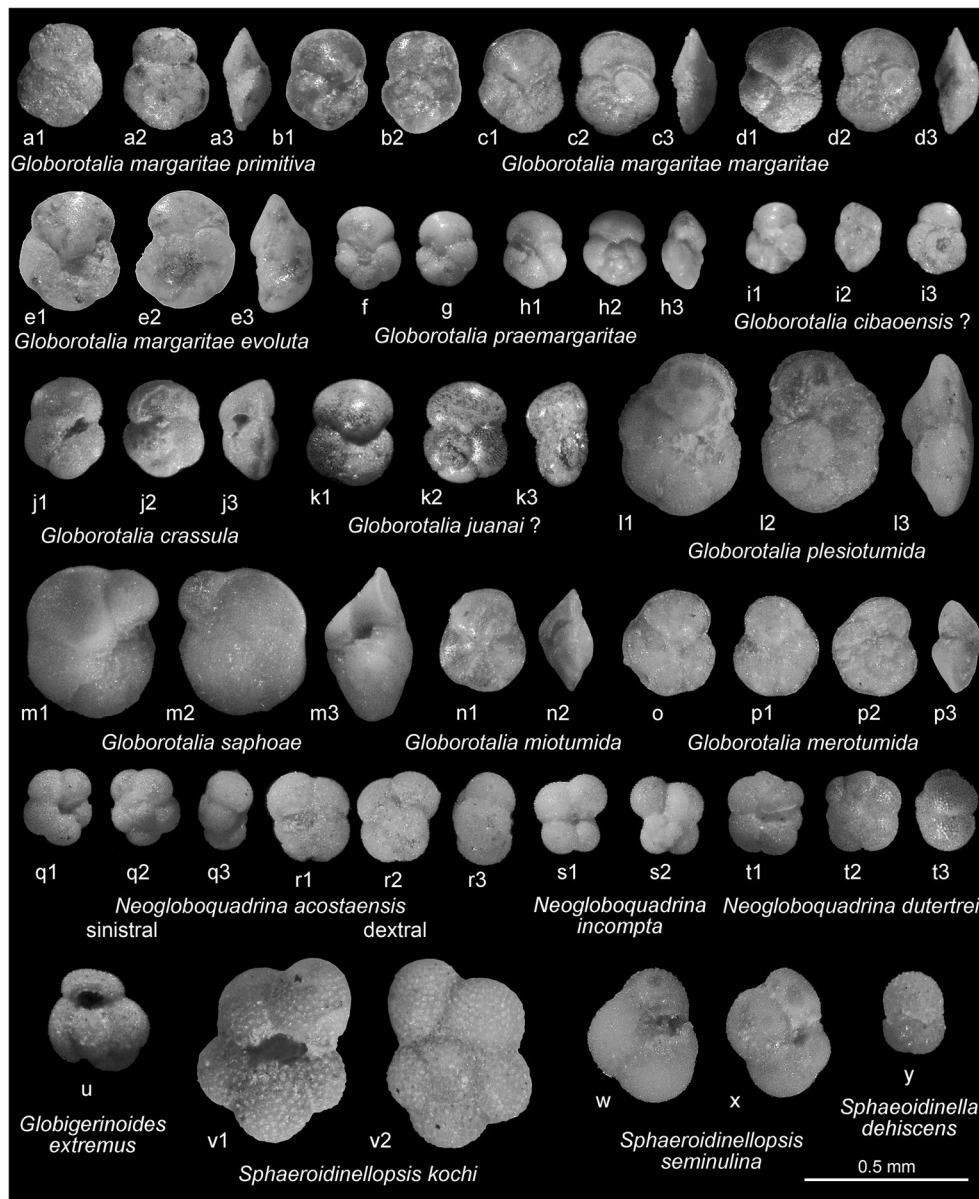


Fig. 6 Photoplate of selected planktonic foraminifera deemed of stratigraphic significance. *Globorotalia margaritae primitiva*: **a** Sidi Mohamed ech Chleuh (section 2), Zanclean level 2. *Globorotalia margaritae margaritae*: **b**, Kef Nsour (section 4), higher Zanclean; **c**, **d**, Sidi Mohamed ech Chleuh (section 2), Zanclean level 2; *Globorotalia margaritae evoluta*: **e**, Kef Nsour (section 4), higher Zanclean. *Globorotalia praemargaritae*: **f–h**, Sidi bou Sensal (sections 6 and 7), Tortonian clay. *Globorotalia cibaoensis*?: **i** Sidi Mohamed ech Chleuh (section 2), Zanclean level 1. *Globorotalia crassula*: **j** Kef Nsour (section 4), basal Zanclean. *Globorotalia juanai*?: **k** Jebel Zebbouj (section 3), higher Zanclean. *Globorotalia plesiotumida*: **l** Sidi bou Sensal (section 7), basal Tortonian mudstone. *Globorotalia saphoe*: **m** Sidi bou Sensal (section 7), Tortonian clay. *Globorotalia miotumida*: **n** Sidi Mohamed ech Chleuh (section 2), Zanclean level 2 (presumed reworked). *Globorotalia merotumida*: **o**, **p** Dar bel Hamri (section 1), Zanclean, yellow sands of Dar bel Hamri (presumed reworked). *Neogloboquadrina acostaensis*: **q** Sidi bou Sensal (section 7), Tortonian clay; **r** Kef Nsour (section 4), basal Zanclean. *Neogloboquadrina incompta*: **s** Sidi bou Sensal (section 6), Tortonian clay. *Neogloboquadrina dutertrei*: **t** Jebel Zebbouj (section 3), higher Zanclean. *Globigerinoides extremus*: **u** Jebel Zebbouj (section 3), higher Zanclean. *Sphaeroidinellopsis kochi*: **v** Dar bel Hamri (section 1), coquina. *Sphaeroidinellopsis seminulina*: **w**, **x** Sidi bou Sensal (section 7), Tortonian clay. *Sphaeroidinella dehiscens*: **y** Jebel Zebbouj (section 3), higher Zanclean

At section 7 and extending into section 6, this basal unit is overlain by a thick sequence of massive calcareous clay of medium gray to blue-gray color that does not show apparent bedding. This sequence corresponds to the “detritic molasse” of Faure-Muret and Choubert (1971) and indicates a rapid deepening of the sedimentary environment. It is possible that it has been affected by syndimentary redeposition or slumping caused by over-steepening and slope failure along the putative nearby basin flanks. Samples taken at section 6 from this interval were rich in microfossils (Fig. 5). The most common planktonic foraminifera are *Globorotalia praemargaritae* (Fig. 6f–h) and *Sphaeroidinellopsis seminulina* (Fig. 6w, x). Other characteristic species are *Dentoglobigerina altispira*, *Globigerinoides extremus* (Fig. 6), *Neogloboquadrina acostaensis* (sinistral; Fig. 6q), and *Globorotalia saphoe* (Fig. 6m), the latter from a single specimen that very much resembles *G. saphoe* as depicted by Wernli (1988) from the Tortonian, while in the Mediterranean it occurs only in the early Messinian. Benson and Rakic-El Bied (1991) showed *G. praemargaritae* in the late Tortonian. Achalhi et al. (2016) used *G. juanai* (priorized by *praemargaritae* according to Wernli, 1988) as diagnostic for Tortonian (M13a in that case) and Wernli (1988) for zone N17. The sinistral coiling orientation found in *N. acostaensis* is also characteristic (Barhoun & Bachiri Taoufiq, 2008; Yousfi et al., 2013). The predominance of the coiling direction in *N. acostaensis* changed from sinistral to dextral at about 6.35 Ma (Lourans et al. 2004). *Neogloboquadrina incompta* occurs for the first time in this interval and according to Wernli (1988) is found regularly in Morocco beginning with N17. Because of these occurrences and the further co-occurrence with *G. extremus*, the sedimentary sequence of section 6 is here interpreted as representing the late Tortonian, zone M13b (N17a). The top of this unit is uncertain, because no adequate outcrops for sampling have been identified for the higher section. The top of the Jebel Boutouil (Fig. 2) shows a clear lithology change. Samples from above and below that lithology change did not yield fossils. I consider it to mark the highest possible base for the Messinian, but it is also plausible that the Tortonian–Messinian boundary has to be expected within the un-sampled section between the top of section 6 and the lithology change observed on Jebel Boutouil. The well KC1 to the west of Dar bel Hamri had about 800 m thickness of Late Miocene and probably coeval sediments (Wernli, 1988). In the study area, the sequence is in the order of over 200 m thickness and is found all across the terrain between the Oued Boudokara fault and the Jebel Kansera-Lahfari thrust

front fault (see also chapter titled “Structural geology”; Fig. 2).

The recognition of the Messinian in the Atlantic Moroccan Neogene has remained a matter of conflicting interpretations, particularly as far as the delimitation toward the Early Pliocene is concerned, as can for instance be observed in the studies of micropaleontological findings (compare Barbieri & Ori, 1997; Benson & Rakic-El Bied, 1991; Krijgsman et al., 2004; Rakic-El Bied & Benson, 1996; Wernli, 1988; Yousfi et al., 2013). However, the stratotype for the global boundary of the base of the Messinian was established at Oued Akrech near Rabat by Hilgen et al. (2000). Along the Oued Beth section, the recognition of Messinian strata has remained problematic. This is mainly because species considered to be indicative of the Messinian have not been found (e.g., *Globorotalia conomiozea*, *G. nicolae*, *G. mediterranea*, *G. multiloba*, or *G. saheliana*). At the base of the Kef Nsour section, however, specimens of *Globorotalia margaritae primitiva* (Fig. 6a) were found not associated with *G. margaritae margaritae*. The first occurrence date (FOD) of both subspecies is within the Messinian, but that of *G. m. primitiva* is considered by Maniscalco and Brunner (1998) to be earlier at about 6.55 Ma. This level at Kef Nsour and certain higher levels in various sections also contained a *Globorotalia* species apparently not reported in Wernli (1988) and interpreted here as possibly representing *G. juanai*? (Fig. 6k), but it seems to occur stratigraphically higher than recorded in the literature. However, distinction or synonymization of the formal species *G. juanai*, *G. praemargaritae*, and *G. margaritae primitiva* vary in the literature (see Stainforth et al., 1975; Kennet & Srinivasan, 1983; Wernli, 1988; Aze et al., 2011). *Neogloboquadrina acostaensis* is found rarely and in dextral coiling orientation, which according to Benson and Rakic-El Bied (1991) corresponds to a late Messinian event at about 5.55 Ma but is shown earlier in the Messinian at 6.35 Ma in Lourens et al. (2004) and Krijgsman et al. (2004). This interval at Kef Nsour is interpreted to be of Messinian age, probably late Messinian. An outcrop at the base of the Chaba Kaudiat el Mogen ravine (section 5) is also considered to probably be of Messinian age. It did not contain any indicative planktonic foraminifera but is unique in containing thin laminae (a few centimeters thick) of gypsum. This indicates a restricted evaporitic environment for these sediments. Even though the sediments are probably of Messinian age they may not be related in any way to the evaporites of the Mediterranean Messinian Salinity Crisis but may rather represent an ephemeral local event in a small semi-enclosed sub-basin at the time.

Most of the sediment sequence cut by the Oued Beth between the Oued Boudokara Fault and Dar bel Hamri

is considered to be of Pliocene age. This is in agreement with the geological map of the Rifian region (Saadi et al., 1980), but in conflict with the regional map in Capella et al. (2017), where the area is shown as late Messinian. The basal part of the sequence in question is particularly well exposed in the sections of Sidi Mohamed ech Chleuh (section 2; Fig. 3a) and Kef Nsour (section 4; Fig. 3b). It starts with a 3 to 5 m thick dark bluish-gray clayey silt (level 1), overlain by a similarly thick medium gray clayey silt (level 2) and in turn by a light gray silty and clayey sand (level 3) of which the thickness could not be ascertained (Fig. 3a). The lower two levels are rich in *Globorotalia margaritae margaritae* and form an acme for that species (Figs. 5, 6b–d). It also represents the first occurrence of *G. m. margaritae* in the studied area. These two levels further contain certain other, more rare, diagnostic species, namely *G. m. primitiva*, *G. crassula* (Fig. 6j), and possibly *G. cibaoensis?* (Fig. 6i) and a single specimen of *G. miotumida* in level 2 (Fig. 6n), which is considered to be reworked (see also the discussion below on the coquina). *Neogloboquadrina acostaensis* is relatively common and is always in dextral coiling orientation (Figs. 5, 6r). The FOD of *G. m. margaritae* is given as 5.90 Ma by Maniscalco and Brunner (1998) and 5.95 Ma by Wade et al. (2011), respectively, in the late Messinian and that of *G. crassula* (Fig. 6) within zone N18, but Chaisson and Pearson (1997) show it commencing only in the Early Pliocene. The highest sequence consisting of light gray silty sand also includes *G. m. evoluta* (Fig. 6), which differs from *G. m. margaritae* in the last chamber being widened and the spiral side being even more convex. The FOD of *G. m. evoluta* is within zone PL1 and terminates with PL2. Wernli (1988) regarded both subspecies (*G. m. margaritae* and *G. m. evoluta*) as indicative of the Early Pliocene, a view that is more or less in agreement with Yousfi et al. (2013) and Barbieri and Ori (1997), in particular as to the range of *G. m. evoluta*. Benson and Rakic-El Bied (1991) recognized an event with *G. margaritae* becoming abundant at about 5.3 Ma in the latest Messinian. A *G. margaritae* acme was observed by Rakic-El Bied and Benson (1996) in Ain el Beda near Rabat and was associated with polarity chron C3r (Gilbert), and Krijgsman et al. (2004) correlated it with an interval from 5.84 to 5.56 Ma during the latest Messinian. However, Krijgsman et al. (2004) also state that the top of the *G. margaritae* acme does not correspond to a real drop in abundance, as the taxon is still common in the Pliocene. The identification of *G. crassula* and *G. cibaoensis?* requires some explanation, since neither has been recorded in other studies. Wernli (1988) studied the Dar bel Hamri section (section 1, see below) and found *G. crassaformis* throughout, from which he interpreted the sediments to be of late Early Pliocene age (PL2). He also

noted that the specimens were unusually small. In my view, other possible differences, albeit subtle, are the less convex umbilical side and the more rounded periphery. Therefore, attributing these specimens to the precursor of *G. crassaformis*, namely *G. crassula*, appears justified to me. Very rarely, an even smaller species occurs with 4.5 to 5 chambers in the last whorl that are here tentatively interpreted as *G. cibaoensis?*. Thus, in the case of sections 2 and 4 of the Oued Beth outcrop sequence, the presence of *G. crassula* throughout and of *G. m. evoluta* in the higher part of the interval strongly indicate zone PL1 and is here interpreted to belong to the Early Pliocene (Zanclean; Figs. 4, 5).

A special situation is observed in section 1, 1.5 km south of Dar bel Hamri, because of the presence of the coquina at the base of the section and only a very thin, less than 1 m thick bluish-gray silty marl section above, both of which (plus an unknown possible deeper section) are thought to represent the lateral equivalent of the unit described above from Sidi Mohamed ech Chleuh and Kef Nsour. The lateral extent of the coquina is apparently limited and not known from any other outcrop in the area. Apart from the coquina and sediments immediately above and on the higher section of the cliff, most of the outcrop was obscured during the times of the visit. The coquina is rich in fossils, mainly molluscs (Fig. 7), but also small solitary corals, shark teeth, fish otolith, ostracods, and benthic foraminifera. Planktonic foraminifera are relatively rare. Wernli (1988) assumed a depositional water depth of 30–70 m based on the planktonic–benthonic foraminifera ratio. The section was studied by Wernli (1988), and my own observations confirm the findings reported in his monograph, except for *G. crassaformis*, which is here interpreted as *G. crassula* and which in my samples only occurred in the higher part of the section and not in the coquina. In addition to Wernli and the ubiquitous *G. m. margaritae*, *Sphaeroidinella kochi* (Fig. 6v), *S. seminulina*, and *Sphaeroidinella dehiscens* (Fig. 6y) were identified. As noted by Wernli (1988), the coquina also contains several reworked planktonic foraminifera of Late Cretaceous age (*Globotruncana* spp.), Eocene (*Globorotalia cerroazulensis*, *G. gracilis*), and Late Miocene (*Globorotalia merotumida*, *Globoquadrina dehiscens*). A similar situation has been observed with molluscs, which probably led to the different assignments of Late Miocene and Early Pliocene and was commented on by Lecointre and Roger (1943). Lecointre and Roger mentioned four gastropod species that they considered reworked from Miocene strata. One of them, *Ancillaria glandiformis* Lamarck 1810 (Fig. 7h), is relatively commonly found in the coquina, but almost always severely eroded. A common shell in the coquina and equivalent strata is *Amussium cristatum*

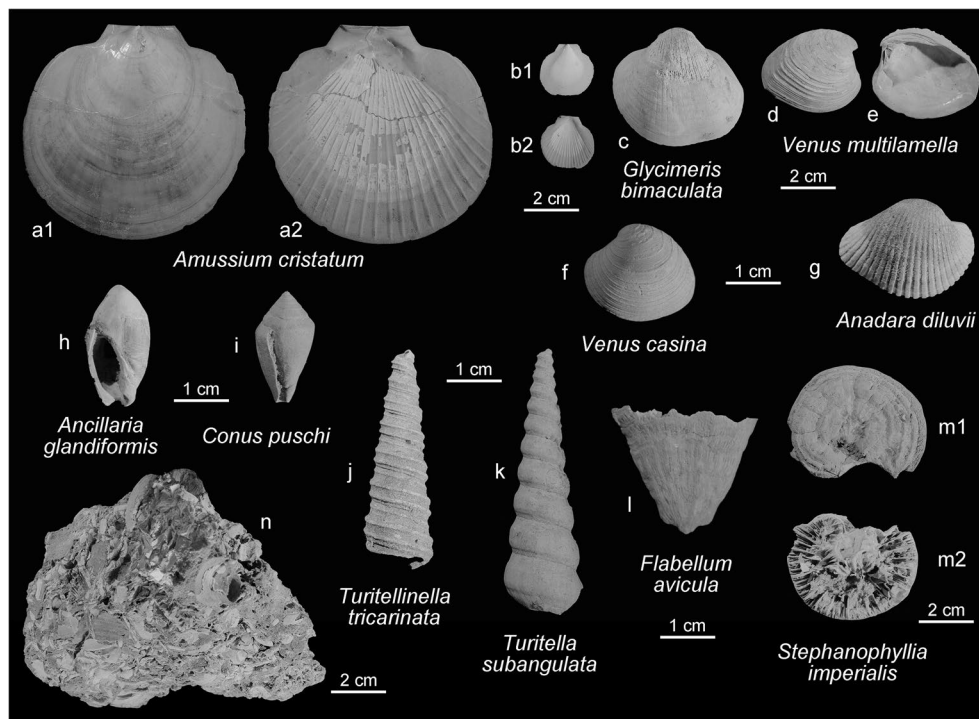


Fig. 7 Photoplate of selected macrofossils from the Early Pliocene coquina of section 1, ca. 1.5 km south of Dar bel Hamri. A rock sample is shown in n

(Bron, 1827), a thin-walled large pectinid, which is easily recognized by its smooth outer surface and the presence of multiple thin radial ridges on the inner surface (Fig. 7a,b). Such a shell would not survive redeposition in good shape and is, therefore, regarded as autochthonous. Ben Moussa (1994) described it as particularly common and large in size in Early Pliocene localities of Asilah, Tétouan, and Boudinar, but also recorded it from the Messinian in Mediterranean sections (Melilla). The shark teeth of *Notorynchus primigenius* (Agassiz, 1835), which according to F. von der Hocht (personal communication) are always strongly eroded, are also considered to be reworked. *Notorynchus* is a species ranging into the Miocene, but not the Pliocene. He also mentioned two morphotypes of *Galeocерdo*, one of Miocene origin and always eroded, and another Pliocene species well preserved. It thus appears that the basal Pliocene strata in Dar bel Hamri contain significant amounts of reworked fossils, which is also seen in time-equivalent strata further to the south (Sidi Mohamed ech Chleuh and Kef Nsour) but to a much lesser degree. The origin of the reworked fossils will be elucidated in more detail in the chapter titled “Structural geology” and is probably related to erosion from the Nappe Prerifaine in the North and directly underlain and apparently eroded Late Miocene strata. A selection of common and typical macrofossils in

the coquina of gastropods, lamellibranchiates, and solitary corals is depicted in Fig. 7.

The main, upper part of the section at Dar bel Hamri (section 1) is composed of a yellow sand (the “sables jaune de Dar bel Hamri”) with a few interbeds (see Tilloy, 1952, for detailed lithology section). Aragonitic fossils are not preserved, and the contents of planktonic foraminifera decreases probably because of a shallowing environmental setting. Southward, at Sidi Mohamed ech Chleuh and Kef Nsour, this sequence gradually thickens, indicating that the depocenter was further south, and the sediments change to a silty fine sand and clayey silt. In a section relatively high in the sequence at Jebel Zebbouj (section 3), a relatively deep water environment continued and aragonitic fossils are still preserved. The composition of the planktonic foraminifera does not change significantly, except for *G. m. margaritae* becoming increasingly rarer and disappearing in the higher part of section 1 and being absent in section 3. Some reworked specimens still occur in the higher part of section 1, notably *G. merotumida*. The higher parts of sections 1, 2, and 4 are interpreted as undifferentiated PL1-2. Section 3 represents the highest point in the sequence, bears more and better preserved specimens than its rather lean equivalents in sections 1, 2, and 4, and may represent biozone PL2. *Neoquadrina dutertrei* (Fig. 6t) occurs here for the first time.

The marine Neogene section terminates with the interval considered to represent biozone PL2 in most studied sections, but at Kef Nsour a higher stratigraphic interval is preserved at the top of the cliff (Fig. 3c). It is about 10 m thick and composed of relatively coarse, cross-bedded medium to coarse sands with some pockets of finer sand. These finer sand pockets contained few planktonic foraminifera (i.e., *Dentoglobigerina altispira*, *Globorotalia crassaformis*, and *Pulleniatina obliqueloculata*), indicating a Piacenzian age, in agreement with the stratigraphic assessment of Yousfi et al. (2013) in a well in the center of the Rharb Basin. These rocks represent the last marine sediment found along the studied Oued Beth section.

In summary, a review of the preserved samples from my unpublished master's thesis and a review of the results in the light of modern biostratigraphic research in Morocco have demonstrated that the outcrop sequence along the right river banks of the Oued Beth between Dar bel Hamri and El Kansera represents a stratigraphic sequence from the late Tortonian (M13b) up to the Early Piacenzian (Figs. 2, 3, 4, 5). The sequence may have some local interruptions or hiatuses at undefined levels of the Messinian, but otherwise appears to be continuous. A dense stratigraphic interval sampling should be possible, and the sections of Kef Nsour and Sidi bou Sensal appear particularly promising for that purpose. The higher part of the section of Sidi bou Sensal may require shallow hand drills for optimal sampling. The sequence *Globorotalia prae-margaritae*, *G. m. primitiva*, *G. m. margaritae*, and *G. m. evoluta* as well as the occurrence of *G. plesiotumida* and *G. crassula* appear to provide particularly promising results. An unambiguous Messinian interval with

(common) *G. conomiozea* or *G. nicolae* is yet to be found in this sequence.

Structural geology

The study area is located at the southern rim of the larger Rharb Embayment of the Neogene Northeast Atlantic and covers terrain at the westernmost Prerif Ridges and thus along the hinge between the Saiss sub-basin and the Mamora platform (Fig. 1). The exposures are basically structured into three parts: (1) the southern part is characterized by the upthrust Jurassic rocks of the east-verging Jebel Kansera/Lahfari thrust front; (2) the central part is characterized by uplifted Late Miocene sediments bound to the North by the Oued Boudokara fault; and (3) the northern part is characterized by a flat-lying and essentially undisturbed Early Pliocene sedimentary cover. The Prerif Ridges were formed as a response to compressional and rotational forces that affected the stable NW-African plate margin during the Neogene to the south of the bethic-rifian orogeny. The Prerif Ridges form an arcuate geometry in map view with trending southwest to west to northwest fault fronts and have been intensely studied for decades (see Faure-Muret & Choubert, 1971; Sani et al., 2006; Roldán et al., 2014 and literature cited therein). Following the principles of section balancing in compressional regimes, Flinch (1993), Zizi (1996), Haddaoui et al. (1997), and Roldán et al., (2014) explained the Prerif Ridges by compression exerted from the approaching Rif orogeny beginning in the Late Miocene and culminating in the Late Pliocene (Zizi, 1996). The decollement of the sole thrust from which the individual Prerif Ridges would represent splays is located within Triassic evaporites. The basement is not involved in the deformation of the Prerif Ridges (Zizi, 1996). Commercial oil wells have shown thicknesses of about 1000 m

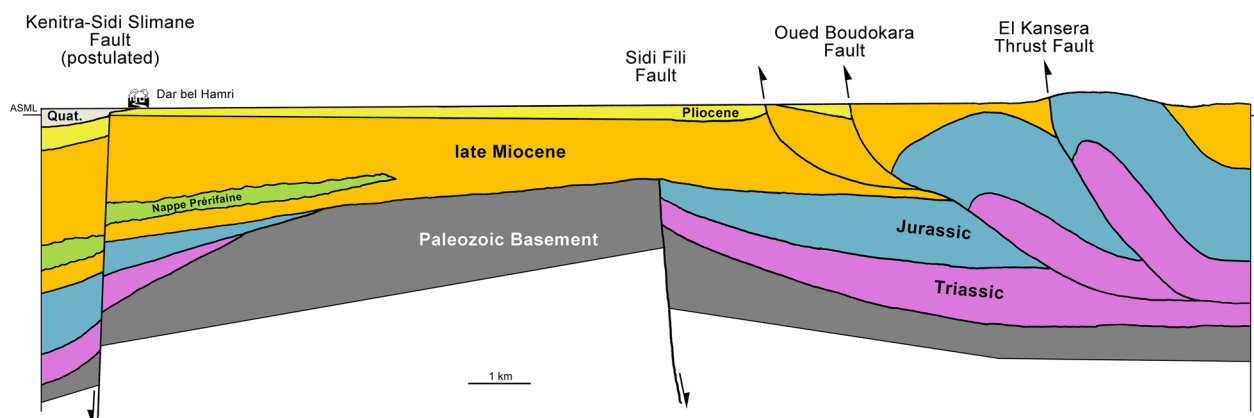


Fig. 8 Conceptual structural cross-section through studied area based on Zizi (1996) and own field observations (scale 1:1). Subsurface thicknesses are extrapolated from sections of nearby wells published in Saadi et al. (1980) and Sani et al. (2006). Subsurface positions of not-exposed tectonic elements after Tilloy (1952), Zizi (1996), and Zouhri et al. (2002)

of Triassic and about 1400 m of Jurassic rocks about 10 to 20 km west of the study area (geological map by Saadi et al., 1980). The thrust model is depicted in an interpreted seismic line and geo-seismic interpretation tying up Jebel Jebil and Jebel Kansera by Zizi (1996, pl. 22). The model is consistent with the observations I made on Jebel Kansera along the Oued Beth gorge (Figs. 3f, 8) (see also Roldán et al., 2014). A small, deep, and rather shallow anticline located in the study area in front of Jebel Kansera (section 7; see above) probably represents a buckling in the foreland of the Kansera thrust fault that could lead up to the Jebel Balaas thrust front (Figs. 2, 4, 8; see also Balaas cross section in Zizi, 1996; Fig. 3.33). The Oued Boudokara fault represents the outermost thrust-related reverse fault of the Prerif Ridges in the study area, connecting the northern termination of Jebel Jebil with the foreland of Jebel Balaas (Figs. 2, 4, 8). Tortonian is displaced against Pliocene across the fault and, because of the soft nature of the affected sediments, the fault is expressed as a wadi erosion on the surface (Oued Boudokara) along the zone of weakness. Generally, the thrust faults of the Prerif Ridges cut through Early and Late Pliocene strata, and while they may have been active synsedimentarily through the Late Miocene and Early Pliocene (Haddaoui et al., 1997), they must still have had a strong tectonic pulse after the deposition of the Piacenzian. However, the observed thickening of the Pliocene section in the study area from Dar bel Hamri toward the Oued Boudokara fault (Fig. 4) is probably caused by synsedimentary depression and sedimentary accretion in the foreland of the propagating thrust faults.

An important tectonic element in the context of the formation of the Prerif Ridges is the Sidi Fili fault (Figs. 2, 8). The Sidi Fili fault is named after an oil field discovered in the 1950s, which itself was named after a small village, Sidi Fili (Fig. 2), on the left bank of the Oued Beth. It is not expressed on the surface but well constrained by commercial oil wells (Saadi et al., 1980). The Sidi Fili fault represents a major SW–NE trending Mesozoic basin margin fault with Paleozoic rocks exposed under the Neogene cover on the northwestern shoulder (foot wall) and Mesozoic, chiefly Triassic and Early Jurassic, sediments of about 2500 m thickness in the hanging wall within the study area (Sani et al., 2006; Fig. 8). The long-ranging sedimentary hiatus in the Rharrb Basin (Early Jurassic to Late Miocene in the study area) has resulted in a complex pre-Neogene subcrop map (Zizi, 1996; Fig. 3.39). The Prerif Ridges only extend over the downthrown side of the Sidi Fili fault in the presence of evaporitic Triassic sediments in the basin, whereas the foot wall of the Sidi Fili fault may have acted as an abutment against the propagating thrusts (Fig. 8). Sani et al. (2006) assumed that the Sidi Fili fault may have been

reactivated during the time as a dextral strike slip fault. While strike slip faults no doubt accompany compressional tectonics, the seismic sections depicted in their study do not suggest reactivation along the Sidi Fili fault. More likely, strike slip movements occurred basinward of the Sidi Fili fault. For instance, the steep symmetrical flanks of Jebel Jebil, which was not studied in the course of my field work, could represent a strike slip fault-related flower structure. The sharp drop-off into the Rharrb Plain north of Dar bel Hamri and the sudden increase of the Neogene sedimentary sequence from about 800 m at Sidi Fili in the study area to more than 2,000 m in well OR3 near Sidi Kacem (see Saadi et al., 1980 and Sani et al., 2006) indicates that a north-verging normal fault may cut the Sidi Fili basement high to the north. Zouhri et al. (2002) show such a configuration in seismic sections a little further to the west limiting the Mamora platform to the north, which they termed the Kenitra–Sidi Slimane fault. It is here postulated that this fault extends eastward into the study area just north of Dar bel Hamri (Figs. 2, 8). The fault is younger than the Mesozoic Sidi Fili fault and seems to cut through the older NE–SW trending fault system (Zouhri et al., 2001). It probably represents a Mio-Pliocene growth fault controlling the sedimentation in the Rharrb depocenter.

In addition to the tectonic elements described above, further tectonic-related events influenced the basin history in the study area. In particular, the Nappe Prerifaine (see Bruderer & Lévy, 1954, for a historic review) should be mentioned in this respect, which is composed of imbricates and chaotically mixed sediments of Late Cretaceous to Early Miocene age and can reach up to 3000 m in the northern part of the Rharrb Basin (Zizi, 1996). Long recognized as olistostromatic in nature, it was originally postulated to be caused by gravitational gliding from the shoulders of the Rif orogeny (Bruderer & Lévy, 1954) and more recently was interpreted as a large accretionary wedge in front of the Rif orogeny with superimposed slides by Flinch (1993). It was emplaced during the Late Miocene (Tortonian; Roldán et al., 2014) and terminated during the Early Pliocene (Flinch, 1993; Zizi, 1996). Interpreted seismic lines to the west of the study area show relatively thin slabs of the Nappe Prerifaine, sometimes with irregular, probably erosional tops (Sani et al., 2006), indicating the slump-type nature of the front of the nappe and its partial erosion. This observation would explain the occurrence of reworked Cretaceous and Paleogene planktonic foraminifera found in the Pliocene sediments of the Oued Beth outcrops (see above) and in particular in the coquina of section 1.

Capella et al. (2017) depict in their Fig. 3 a buried channel of Late Miocene to Pliocene age that they extracted from a proprietary SCP/ERICO report of 1991 (see

Capella et al., 2017, for reference), which they interpreted as a contourite moat. This buried channel is shown passing through the study area in a northward direction just west of Jebel Balaas. Later, de Weger et al., (2020a, 2020b, 2020c, 2021, 2022) interpreted certain sediment sequences identified in outcrops further to the east as related to paleo-Mediterranean Outflow Water (paleo-MOW) channels and contourites that occurred between 7.8 Ma and 7.51 Ma (late Tortonian). If further verified and made public, the buried channel west of Jebel Balaas may have been younger in time and not related to a paleo-MOW. During the Early Pliocene, the Rharrb Basin formed a funnel-shaped inland extension of the adjacent Northeast Atlantic, and the channel observed on the seismic sections could be related to the charge of tidal water into the funnel and water reflux during low tide. However, it would have certainly had some influence on the depositional environment along the Oued Beth outcrops, having been lateral by only about 2 km and having been coeval in time. One could speculate that it influenced the apparent sedimentary hiatus and erosion of (part of) the Messinian and the accumulation of a submarine coquina in section 1. This could have resulted in the reworked Late Miocene planktonic foraminifera found in the Early Pliocene section.

Paleontology

Material and methods

Most of the studied otoliths were obtained from the coquina of section 1 (Dar bel Hamri). The sediment was washed and screened in two fractions (1 mm and 1 cm mesh sizes) in the Oued Beth. The large mesh size was chosen to collect otoliths in the field, while the sieve concentrate of the small mesh size was taken to the laboratory at the facilities of the Paleontological Institute of the Freie Universität Berlin, where I was enlisted as a student at the time. The sieve concentrate was further processed with H_2O_2 and otoliths were picked under the microscope. Sieve concentrate from 1 mm mesh size was also produced from locations 2 (Sidi Mohammed ech Chleuh) and 4 (Kef Nsour) (Fig. 2) and processed in the same way. Bulk sediment samples were taken from the other locations mainly for extraction of planktonic foraminifera for biostratigraphic purposes. A few otoliths were obtained from the bulk samples of location 3 (Jebel Zebouj) and location 5 (Chaba Kaudiat el Mogen). The large collection of otoliths made by F. von der Hocht and provided for this study was mostly done with a 2 mm mesh size. Further to the north, in a temporary outcrop along a local street south of Asilah, a few otoliths were obtained from sieve concentrate. All otoliths originate from Zanclean sediments except those from Kef Nsour and Chaba

Kaudiat el Mogen, which are from late Tortonian or early Messinian sediments.

The coquina of location 1 was found to be rich in otoliths, mostly from large specimens of the respective species, which is favorable for their identification. However, they also often showed a moderate degree of erosion, probably caused by physical abrasion during the sedimentation process. The erosion effect is mostly minor, but in the case of myctophid otoliths has often led to abrasion of the delicate denticles along the ventral rim of the otoliths, which are important for identification. Locations 2 and 4 provided much fewer otoliths, but they were mostly well preserved. Due to their deeper paleoenvironment, many myctophid otoliths were recovered. As some well-preserved otoliths were obtained from the most critical groups, it was also possible to allocate many eroded specimens, which is crucial for statistical distribution evaluations. Unidentifiable otoliths are not recorded, unless they clearly represent different taxa. A total of 4377 identifiable otoliths were obtained, representing 96 species, including 16 new species and 13 in open nomenclature. In addition, 45 species also occur today.

The otoliths were photographed with a Wild M400 photomicroscope that was remotely controlled from a computer. Individual images of every view of the objects taken at a range of depths of field were stacked using the Helicon Focus software from Helicon Soft (Charkiv, Ukraine). Adjustment of exposure and contrast and retouching were applied in Adobe Photoshop when necessary to improve the images without altering any morphological features. All otoliths are shown from the inner face (if not annotated otherwise) of the right side and mirror imaged when necessary. Pleuronectiform otoliths are shown from left and right sides to demonstrate potential side dimorphism.

The morphological terminology used is that established by Koken (1884) with amendments by Chainé and Duvergier (1934) and Schwarzhans (1978b), and the morphometrics for gobies are as established in Schwarzhans (2014). The abbreviations used are as follows: OL, otolith length; OH, otolith height; OT, otolith thickness; OsL, ostium length; CaL, cauda length; OCL, length of ostial colliculum; CCL, length of caudal colliculum; SuL, sulcus length; and SL, standard length (in fish).

Since this study represents the first major fossil record for the region, much effort was made to produce comprehensive photographic documentation. The descriptive section is kept concise with diagnoses and full descriptions only given for new species and short synonymy listings and brief discussions for all other species. The systematics follow Nelson et al. (2016) except for the sequence of orders, which departs in a few instances.

Depository: All types (holotypes and paratypes) and figured specimens are deposited at the Senckenberg Forschungsinstitut und Naturmuseum (SMF), Frankfurt am Main, under the collection registrations SMF PO 101.184 to .296 and .336, except specimens of *Rhynchonger carnevalei* n. sp. and of *Pterothrissus compactus*

from the Tortonian of Piedmont which are deposited at the Museo di Geologia e Paleontologia, Università degli Studi Torino, Torino, Italy (MGPT-PU). Some non-type specimens remain in the comparative collections of the author and F. von der Hocht.

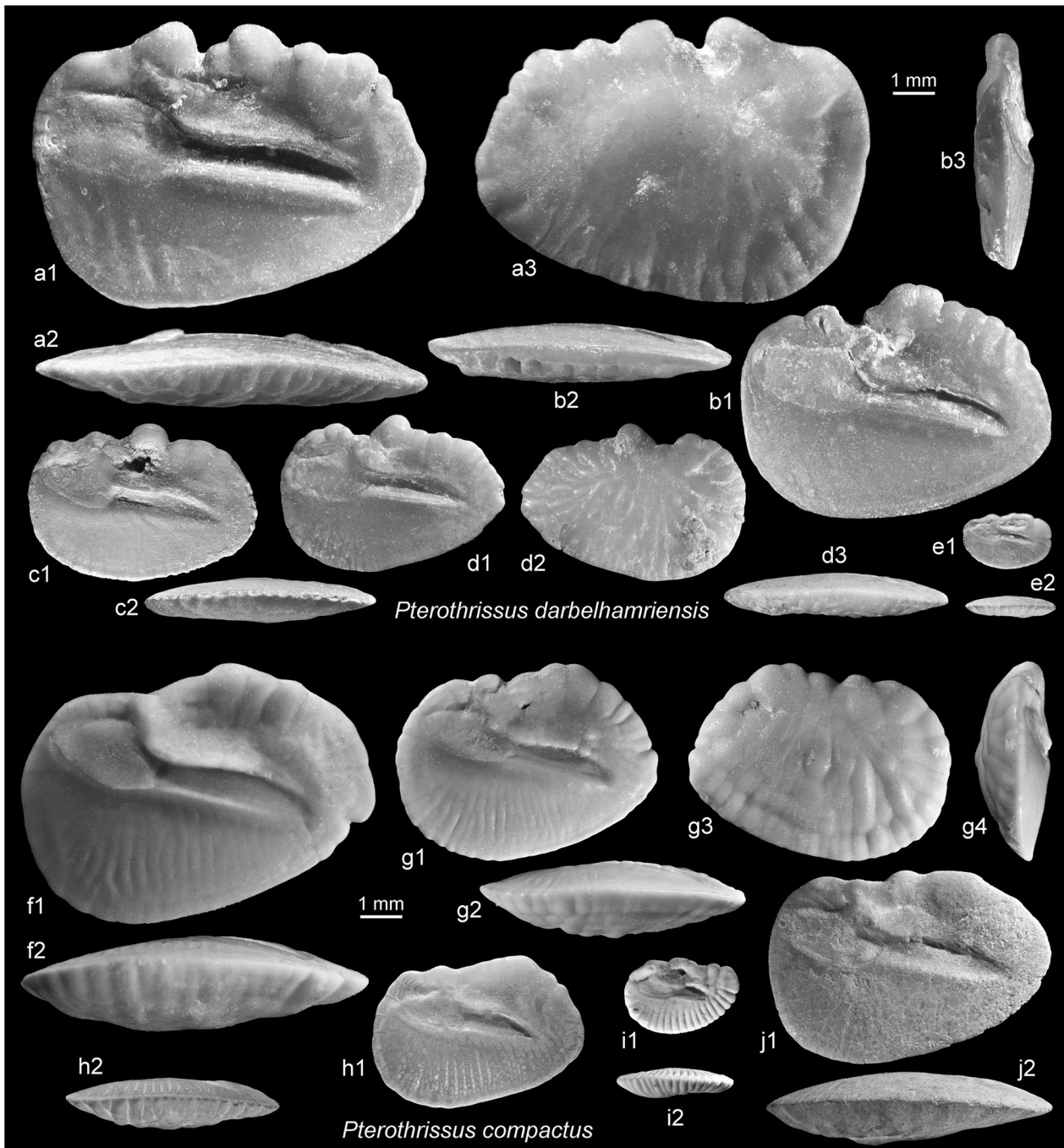


Fig. 9 Pterothrissidae. **a–e**, *Pterothrissus darbelhamriensis* Schwarzahns, 1981, Dar bel Hamri, Zanclean; **a** holotype, SMF P 6234; paratypes, **b** SMF 6235 (reversed), **d** SMF P 6237 (reversed), **e** SMF P 6236; **c** Asilah, coll. WWS. **f–j** *Pterothrissus compactus* Schwarzahns, 1981, Le Puget, southern France, Zanclean; **f** holotype, SMF P 6239; paratypes, **g** SMF P 6240, **i** SMF P 6243 (reversed); **h**, **j** (reversed), MGPT-PU 139453, Stazzano, Piedmont, Italy, Tortonian

Systematic paleontology

Class Osteichthyes Huxley, 1880

Subclass Actinopterygii sensu Goodrich, 1930

Division Teleostei Müller, 1846

Order Albuliformes Jordan, 1923

Family Pterothrissidae Gill, 1893

Genus *Pterothrissus* Hilgendorf, 1877

Pterothrissus darbelhamriensis Schwarzhans, 1981

Figure 9a–e

1981 *Pterothrissus darbelhamriensis*—Schwarzhans: Figs. 6–8.

1997 *Pterothrissus darbelhamriensis* Schwarzhans, 1981—Nolf & Marques da Silva: pl. 1, Figs. 1–3.

2022 *Pterothrissus darbelhamriensis* Schwarzhans, 1981—van Hinsbergh & Hoedemakers: pl. 1, Fig. 1.

Material 80 specimens, Zanclean, 79 from Dar bel Hamri (refigured holotype SMF P6234, and refigured paratypes SMF P6235–6237) and one from Asilah.

Discussion *Pterothrissus darbelhamriensis* is known from the Zanclean and Piacenzian of Atlantic Morocco and Portugal and has recently also been found in the Piacenzian of Estepona near Málaga, Andalusia, Spain by van Hinsbergh & Hoedemakers. It differs from the coeval Mediterranean species *P. compactus* Schwarzhans, 1981 in the thinner appearance and the rectangular outline. Otoliths of *P. compactus* from the Zanclean of Le Puget, southern France (Fig. 9f–g, j) and from the Tortonian of Stazzano, Piedmont, Italy (Fig. 9h, j) are figured for comparison.

Order Anguilliformes Regan, 1909

Family Heterenchelyidae Regan, 1912

Genus *Panturichthys* Pellegrin, 1913

Panturichthys cf. *fowleri* (Ben-Tuvia, 1953)

Figure 10a–d

1980 *Panturichthys subglaber* (Schubert, 1906)—Nolf & Martinell, pl. 1 Figs. 3, 6 (4, 5?).

1989 *Panturichthys subglaber* (Schubert, 1906)—Nolf & Cappetta: pl. 1, Fig. 8.

1998 *Panturichthys subglaber* (Schubert, 1906)—Nolf, Mané & Lopez, pl. 1, Fig. 4.

2020 *Panturichthys* sp.—Agiadi & Albano: Figs. 4.3.

2022 *Panturichthys subglaber* (Schubert, 1906)—van Hinsbergh & Hoedemakers: pl. 1, Fig. 3.

Material 4 specimens SMF PO 101.184, Zanclean, Dar bel Hamri.

Discussion Heterenchelyid otoliths have a simplified otolith morphology with an oval shape, a convex inner face, a nearly flat outer face, and an essentially unstructured shallow sulcus that closely approaches the anterior rim or opens to it. The specimens found in the Pliocene of the Mediterranean have traditionally been placed in *P. subglaber* (Schubert, 1906), which was originally described from the Middle Miocene of Austria. However, the Pliocene otoliths differ in being more slender (OL:OH=1.45–1.6 vs. 1.3–1.4), in the lack of a rostrum (vs. present in most other cases), and in a shorter sulcus (OL:SuL=1.5–1.75 vs. 1.4–1.5). Instead, the Pliocene otoliths match well with an otolith figured as *Panturichthys* sp. from the Holocene off Lebanon (Agiadi & Albano, 2020) and an otolith of the extant *P. fowleri*, which I had the opportunity to investigate in the collection of IRSNB courtesy of D. Nolf (Bruges). Otoliths of *P. mauretanicus* Pellegrin, 1930, an extant species living at the Northwest African shelf are more compressed (OL:OH=1.35 vs. 1.45–1.6) (for figures see Nolf, 2013). Two further extant species occur along the tropical West African coast chiefly south of the equator are *P. isognathus* Poll, 1953 and *P. longus* (Ehrenbaum, 1915). Their otoliths are not known. An otolith identified as *Panturichthys* sp. in Schwarzhans (2013a) from dredges in the Gulf of Guinea may represent one of the two species and is distinguished by its very short, narrow and tapering sulcus. In the light of the occurrence of this morphotype in the Early Pliocene of the Mediterranean as well, all Pliocene records, including the finds in Morocco, may represent the extant *P. fowleri* except for two figured specimens in Nolf and Martinell (1980), which are more compressed but cannot be evaluated based on the documentation. Because of some remaining uncertainty related to the fact that no otoliths are known of the two

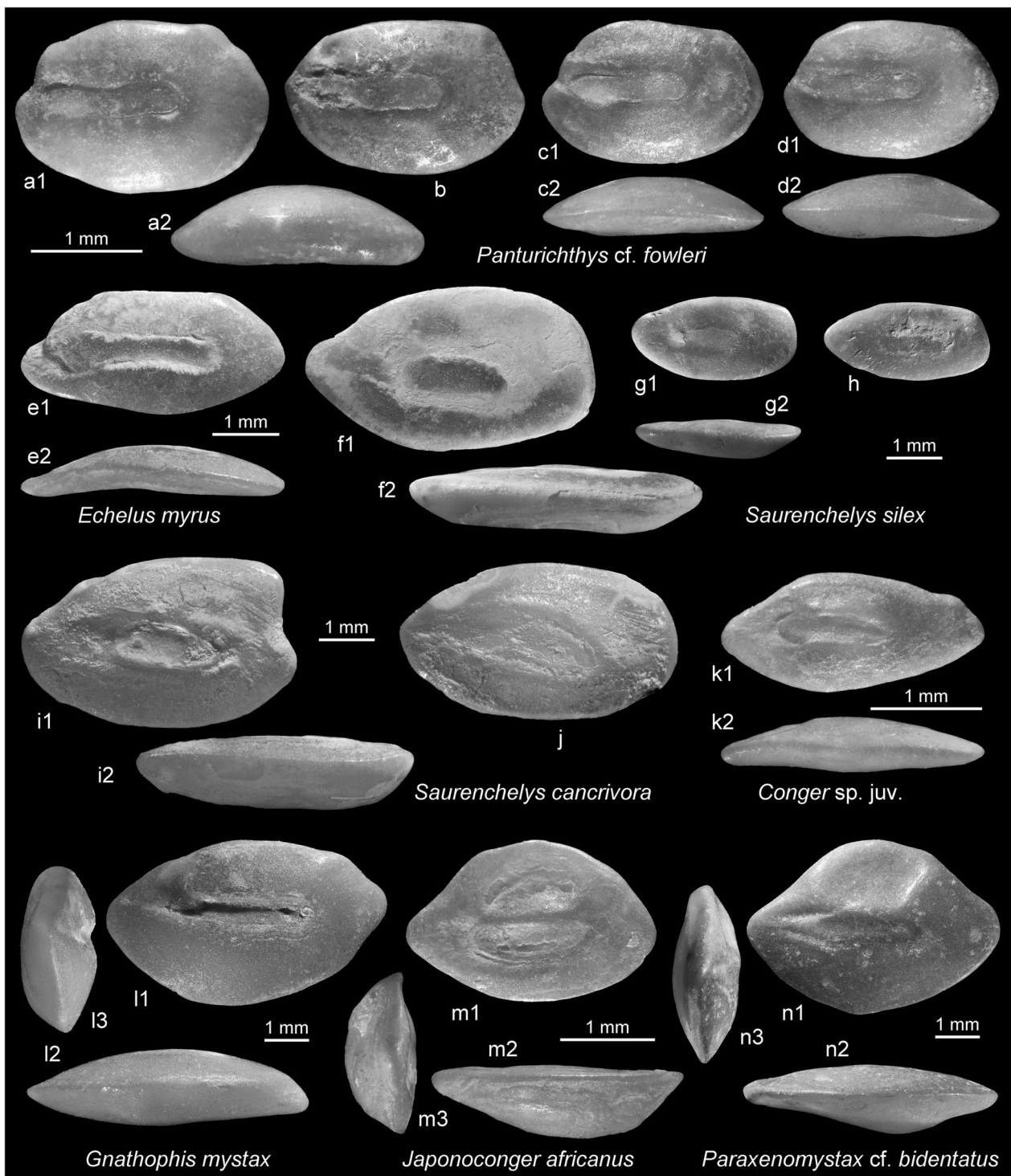


Fig. 10 Anguilliformes. **a–d** *Panturichthys cf. fowleri* (Ben-Tuvia, 1953), SMF PO 101.184 (**a** reversed), Dar bel Hamri. **10e**, *Echelus myrus* (Linnaeus, 1758), SMF PO 101.216 (reversed), Dar bel Hamri. **f–h**, *Saurenehelys silex* van Hinsbergh & Hoedemakers, 2022, Dar bel Hamri, Zanclean, **f** SMF PO 101.186, **g–h** tentatively assigned specimens, SMF PO 101.815 (reversed). **i–j**, *Saurenehelys cancrivora* Peters, 1864, extant, West Pacific, **i** BSKU 69087, **j** BSKU 75296. **k**, *Conger* sp. juv., SMF PO 101.187 (reversed), Dar bel Hamri. **l**, *Gnathophis mystax* (Delaroche, 1809), SMF PO 101.188 (reversed), Dar bel Hamri. **m**, *Japonoconger africanus* (Poll, 1953), SMF PO 101.189 (reversed), Dar bel Hamri. **n**, *Paraxenomystax cf. bidentatus* Reid, 1940, SMF PO 101.273, Dar bel Hamri

extant tropical West African species, I describe the Pliocene otoliths as *P. cf. fowleri*.

Family Ophichthidae Rafinesque, 1815

Genus *Echelus* Rafinesque, 1810

Echelus myrus (Linnaeus, 1758)

Figure 10e

2022 *Echelus myrus* (Linnaeus, 1758)—van Hinsbergh & Hoedemakers: pl. 1, Fig. 5.

Material 1 specimen SMF PO 101.216, Zanclean, Dar bel Hamri.

Family Nettastomatidae Bleeker, 1864

Genus *Saurenehelys* Peters, 1864

Saurenehelys silex van Hinsbergh & Hoedemakers, 2022

Figure 10f–h

2022 *Saurenehelys silex*—van Hinsbergh and Hoedemakers: pl. 1, Figs. 7, 8.

Material 2 specimens SMF PO 101.185 (Fig. 10f) and 2 juvenile specimens SMF PO 101.186 (Fig. 10g–h), Zanclean, Dar bel Hamri.

Description Small otoliths up to 3 mm in length are slender ($OL:OH=2.0–2.15$), specimens from 4 to 6 mm in length are more compressed ($OL:OH=1.65–1.8$); $OH:OT=2.1–2.2$. Dorsal and ventral rims shallow, regular. Anterior tip slightly pointed; posterior tip blunt with rounded angles at junction with dorsal and ventral rims. All rims smooth.

Inner face flat with slightly inclined, centrally positioned, elongate oval and shallow sulcus filled with a single colliculum. $OL:SuL=2.5–2.6$. Sulcus not extending anterior of colliculum. No dorsal depression and no ventral furrow. Outer face smooth, moderately convex, thickest behind the middle.

Discussion Nettastomatid otoliths show a low degree of morphological diversity, which renders identification difficult. Otoliths of representatives of all extant genera in the family are figured in Schwarzhans (2019b). Those of *Saurenehelys* most closely resemble in otolith and sulcus shape. *Saurenehelys cancrivora* Peters 1864 is the only

extant species in the genus occurring off West Africa (and in the Indo-West Pacific). Two extant otoliths figured (Fig. 10i, j) show a distinct variability in the shape of the postdorsal angle, which is pronounced in one specimen (Fig. 10i) and completely rounded in the other (Fig. 10j). The index $OL:OH$ ranges from 1.62 to 1.75. *Saurenehelys silex* described by van Hinsbergh & Hoedemakers, 2022, from the Piacenzian of Estepona near Málaga, Spain shows similar proportions in specimens of 4–5.5 mm in length, which is also matched with large specimens from Dar bel Hamri (Fig. 10e), but differs in the deepened ventral rim and the posterior thickening of the outer face. Two smaller specimens (3 mm in length) from Dar bel Hamri, however, are considerably more slender in shape and could potentially represent a second species. However, it is likely that this difference is due to allometric ontogenetic growth. Despite the lack of specimens of intermediate sizes the small specimens are, therefore, also placed in *S. silex*.

Family Congridae Kaup, 1856

Genus *Conger* Bosc, 1817

Conger sp. juv.

Figure 10k

Material 5 small specimens the largest being 2.3 mm in length from the Zanclean of Dar bel Hamri (figured specimen SMF PO 101.187).

Discussion These are typical otoliths of the genus *Conger* but too small in size for a specific identification and probably stem from juvenile fishes.

Genus *Gnathophis* Kaup, 1859

Gnathophis mystax (Delaroche, 1809)

Figure 10l

2017 *Gnathophis mystax* (Delaroche, 1809)—Lin et al.: pl. 2, Fig. 2j, K.

2022 *Gnathophis mystax* (Delaroche, 1809)—van Hinsbergh and Hoedemakers: pl. 3, Figs. 1, 2.

Material 2 specimens, Zanclean, Dar bel Hamri (SMF PO 101.188).

Discussion An extant species that has been recorded in the Mediterranean since Late Miocene. A second, extinct

species (*Gnathophis kanazawai* Nolf & Martinell, 1980) was described from the Early Pliocene of Catalonia, Spain.

Genus *Japonoconger* Asano, 1958

Japonoconger africanus (Poll, 1953)

Figure 10m

2019b *Japonoconger africanus* (Poll, 1953)—Schwarzhans: pl. 6, Figs. 11, 12.

2022 *Japonoconger africanus* (Poll, 1953)—van Hinsbergh & Hoedemakers: pl. 3, Figs. 12–14 (see there for further references).

Material 1 specimen, Zanclean, Dar bel Hamri (SMF PO 101.189).

Discussion *Japonoconger africanus* today is found at a depth of 250–650 m off tropical West Africa from Gabon to Angola. During the Pliocene, it was much more widely distributed and has regularly been reported from the Mediterranean and now also from Atlantic Morocco. In all these fossil locations, however, it is rare, except for the Piacenzian of Estepona near Málaga, Spain (van Hinsbergh & Hoedemakers, 2022).

Genus *Paraxenomystax* Reid, 1940

Paraxenomystax cf. *bidentatus* Reid, 1940

Figure 10n

Material 2 specimens, Zanclean, Dar bel Hamri (SMF PO 101.273).

Discussion *Paraxenomystax* is commonly recorded as a junior synonym of *Xenomystax* Gilbert, 1891 (see Fricke et al. 2022). The otoliths of the type species *P. bidentatus* show a centrally positioned colliculum with an anterior spur and thus differ from those of other *Xenomystax* species (see Lin et al., 2017 and Schwarzhans, 2019b for extant otoliths). I, therefore, keep *Paraxenomystax* provisionally valid here. The single extant species, *Paraxenomystax bidentatus* is only known from the tropical West Atlantic. The fossil record from Morocco is only tentatively placed in the extant species because of the geographic difference and only two specimens being available from Morocco.

Genus *Rhynchoconger* Jordan & Hubbs, 1925

Rhynchoconger pantanellii (Bassoli & Schubert, 1906)

Figure 11d–e

1906 *Otolithus* (*Ophidiidarum*) *pantanellii*—Bassoli & Schubert (in Bassoli): pl. 1, Figs. 41–42.

1983 *Hildebrandia pantanellii* (Bassoli & Schubert, 1906)—Nolf & Steurbaut: pl. 1, Figs. 4–9 (see there for further references)

1989 *Hildebrandia pantanellii* (Bassoli & Schubert, 1906)—Nolf & Cappetta: pl. 2, Figs. 1–4.

2013a *Rhynchoconger pantanellii* (Bassoli & Schubert, 1906)—Schwarzhans: pl. 1, Fig. 14.

2017 *Rhynchoconger pantanellii* (Bassoli & Schubert, 1906)—Lin et al.: Fig. 2F.

2022 *Rhynchoconger pantanellii* (Bassoli & Schubert, 1906)—van Hinsbergh & Hoedemakers: pl. 3, fig. 16.

Material 117 specimens, Zanclean, 116 from Dar bel Hamri (figured specimens SMF PO 101.190) and one from Asilah.

Discussion *Rhynchoconger pantanellii* is relatively common and widely recorded from the Tortonian to the Zanclean of the Mediterranean and the Zanclean of Atlantic Morocco. No extant species of *Rhynchoconger* have been recorded from the East Atlantic, but Smith (1990, in Quéro et al.) mentioned unidentified larval *Rhynchoconger* specimens from the Gulf of Guinea to Angola. Schwarzhans (2013a) found *Rhynchoconger* otoliths from adult specimens in dredged sediments of Holocene age off Ivory Coast that indicate that an extant eastern Atlantic species of *Rhynchoconger* indeed exists and that it closely resembles the fossil *R. pantanellii*.

Rhynchoconger carnevalei n. sp.

Figure 11a–c

1978a *Gnathophis* sp.—Schwarzhans: Figs. 55, 139.

Holotype SMF PO 101.191 (Fig. 11b), Agrigento, below Rupe Athenae, Sicily, Italy, Zanclean.

Paratype Two specimens: one specimen MGPT-PU 130452, Borelli, Piedmont, Italy, late Tortonian; one

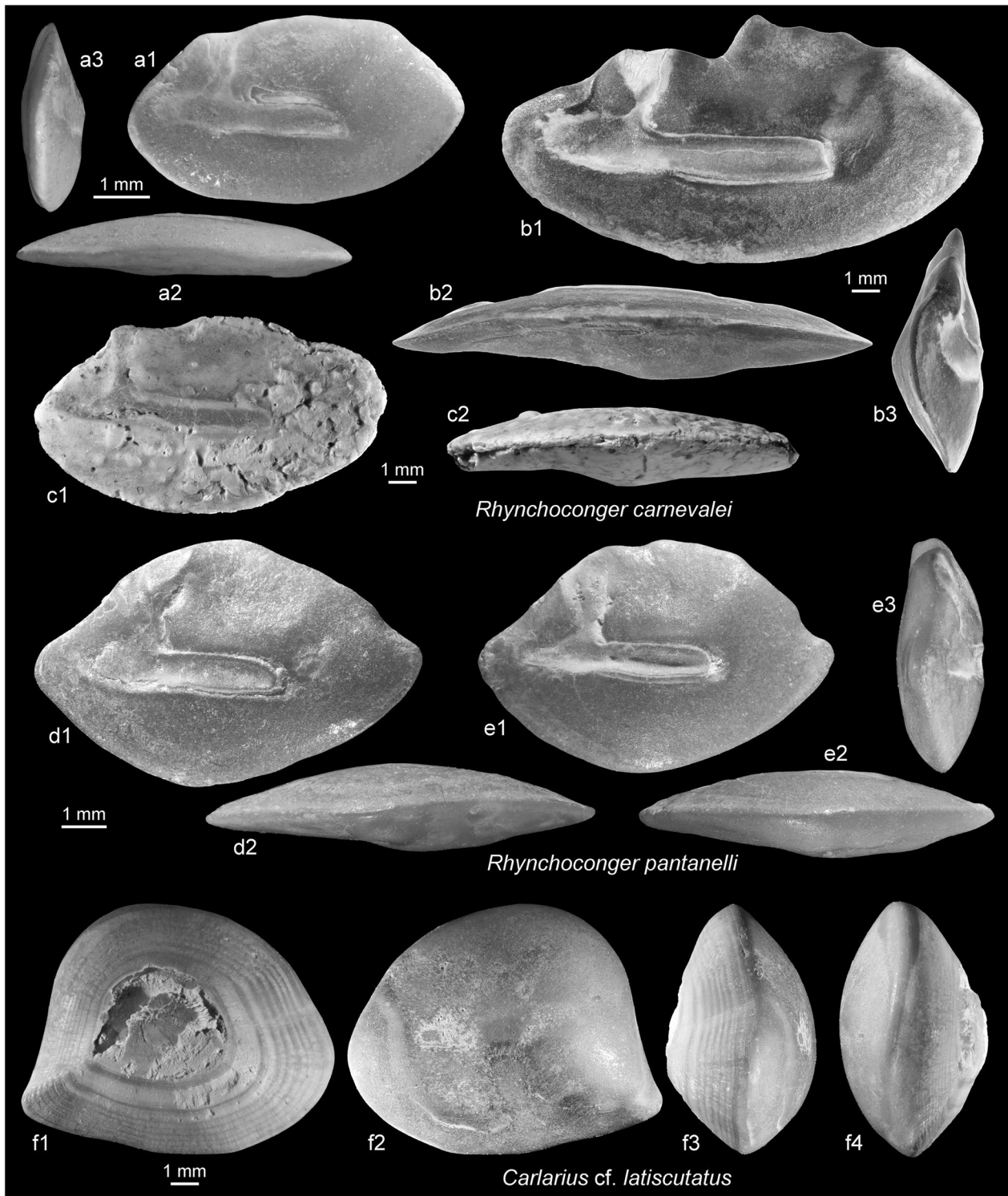


Fig. 11 Anguilliformes and Siluriformes. **a–c** *Rhynchoconger carnevalei* n. sp. 10a paratype, MGPT-PU 130,452 (reversed), Borelli, Piedmont, Italy, late Tortonian, **b** holotype, SMF PO 101.191, Agrigento, Sicily, Italy, Zanclean, **c** paratype, SMF PO 101.336 (reversed), Orciano near Pisa, Italy, Zanclean. **d**, **e** *Rhynchoconger pantanelli* (Bassoli & Schubert, 1906), SMF PO 101.190 (**e** reversed), Dar bel Hamri. **f** *Carlarius cf. latiscutatus* (Günther, 1864), SMF PO 101.192, Dar bel Hamri

specimen SMF PO 101.336, Orciano near Pisa, Tuscany, Italy, Zanclean.

Etymology In honor of Giorgio Carnevale, Torino, Italy, for his many contributions to the understanding of fossil bony fishes.

Diagnosis OL:OH=1.8–2.1; OH:OT=2.5–3.1. Dorsal rim anteriorly depressed and generally low; ventral rim shallow, regularly curved. Ostium closely approaching anterior rim of otolith.

Description Slender, large, elegant otoliths reaching sizes of 17 mm in length (holotype). OL:OH=1.8–2.1, increasing with size; OH:OT=2.5–3.1, decreasing with size. Dorsal rim shallow, anteriorly depressed and irregular, highest behind middle of otolith. Ventral rim shallow, smooth and very regularly curved. Anterior tip rounded, posterior tip slightly tapering.

Inner face convex, with a long, nearly horizontal and relatively narrow sulcus. Ostium marked against cauda at ventral sulcus rim by slight indentation, its anterior tip reaching close to anterior rim of otolith. Ostial channel narrow, short, positioned perpendicular on rear part of ostium. Cauda narrow, straight. Single colliculum contiguous from ostium, including ostial channel and cauda. OL:SuL=1.6–1.7; CaL:OsL=1.3–1.4. Dorsal depression narrow, relatively shallow and with indistinct margins; no ventral furrow. Outer face smooth, flat or with moderate central umbo.

Discussion The presence of a second species of *Rhynchoconger* in the young Neogene of the Mediterranean was already recognized by Schwarzhans (1978a), who refrained from describing a new species based on a single large specimen. With the finding of two additional specimens of smaller and intermediate size, it is now clear that the morphological characteristics are stable through ontogeny. The species is much rarer than *R. pantanellii* and differs mainly in being distinctly more elongate (OL:OH=1.8–2.1 vs. <1.6), the depressed predorsal rim and the ostium approaching the anterior rim of the otolith more closely than in *R. pantanellii*. Its stratigraphic range in the Mediterranean reaches from the late Tortonian to the Zanclean. It is described here because it is considered relevant for the faunal evaluation discussed later.

Order Clupeiformes Bleeker, 1859

Family Clupeidae Rafinesque, 1810

Material Three clupeid otolith fragments from Dar bel Hamri that cannot be identified to genus or species level.

Order Siluriformes Cuvier, 1817

Family Ariidae Bleeker, 1862

Genus *Carlarius* Marceniuk & Menezes, 2007

Carlarius cf. *latiscutatus* (Günther, 1864)

Figure 11f

Material 2 specimens, SMF PO 101.192, Dar bel Hamri, Zanclean.

Discussion The two, large, and thick otoliths of 11.4 and 12.4 mm in length resemble closely the extant specimen figured by Veen and Hoedemakers (2005; pl. 2, Fig. 2). The outline of the otolith and its proportions match well, but Veen & Hoedemakers did not figure the ventral face with the diagnostic sulcus-like mesial depression and the mesial inward curve (terminology of Ohe in Aguilera et al., 2013). In the case of the specimen from Morocco, this inward curve is relatively long and narrow and only slightly inclined, which would probably represent a distinctive feature. Therefore, this specimen is only tentatively placed in *C. latiscutatus*. Today, *C. latiscutatus* occurs south of the northwest African upwelling system from Senegal to Angola.

Order Myctophiformes Regan, 1911

Family Myctophidae Gill, 1893

Subfamily Myctophinae Fowler, 1925

Genus *Hygophum* Bolin, 1939

Hygophum cf. *hygomi* (Lütken, 1892)

Figure 12d

Material 2 fragmented specimens, SMF PO 101.193, Dar bel Hamri, Zanclean.

Discussion The figured specimen lacks most of the dorsal portion but is the better preserved one of the two fragments. The regularly curved and somewhat undulating ventral rim is similar to the appearance in extant otoliths of *H. hygomi*. This species has commonly been recorded from the Mediterranean Pliocene following the synonymization of the fossil otolith-based *Hygophum*

agrigentense Schwarzhans, 1978, with the extant *H. hygomi* by Brzobohatý and Nolf (1996). It is likely that the specimens from Dar bel Hamri represent the same species.

Genus *Myctophum* Rafinesque, 1810

Myctophum fitchi (Schwarzhans, 1978)

Figure 12c.

1978a *Gymnoscopelus fitchi*—Schwarzhans: Figs. 30, 31, 129.

2022 *Myctophum fitchi* (Schwarzhans, 1978)—Carnevale & Schwarzhans: Fig. 8I–K (see there for further references).

2022 *Myctophum fitchi* (Schwarzhans, 1978)—van Hinsbergh & Hoedemakers: pl. 12, Figs. 19–25.

Material 4 specimens, Zanclean, 2 specimens Dar bel Hamri (SMF PO 101.194), 1 specimen Jebel Zebbouj, 1 specimen Asilah.

Subfamily Lampanyctinae Paxton, 1972

Genus *Ceratoscopelus* Günther, 1864

Ceratoscopelus maderensis (Lowe, 1839)

Figure 12e

1971 *Ceratoscopelus maderensis* (Lowe, 1839)—Weiler: pl. 1, Fig. 10.

1978a *Ceratoscopelus maderensis* (Lowe, 1839)—Schwarzhans: Figs. 33–35, 37.

1986 *Ceratoscopelus maderensis* (Lowe, 1839)—Schwarzhans: Fig. 22.

1989 *Ceratoscopelus maderensis* (Lowe, 1839)—Nolf & Cappetta: pl. 6, Figs. 17–20.

Material 1 specimen, SMF PO 101.195, Dar bel Hamri, Zanclean.

Genus *Lampanyctus* Bonaparte, 1840

Lampanyctus sp.

Figure 12f

Material 2 specimens, SMF PO 101.196, Dar bel Hamri, Zanclean.

Discussion Small and high-bodied otoliths that resemble *Lampanyctus latesulcatus* Nolf & Steurbaut, 1983, from the Tortonian of Italy. The specimens from Dar bel Hamri differ slightly in the caudal pseudocolliculum extending beyond the entire cauda, while it is posteriorly reduced in *L. latesulcatus*. They may thus represent a different species. Van Hinsbergh and Hoedemakers (2022) identified the extant *L. crocodilus* and *L. photonotus* from the Piacenzian and the latter also from the Zanclean of Estepona near Málaga, Spain.

Subfamily Diaphinae Paxton, 1972 (sensu Martin et al. 2018)

Genus *Diaphus* Eigenmann & Eigenmann, 1891

Diaphus adenomus Gilbert, 1905

Figure 12g

2022 *Diaphus adenomus* Gilbert, 1905—van Hinsbergh & Hoedemakers: pl. 11, Figs. 9–11 (see there for further references).

Material 4 specimens SMF PO 101.274, Dar bel Hamri, Zanclean.

Diaphus cavallonis Brzobohatý & Nolf, 2000

Figure 12h–l

2000 *Diaphus cavallonis*—Brzobohatý & Nolf: pl. 5, Figs. 7–14 (see there for further references).

2017 *Diaphus cavallonis* Brzobohatý & Nolf, 2000—Agadi et al.: Fig. 5.14.

2022 *Diaphus cavallonis* Brzobohatý & Nolf, 2000—Carnevale & Schwarzhans: Fig. 7I (see there for further references after 2000).

?2022 *Diaphus cavallonis* Brzobohatý & Nolf, 2000—Agathangelou et al.: Fig. 3A.

2022 *Diaphus cavallonis* Brzobohatý & Nolf, 2000—van Hinsbergh & Hoedemakers: pl. 8, Figs. 7–18.

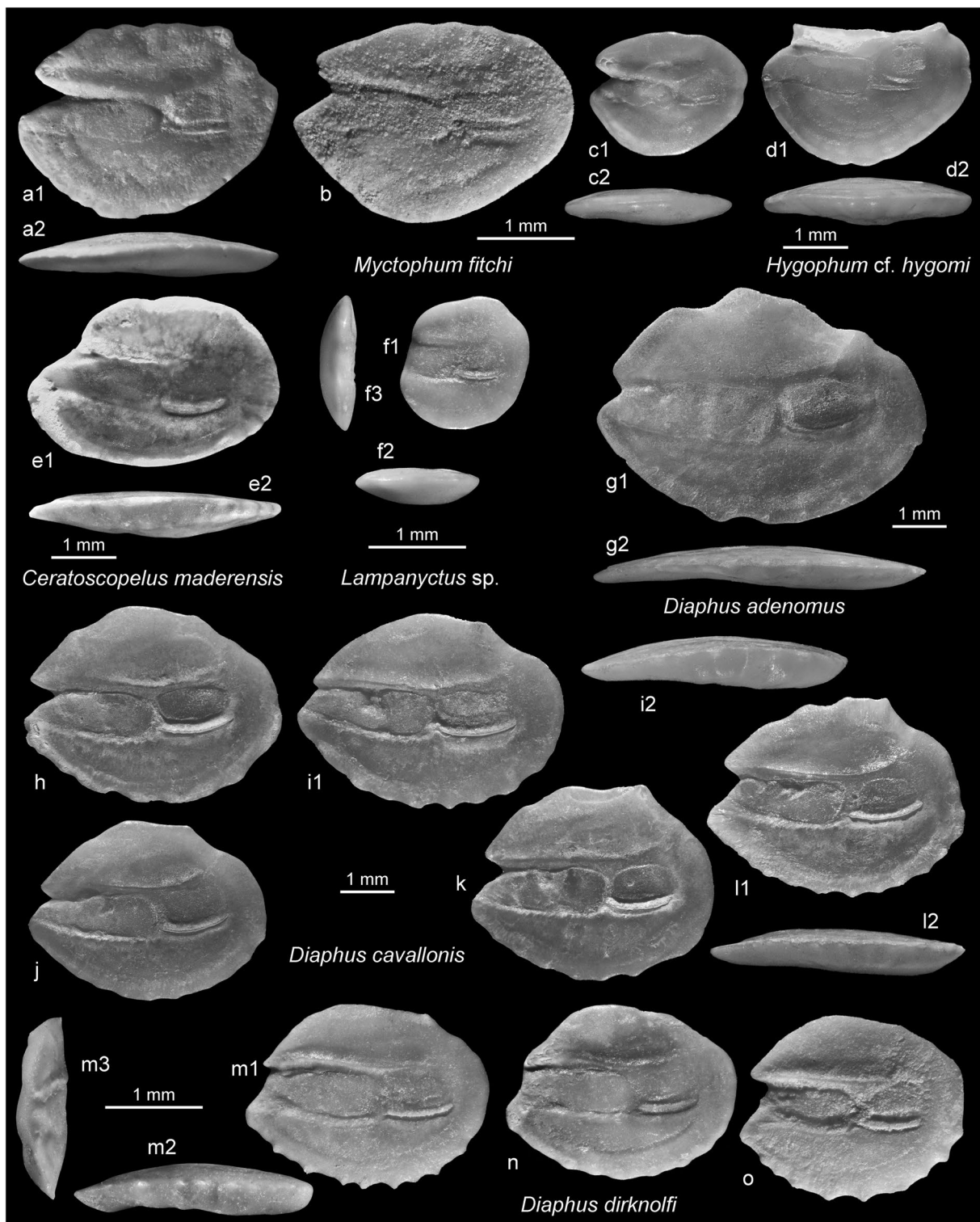


Fig. 12 Myctophidae. **a–c** *Myctophum fitchi* (Schwarzahns, 1978), **a, c** SMF PO 101.194 (**a** reversed), Dar bel Hamri, **b** Asilah, **d**, *Hygophum* cf. *hygomi* (Lütken, 1892), SMF PO 101.193, Dar bel Hamri. **e** *Ceratoscopelus maderensis* (Lowe, 1839), SMF PO 101.195, Dar bel Hamri. **f**, *Lampanyctus* sp. SMF PO 101.196, Dar bel Hamri. **g**, *Diaphus adenomus* Gilbert, 1905, SMF PO 101.274 (reversed), Dar bel Hamri. **h–l** *Diaphus cavalloni* Brzobohatý & Nolf, 2000, SMF PO 101.197 (**j** reversed), Dar bel Hamri. **m–o** *Diaphus dirknolfi* Schwarzahns, 1986, **n** SMF PO 101.198, Dar bel Hamri, **m, o** SMF PO 101.199, Sidi Mohammed ech Chleuh

Material 146 specimens, figured specimens SMF PO 101.197, Dar bel Hamri, Zanclean.

Discussion *Diaphus cavallonis* has 8 to 12 delicate denticles along the ventral rim, according to van Hinsbergh and Hoedemakers (2022), based on more than 1000 specimens from Spain. Schwarzhans & Aguilera (2013) noted 10 to 12 denticles on much fewer specimens, which may reflect the predominant range. In the case of the Moroccan specimens, the denticles are eroded except for few specimens (e.g., Fig. 10i, k, l), which show 8–11 denticles. The Moroccan specimens show a considerable variability in respect to the predorsal rim which can be shallow (Fig. 12l) or expanded (Fig. 12h, i), the shape of the posterior rim which can be rounded (Fig. 12i) or relatively blunt (Fig. 12l) and the opening of the ostium. The variability appears to be within the range observed in the types of Brzobohatý and Nolf (2000) and figures shown in Schwarzhans & Aguilera (2013) and van Hinsbergh and Hoedemakers (2022). The specimens currently available to me do not warrant a further investigation of the nature of the species but indicate that a detailed review of its morphologic limit may be required. *Diaphus cavallonis* was apparently widely distributed in the North Atlantic and the Mediterranean during the Zanclean; the oldest records in the Mediterranean date from the Tortonian (Lin et al., 2015, 2017). Van Hinsbergh and Hoedemakers (2022) found that *D. cavallonis* is lacking in the Piacenzian of the Mediterranean and instead is replaced by *D. postcavallonis* van Hinsbergh & Hoedemakers, 2022. In contrast, Agathangelou et al. (2022) reported *D. cavallonis* from the Piacenzian of Cyprus. *Diaphus cavallonis* is the second largest *Diaphus* species in Dar bel Hamri, reaching 5 mm in length, surpassed only by *D. adenomus* (see above) with 6 mm in length.

***Diaphus dirknolfi* Schwarzhans, 1986**

Figure 12m–o

1986 *Diaphus dirknolfi*—Schwarzhans: pl. 3, Figs. 34, 35.

2022 *Diaphus dirknolfi* Schwarzhans, 1986—Carnevale & Schwarzhans: Fig. 7 J–P (see there for further references).

2022 *Diaphus dirknolfi* Schwarzhans, 1986—van Hinsbergh & Hoedemakers: pl. 11, Figs. 4–8.

Material 90 specimens, Zanclean: 84 specimens Dar bel Hamri (figured specimen SMF PO 101.198), 4 specimens Sidi Mohamed ech Chleuh (SMF PO 101.199), 2 specimens Asilah.

Discussion *Diaphus dirknolfi* was originally established on specimens from Dar bel Hamri with incompletely preserved denticles along the ventral rim, which resulted in a too high count of 12–14 denticles. The species was redefined in 2022 by Carnevale and Schwarzhans (2022) based on better preserved specimens from the type locality and the nearby location Sidi Mohammed ech Chleuh, which yielded uneroded specimens. The recount of the denticles along the ventral rim resulted in 6–8. Van Hinsbergh and Hoedemakers (2022) reported 7–11 denticles. These records show that the number of denticles is quite variable in this species, but mostly seems to fall in the range of 7–9. Obviously, this characteristic cannot be used as a distinguishing trait between *D. dirknolfi*, the Early to Middle Miocene *D. hataii* (Ohe & Araki, 1973), and the extant *D. dumerilii* (Bleeker, 1856), but other characteristics such as the proportional length of rostrum to antirostrum and the proportions of ostium and cauda remain valid (see Carnevale & Schwarzhans, 2022, for details). *Diaphus dirknolfi* is known from the latest Messinian (Lago Mare interval) to the Piacenzian of the Mediterranean and the Zanclean of Morocco.

***Diaphus draconis* Schwarzhans, 2013**

Figure 13a–c

2013c *Diaphus draconis*—Schwarzhans: pl. 4, Fig. 8–12.

2019a *Diaphus draconis* Schwarzhans, 2013—Schwarzhans: Fig. 57.1–3.

2022 *Diaphus* cf. *draconis* Schwarzhans, 2013—Carnevale & Schwarzhans: Fig. 7Q–T.

Material 3 specimens Kef Nsour, Messinian (SMF PO 101.200), 5 specimens Sidi Mohamed ech Chleuh, Zanclean, possibly reworked from Messinian.

Discussion *Diaphus draconis* is an inconspicuous small species reaching about 2 mm in length in the Moroccan localities. It can be easily confused with small specimens of larger species (see extensive discussion in Carnevale & Schwarzhans, 2022). It may be recognized best by its 4–6 widely spaced strong denticles along the ventral rim. *Diaphus draconis* was originally described from the Serravalian/Tortonian of Gabon (Schwarzhans, 2013c) and also recorded from the Tortonian of New Zealand (Schwarzhans, 2019a), indicating a wide geographic distribution. Specimens from the latest Messinian Lago Mare phase of Italy were only tentatively allocated (Carnevale & Schwarzhans, 2022). In the Rharrb Basin of Morocco, the

best preserved specimens were obtained from the basal levels of Kef Nsour, which are supposed to be Messinian in age. Specimens from the basal level of Sidi Mohamed ech Chleuh are slightly leached, possibly indicating an origin from reworked Messinian strata below. There are no positive records from the Zanclean.

Diaphus maghrebensis n. sp.

Figure 13d–j

2022 *Diaphus taaningi* Norman, 1930—van Hinsbergh & Hoedemakers: pl. 8, Figs. 1–5.

Holotype SMF PO 101.201 (Fig. 13f), Dar bel Hamri, coquina at river level of Oued Beth, Zanclean.

Paratype 7 specimens, 4 specimens SMF PO 101.202, Dar bel Hamri, Zanclean, 1 specimen SMF PO 101.203, Kef Nsour, Messinian, 2 specimens SMF PO. 101.204, Sidi Mohamed ech Cleuch, Zanclean.

Further material 291 specimens, 23 Kef Nsour and Chaba Kaudiat el Mogen, Messinian, 213 specimens Dar bel Hamri, Zanclean, 38 specimens Sidi Mohamed ech Chleuh, Zanclean, 17 specimens Jebel Zebbouj, Zanclean.

Etymology After Maghreb, the name of the northwestern region of Africa.

Diagnosis OL:OH=1.1–1.2; OH:OT=3.25–3.35. Ventral rim regularly and deeply curved, with 6–9 denticles. OCL:CCL=1.95–2.7. Inner face convex; outer face with distinct postcentral umbo.

Description Relatively small otoliths reaching sizes of 2.5 mm in length (holotype 2.3 mm). Dorsal rim high, regularly curved or anteriorly expanded; posteriorly rounded or with mild, short depression. Ventral rim deep, regularly curved, with 6–9 denticles (mostly 7–8). Rostrum slightly longer than antirostrum, 8–15% of OL, ratio rostrum to antirostrum about 2:1. Posterior rim broadly rounded, blunt.

Inner face distinctly convex in horizontal direction, less bent in vertical direction. Sulcus long, slightly supra-median, shallow, straight, OL:SuL=1.25–1.35. Ostium slightly wider than cauda and twice to 2.5 times the length of the cauda (OCL:CCL=1.95–2.7). Upper margin of ostium straight. Cauda short, with equally long caudal pseudocolliculum. Dorsal depression wide; ventral furrow mostly distinct, relatively close to ventral rim of otolith. Outer face relatively smooth, with distinct, broad postcentral umbo.

Discussion Many small and somewhat inconspicuous otoliths from the Miocene and Pliocene from the Mediterranean and Paratethys have been placed in the extant *Diaphus taaningi* Norman, 1930, by Brzobohatý and Nolf (2000). *Diaphus taaningi* is a pseudoceanic species occurring in the tropical West and East Atlantic (Froese & Pauly, 2022). In dredge samples from the Gulf of Guinea and in a comparative morphological study of extant otoliths of the genera *Diaphus*, *Idiolychnus*, and *Lobianchia*, Schwarzahans (2013a, 2013b) figured several extant otoliths of *D. taaningi* from both areas of its distribution and found slight but consistent differences between the West and East Atlantic populations. Schwarzahans & Aguilera (2013) concluded on this basis that none of the fossil otoliths figured as *D. taaningi* until then actually pertains to this species and also figured presumably valid *D. taaningi* otoliths from the Gelasian of Atlantic Panama. More recently, van Hinsbergh and Hoedemakers (2022) figured, without description or explanation, *Diaphus taaningi* otoliths from the Zanclean and Piacenzian of Estepona near Málaga, Spain.

In the late Tortonian/early Messinian and Zanclean of the locations in the Rharb Basin of Morocco studied here, the otoliths of *Diaphus maghrebensis* represent the most common myctophid species. They clearly represent the same species as the otoliths figured by van Hinsbergh & Hoedemakers as *D. taaningi* from Estepona near Málaga, but reach larger sizes (2.5 mm in length vs. <2 mm). Therefore, I assume that these otoliths from Morocco represent true adult forms of the species in question. In many aspects, they resemble extant *D. taaningi* otoliths (Fig. 13k–m), which reach nearly 3 mm in length, but they also differ in some consistent aspects as follows (*D. maghrebensis* first, *D. taaningi* second): OH:OT=3.25–3.35 vs. 4.3–4.5, OCL:CCL=1.95–2.7 vs. 1.1–1.4, outer face with distinct postcentral umbo vs. flat or with shallow umbo.

The relatively significant difference of the ratio of the ostium to the cauda length in the two species may even indicate that they are not closely related. In fact, I do not know of any the extant species that may be related. *Diaphus maghrebensis* is known from the Messinian and Zanclean of Morocco and from the Zanclean and Piacenzian of the Mediterranean. Earlier records of so-called *Diaphus taaningi* otoliths from the Tortonian of the Mediterranean require specific review; referenced records from the Badenian of the Paratethys have recently been re-identified as *Diaphus cassidiformis* (Frost, 1933) (see Schwarzahans & Radwańska, 2022).

Order Gadiformes Goodrich, 1909

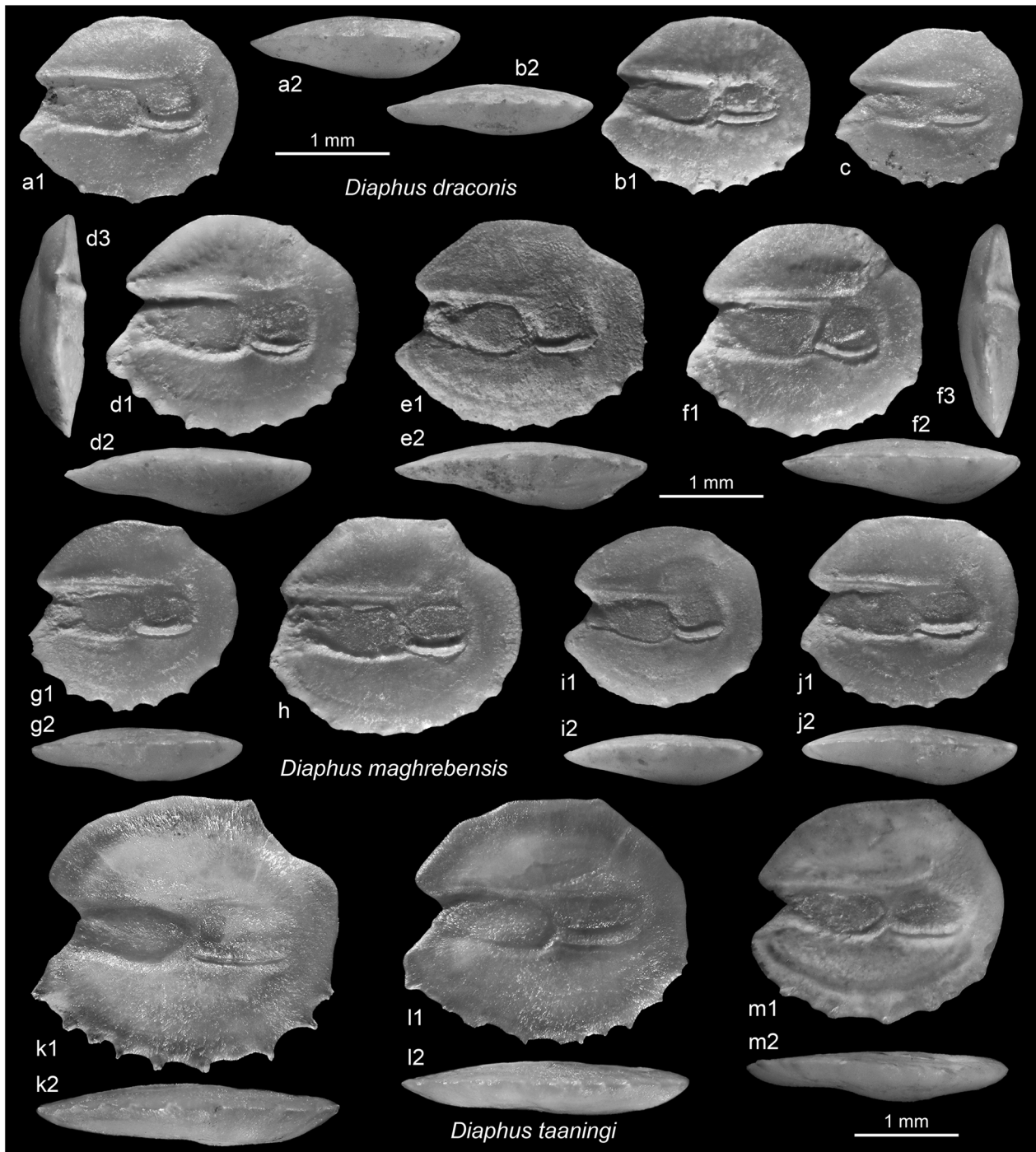


Fig. 13 Myctophidae. **a–c** *Diaphus draconis* Schwarzhans, 2013, SMF PO 101.200 (**c** reversed), Kef Nsour, Messinian. **d–j** *Diaphus maghrebensis* n. sp. **f** holotype, SMF PO 101.201, Dar bel Hamri, Zanclean, paratypes, **h–j** SMF PO 101.202 (**h, j** reversed), Dar bel Hamri, Zanclean, **e** SMF PO 101.203 (reversed), Kef Nsour, Messinian, **d, g** SMF PO 101.204, Sidi Mohamed ech Chleuh, Zanclean. **k–m**, *Diaphus taaningi* Norman, 1930, extant, **k–l** MCZ 150978, 36°17'N, 74°49'W, 13 m refigured from Schwarzhans (2013b), dredge in the Gulf of Guinea, 00°20'S, 08°46'E

Family Moridae Berg, 1940**Genus *Physiculus* Kaup, 1858*****Physiculus* sp.**

Figure 14a–c

Material 21 specimens, 20 specimens Dar bel Hamri (figured specimens SMF PO 101.205), 1 specimen Sidi Mohamed ech Chleuh.

Discussion *Physiculus* is a species-rich genus with two extant species in the tropical and subtropical eastern Atlantic: *P. huloti* Poll, 1953, from Mauritania to Angola and *P. dalwigki* Kaup, 1858, in the eastern Atlantic from about 25°N to 44°N, including Madeira, and in the western Mediterranean. Many of the fossil specimens from the Neogene of Europe have been placed in *P. huloti* (see van Hinsbergh & Hoedemakers, 2022), but Schwarzahns (2013a) questioned many of these allocations. The specimens from Morocco are not well enough preserved to allow for a specific identification, but the relatively high predorsal protrusion does not seem to match the extant specimens figured in Schwarzahns (2013a).

Family Bregmacerotidae Gill, 1872**Genus *Bregmaceros* Thompson, 1840*****Bregmaceros* sp.**

Figure 14d

Material 1 specimen, SMF PO 101.206, Dar bel Hamri, Zanclean.

Discussion The single specimen cannot be identified to species level, but certainly is too much compressed to represent the ubiquitous Mediterranean *B. albyi* (Sauvage, 1880) (OL:OH = 1.0 vs. 0.8–0.9) (see Schwarzahns, 2013c for details).

Family Macrouridae Bonaparte, 1832**Genus *Coelorinchus* Giorna, 1809*****Coelorinchus* cf. *arthaberoides* (Bassoli, 1906)**

Material A single, rather eroded specimen from Dar bel Hamri.

Genus *Nezumia* Jordan, 1904***Nezumia ornata* (Bassoli, 1906)**

Figure 14e

Material 10 specimens (figured specimens SMF PO 101.207), Dar bel Hamri, Zanclean.

Genus *Trachyrincus* Giorna, 1809***Trachyrincus scabrurus* (Rafinesque, 1810)**

Figure 14f

Material 1 specimen SMF PO 101.275, Dar bel Hamri, Zanclean.

Family Merlucciidae Rafinesque, 1815**Genus *Merluccius* Rafinesque, 1810*****Merluccius polli* Cadenat, 1950**

Figure 14j–l

Material 9 fragmentary specimens, 1 specimen from Kef Nsour, SMF PO 101.208, Messinian; 8 specimens Dar bel Hamri, figured specimens SMF PO 101.209, Zanclean.

Discussion None of the specimens available are complete, the best preserved ones are from two-thirds of a specimen. The depressed predorsal projection and the rounded anterior tip are considered typical for *M. polli* in otoliths of *Merluccius* species from the East Atlantic. The most complete specimen of Fig. 14j is 18 mm in length and reconstructed for the broken part would have been about 24 mm in length. The largest, not figured fragmented specimen may have been 33 mm in length when complete. For comparison, extant otoliths are figured of *M. merluccius* (Linnaeus, 1758) (Fig. 14g), *M. senegalensis* Cadenat, 1950 (Fig. 14h), and *M. polli* (Fig. 14i). Today, *M. polli* is known from the west African shelf off Mauritania to Angola from 29° to 19°S in deep water from 50 to 550 m.

Family Gadidae Rafinesque, 1810**Genus *Paratrisopterus* Fedotov, 1971*****Paratrisopterus glaber* Schwarzahns, 2010**

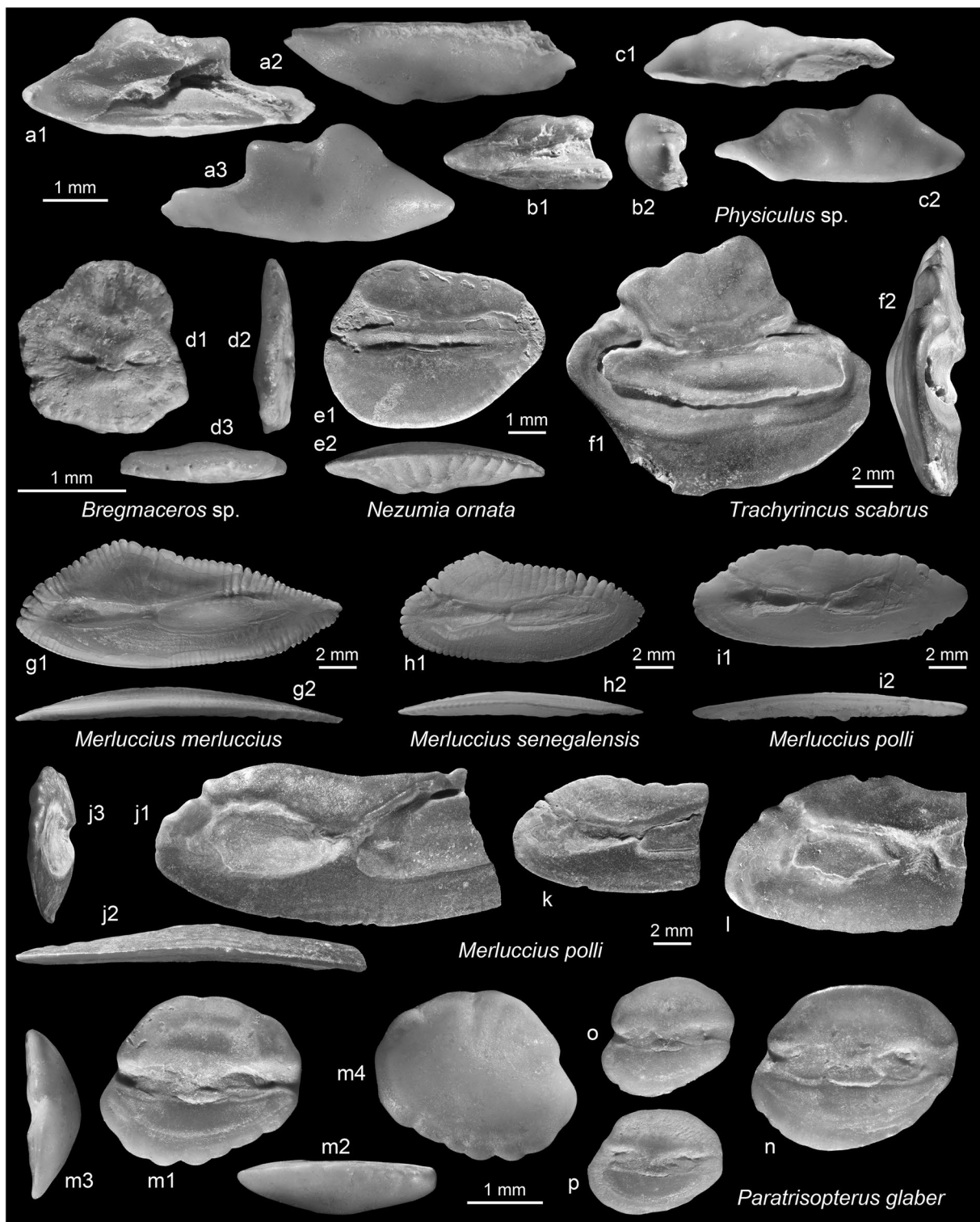


Fig. 14 Gadiformes. **a–c** *Physiculus* sp. SMF PO 101.205, Dar bel Hamri. **d**, *Bregmaceros* sp. SMF PO 101.206, Dar bel Hamri. **e**, *Nezumia ornata* (Bassoli, 1906), SMF PO 101.207 (reversed), Dar bel Hamri. **f**, *Trachyrincus scabrus* (Rafinesque, 1810), SMF PO 101.275, Dar bel Hamri. **g**, *Merluccius merluccius* (Linnaeus, 1758), extant (reversed), Marmara Sea, Turkey. **h**, *Merluccius senegalensis* Cadenat, 1950, extant (reversed), CAS 235494, 14°14'N, 17°32'W. **i**, *Merluccius polli* Cadenat, 1950, extant, CAS 235466, 13°53'N, 17°34'W. **j–l**, *Merluccius polli* Cadenat, 1950, SMF PO 101.209 (**l** reversed), Dar bel Hamri, Zanclean. **m–p**, *Paratrisopterus glaber* Schwarzhans, 2010, SMF PO 210, Dar bel Hamri

Figure 14m–p

2010 *Paratrisopterus glaber*—Schwarzhans: pl. 30, Figs. 12–15.

2022 *Paratrisopterus glaber* Schwarzhans, 2010—van Hinsbergh & Hoedemakers: pl. 15, Figs. 14, 15.

Material 72 specimens, 2 specimens, Kef Nsour, Messinian, 64 specimens, Dar bel Hamri (figured specimens SMF PO 101.210), Zanclean, 2 specimens Sidid Mohamed ech Chleuh, Zanclean, 3 specimens, Jebel Zebbouj, Zanclean. 1 specimen, Asilah, Zanclean.

Discussion *Paratrisopterus glaber* differs from the Middle Miocene species *P. brinki* (Posthumus, 1923) in its more compressed shape and relatively smooth outer face. It is, however, not as compressed as the rare Middle Miocene *P. globosus* (Posthumus, 1923). *Paratrisopterus glaber* was described from the Late Miocene of the North Sea Basin but was apparently more widely distributed in the European seas. It has recently been recorded from the Zanclean and Piacenzian of Spain, where it occurs in parallel with *P. labiatus* (Schubert, 1905) in the Zanclean. The occurrence in the Moroccan Early Pliocene fills a geographic gap in the distribution. Otoliths have been described in situ by Landini and Sorbini (1999) from a fish interpreted as *Gadiculus labiatus* from the Early Pleistocene of Italy. According to the otoliths figured in this article, the species represents *P. glaber*.

Order Ophidiiformes Berg, 1937

Family Carapidae Jordan & Fowler, 1902

Genus *Carapus* Rafinesque, 1810

Carapus acus (Brünnich, 1768)

Figure 15a

2006 *Carapus* sp.—Nolf & Girone: pl. 1, Fig. 10.

2017 *Carapus acus* (Brünnich, 1768)—Lin et al.: Fig. 9D–E.

2019a *Carapus acus* (Brünnich, 1768)—Agiadi et al.: Fig. 3G.

Material A single somewhat eroded specimen of 2.8 mm in length (SMF PO 101.211) from Dar bel Hamri, Zanclean.

Genus *Echiodon* Thompson, 1837

Echiodon dentatus (Cuvier, 1829)

Figure 15b–e

1978a *Carapus acus* (Brünnich, 1768)—Schwarzhans Fig. 112.

1994 *Echiodon praeimberbis* (Weiler, 1971)—Nolf & Cavallo: pl. 5, Fig. 2.

Material 24 specimens, Zanclean, 23 specimens Dar bel Hamri (figured specimens SMF PO 101.212), 1 specimen Sidi Mohamed ech Chleuh (SMF PO 101.213).

Discussion There has been some confusion about the identity of carapid otoliths of the genus *Echiodon* in the Pliocene of the Mediterranean. A large series of extant otoliths of *E. dentatus* has been figured in Lombarte et al. (2006), and one of them is refigured here (Fig. 15e). These otoliths are characterized by being relatively thin, having a relatively narrow sulcus terminating at some distance from the anterior rim of the otolith, and a flat ventral otolith rim. Some specimens found in Morocco and recorded in the literature from the Mediterranean (see synonymy listing) match the morphology of the extant specimens very well. However, there is also a coeval second species known from the Zanclean of the Mediterranean and Morocco that represents a different morphotype and has been described as *Carapus praeimberbis* by Weiler (1971) but is sometimes confused with *E. dentatus* (see below). *Echiodon dentatus* differs from *E. praeimberbis* by the narrower and shorter sulcus (although in large specimens of *E. dentatus*, the sulcus increases in size; see Tuset et al., 2008), the unexpanded (vs. expanded) ventral otolith rim, and the outer face projecting over the dorsal rim of the otolith (vs. unexpanded).

Echiodon praeimberbis (Weiler, 1971)

Figure 15f–i

1971 *Carapus praeimberbis*—Weiler: pl. 2, Fig. 35.

1978a *Echiodon drumondii* Thompson, 1837—Schwarzhans: Fig. 113.

1989 *Echiodon praeimberbis* (Weiler, 1971)—Nolf & Cappetta: pl. 13, Fig. 1.

2006 *Echiodon praeimberbis* (Weiler, 1971)—Girone, Nolf & Cappetta: Fig. 6.8.

2022 *Echiodon dentatus* (Cuvier, 1829) —van Hinsbergh & Hoedemakers: pl. 17, Figs. 17, 18.

Material 79 specimens, Dar bel Hamri, Zanclean (figured specimens SMF PO 101.214).

Discussion Otoliths of *E. praeimberbis* differ from those of *E. dentatus* in being more thickset, showing a distinctly wider and larger sulcus that reaches close to the anterior and dorsal rims of the otolith and a deepened, curved ventral otolith rim. Except for the deepened ventral rim, these otoliths resemble those of the extant *E. drummondii* from the northern North Sea and Norwegian Sea. Schwarzhans (2013a) recorded otoliths of *Echiodon* sp. from Holocene dredge samples off West Africa between Guinea and Nigeria, which are refigured here for comparison (Fig. 15j–k). These otoliths resemble *E. praeimberbis* even more closely in the expanded ventral rim and differ only in the pointed anterior tip and the reduced, rounded posterior tip. No *Echiodon* species is recorded from tropical West Africa today. Thus, the Holocene dredge samples indicate that an undescribed *Echiodon* species may exist in West Africa (Schwarzhans, 2013a), and *E. praeimberbis* would be the fossil species most closely related to it.

Nolf (2013) considered all records of *E. praeimberbis* to represent the extant *E. dentatus*, but this concept is probably a result of the presence of two different species occurring coevally and mostly in small numbers. However, van Hinsbergh and Hoedemakers (2022) listed 328 specimens from Estepona near Málaga, Spain, mostly from the Piacenzian. The two specimens figured pertain to *E. praeimberbis*, but it is quite possible that the assemblage also contained *E. dentatus*.

Family Ophidiidae Rafinesque, 1810

Subfamily Brotulidae Swainson, 1838

Genus *Brotula* Cuvier, 1829

***Brotula* aff. *multibarbata* Temminck & Schlegel, 1846**

Figure 16a

1998 *Brotula* aff. *multibarbata* Temminck & Schlegel, 1846—Nolf, Mañe & Lopez: pl. 5, Fig. 6.

2006 *Brotula* cf. *multibarbata* Temminck & Schlegel, 1846—Nolf & Girone: pl. 1, Fig. 14, pl. 4, Fig. 18.

2022 *Brotula* cf. *multibarbata* Temminck & Schlegel, 1846—van Hinsbergh & Hoedemakers: pl. 18, Figs. 8, 9.

Material 5 specimens SMF PO 101.215, Dar bel Hamri, Zanclean.

Discussion Incomplete, eroded, or small otoliths of *Brotula* have occasionally been reported from the Pliocene of the Mediterranean (see synonymy listing). The large, figured specimen from Morocco is well preserved but lacks the entire rear part of the otolith. Within the extant species of *Brotula*, two slightly different otolith morphotypes are recognized. One morphotype is characterized by elongate otoliths and a long ostium ($CaL:OsL = 1.4–1.6$), comprising the extant species *B. barbata* (Bloch & Schneider, 1801) and *B. clarkae* Hubbs, 1944 (see Nolf, 1980, for figures). The other morphotype has relatively more compressed otoliths with a shorter ostium ($CaL:OsL \cong 2.0$), comprising *B. multibarbata* (Temminck & Schlegel, 1846) (see Nolf, 1980, for figures), *B. flaviviridis* Greenfield, 2005, *B. ordwayi* Hildebrand & Barton, 1949, and *B. townsendi* Fowler, 1900. *Brotula barbata* is the only one of these species living today in the Atlantic. The fossil otoliths from the Pliocene of the Mediterranean and Morocco, however, represent the second morphotype and have usually been tentatively associated with *B. multibarbata*. Today, *B. multibarbata* is known from the Indo-West Pacific, with its closest occurrence to the fossil specimens in southeastern Africa. I follow previous records in recording the Moroccan Pliocene otoliths as *B. aff. multibrabata*. The only known large and complete otolith specimen figured from *B. aff. multibrabata* is by Nolf et al. (1998) from the Pliocene of southern Spain, and it confirms both the short ostium and the moderately elongate shape. Without a review of all relevant fossil specimens from Europe, however, it is not clear whether it could represent an extinct species of *Brotula*.

Subfamily Ophidiidae Rafinesque, 1810

Genus *Ophidion* Linnaeus, 1758

***Ophidion tuseti* n. sp.**

Figure 16b–g

Holotype SMF PO 101.217 (Fig. 16b), Dar bel Hamri, coquina at river level of Oued Beth, Zanclean.

Paratype 5 specimens SMF PO 101.218, same data as holotype.

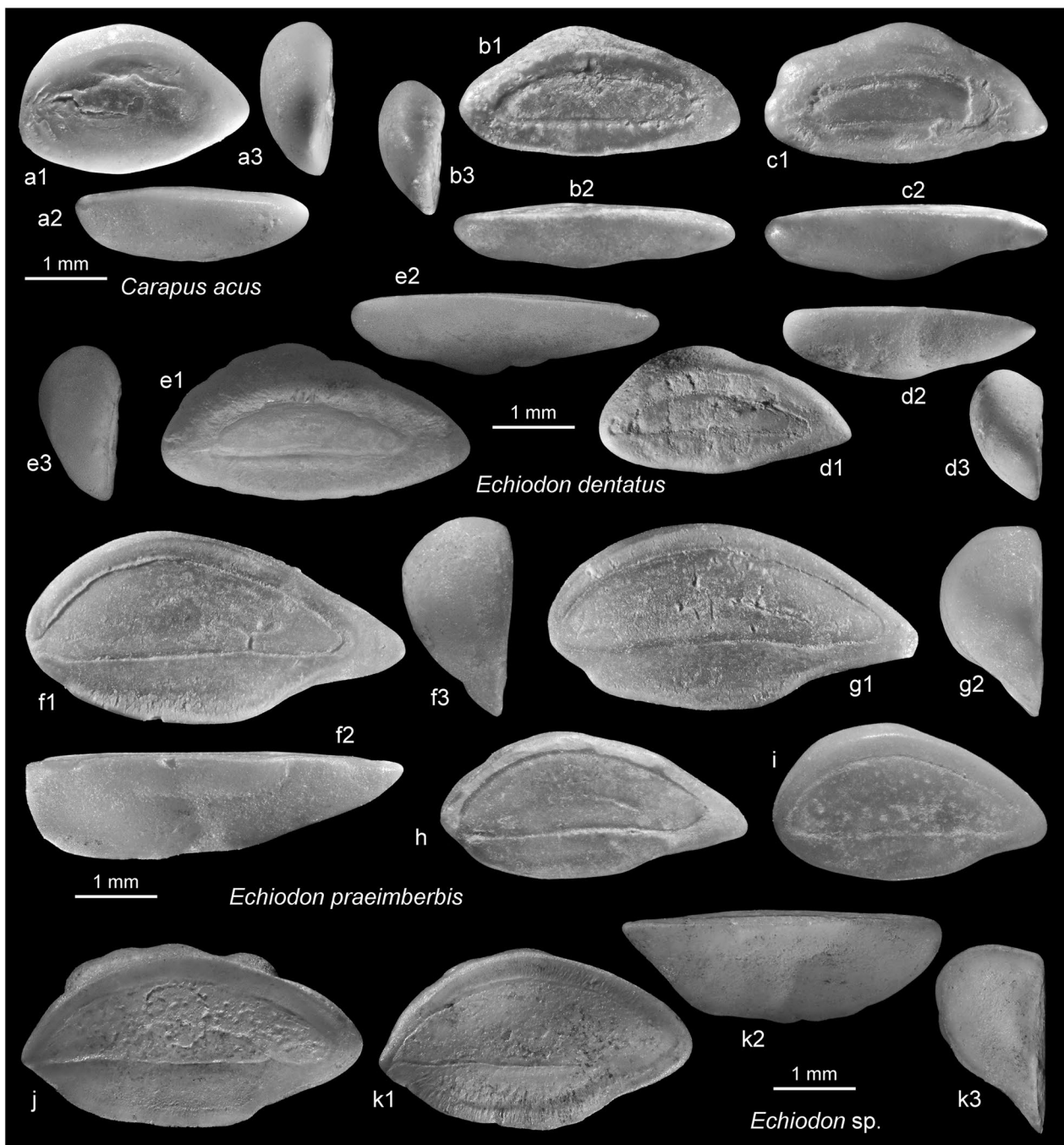


Fig. 15 Ophidiiformes. **a** *Carapus acus* (Brünnich, 1768), SMF PO 101.211, Dar bel Hamri. **b–d**, *Echiodon dentatus* (Cuvier, 1829), **b, c** SMF PO 101.212, Dar bel Hamri, **d** SMF PO 101.213 (reversed), Sidi Mohamed ech Chleuh. **e**, *Echiodon dentatus*, extant, ICM-O 258.6, off Tarragona. **f–i**, *Echiodon praeimberbis* (Weiler, 1971), SMF PO 101.214 (**g, h** reversed), Dar bel Hamri. **j–k**, *Echiodon* sp., Holocene dredge samples off Guinea (15j) and Nigeria (k), refigured from Schwarzhans (2013a)

Further material 238 specimens, same data as holotype.

Etymology Named in honor of Victor M. Tuset Andújar (Las Palmas de Gran Canaria) in recognition of his contribution to the knowledge of extant otoliths.

Diagnosis OL:OH = 1.45–1.52. Predorsal lobe low. Posterior rim of otolith tapering with rounded tip. Sulcus with distinctly convex dorsal rim and ventrally with marked indentation at junction of ostium and cauda; OsL:CaL = 4.0–4.6.

Description Moderately elongate otoliths reaching about 5.5 mm in length (holotype 5.4 mm). OL:OH=1.45–1.52; OH:OT=2.3–2.4. Shape oval with low predorsal lob, rounded anterior rim and tapering posterior rim with rounded tip. Ventral shallow, regularly curved. Rims smooth in specimens above 4.5 mm in length, with increasing marginal crenulation in smaller specimens.

Inner face distinctly convex, smooth, with very shallow sulcus. Sulcus slightly suprmedian, moderately wide, nearly opening to anterior rim of otolith and terminating close to posterior rim. Dorsal rim of sulcus distinctly convex and evenly curved; ventral rim slightly widened, with distinct indentation at junction of ostium and cauda. Colliculi fused, sometimes showing forward bent oblique and narrow junction. No dorsal depression or ventral furrow. Outer face essentially flat, somewhat depressed at center, with irregular nobs and tubercles anteriorly and posteriorly.

Discussion Four species of the genus *Ophidion* live today in the eastern Atlantic and the Mediterranean: *O. barbatum* Linnaeus, 1758, and *O. rochei* Müller, 1845, in the Mediterranean and adjacent northeastern Atlantic, *O. lozanoi* Matallanas, 1990, in the Atlantic from Spain to Angola, and *O. saldanhai* Matallanas & Brito, 1999, in the Atlantic from Cape Verde to the Gulf of Guinea. Otoliths are known from all of them, and they fall into two morphological groups mainly characterized by the expression of the predorsal lobe, otolith proportions and the sulcus. The predorsal lobe is low in *O. rochei* (see Lombarte et al., 2006 for figures) and *O. lozanoi* (Fig. 16h) and expanded in *O. barbatum* (see Lombarte et al., 2006 and Nolf et al., 2009 for figures) and *O. saldanhai* (Fig. 16i). *Ophidion tuseti* differs from the extant *O. barbatum* and *O. saldanhai* from the East Atlantic in the low dorsal projection and the ventrally widened sulcus (vs ventral sulcus margin concave). *Ophidion tuseti* differs from *O. lozanoi* and *O. rochei* in the more elongate shape (OL:OH=1.45–1.52 vs. 1.3–1.4). Specimens of *O. tuseti* of less than 3 mm in length tend to be more compressed than large ones and then distinction from *O. lozanoi* based on otolith proportions can be difficult. In addition, *O. tuseti* differs from all four extant species in the East Atlantic in the mostly well-developed indentation of the ventral sulcus rim at the junction of the ostium and cauda. This characteristic represents a trait only observed in *Ophidion* species from the Americas, such as *O. exul* Robbins, 1991, *O. fulvum* (Hildebrand & Barton, 1949) and *O. galeoides* Gilbert, 1890 (for figures, see Schwarzhans & Aguilera, 2016). Therefore, the relationships of *Ophidion tuseti* are problematic and the species may represent a lineage not present anymore in the East Atlantic. Van Hinsbergh and Hoedemakers (2022) reported *O. barbatum*, *O. rochei*,

and *O. cf. saldanhai* from the Pliocene of Estepona near Málaga.

Order Lophiiformes Garman, 1899

Family Ogcocephalidae Gill, 1893

Genus indet.

Ogcocephalidae indet.

Figure 16j

Material A single, slightly eroded otolith from the Zanclean of Dar bel Hamri (SMF PO 101.276) that is too poorly preserved for further identification.

Order Beryciformes Regan, 1909

Family Berycidae Lowe, 1839

Genus *Centroberyx* Gill, 1862

Centroberyx vonderhocht n. sp.

Figure 17a–d

Holotype SMF PO 101.219 (Fig. 17b), Dar bel Hamri, coquina at river level of Oued Beth, Zanclean.

Paratype 5 specimens SMF PO 101.277, same data as holotype.

Further material 5, mostly fragmentary or eroded specimens, Dar bel Hamri, Zanclean.

Etymology Named in honor of Fritz von der Hocht (Kerpen) who alerted me to this unique location and collected many otoliths of the studied assemblage including the type specimens of this species.

Diagnosis Large otoliths to 20 mm in length. OL:OH increasing from 1.05 at 6 mm in length to 1.35 at 20 mm in length. Dorsal rim strongly lobate; ventral rim flattened at midsection. OsL:CaL=1.10–1.17. Cauda slightly upward directed, with tapering, symmetrical tip.

Description Large otoliths reaching at least 20 mm in length (holotype). OL:OH distinctly allometric, increasing from 1.05 at 6 mm in length to 1.35 in holotype; OH:OT 3.0–3.3. Rostrum and posterior tip moderately strong, superior, with rounded tips, nearly symmetrical. Excisura and antirostrum very small. Dorsal rim anteriorly and posteriorly shortened, relatively shallow,

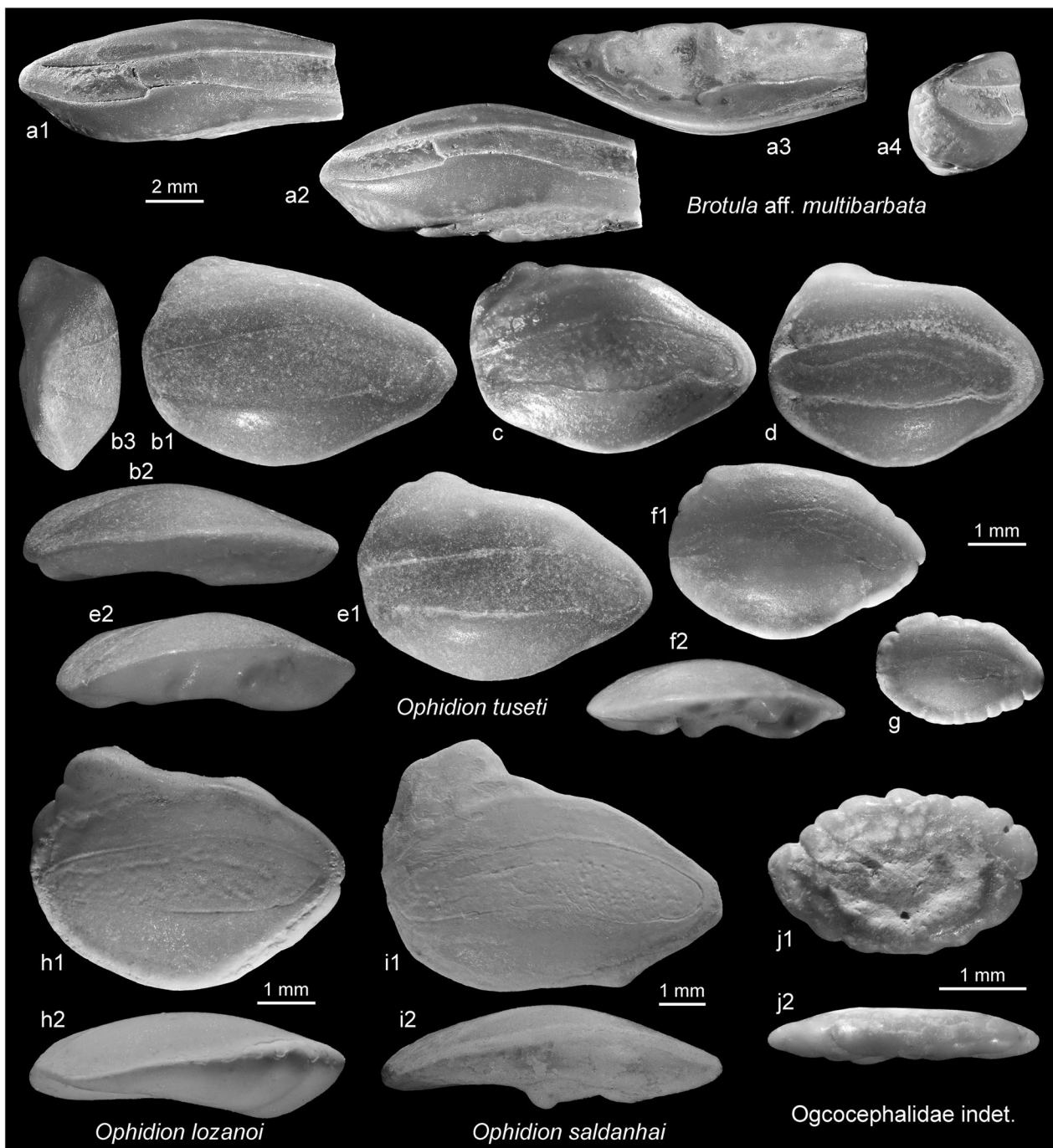


Fig. 16 Ophidiiformes. **a**, *Brotula* aff. *multibarbata* Temminck & Schlegel, 1846, SMF PO 101.215 (reversed), Dar bel Hamri. **b–g**, *Ophidion tuseti* n. sp., Dar bel Hamri, Zanclean, **b** holotype, SMF PO 101.217 (reversed), **c–g** paratypes, SMF PO 101.218 (**c**, **e–g** reversed). **h**, *Ophidion lozanoi* Matallanas, 1990, Holocene dredge samples off Nigeria, refigured from Schwarzhans (2013a). **i** *Ophidion saldanhai* Matallanas & Brito, 1999, extant, Gabon, leg. ZMUC (reversed). **j**, Ogcocephalidae indet., SMF PO 101.276, Dar bel Hamri

deeply and coarsely lobate, usually highest at predorsal angle. Ventral rim moderately deep, with nearly straight, inclined pre- and postventral rims and flattened midsection, relatively smooth.

Inner face distinctly convex, with supramedian positioned, large and wide sulcus. $OsL:CaL=1.13–1.17$ in large and medium sized specimens (Fig. 17a–c), not measurable in smallest specimen (Fig. 17d) because of

incomplete rostrum but probably 1.10 or smaller. Ostium slightly upward oriented, its ventral margin deeply lobed, slightly narrowing toward anterior. $OsL:OsH=1.45-1.75$. Cauda slightly upward oriented, nearly symmetrically tapering. Dorsal depression marked by distinct crista superior. Ventral furrow indistinct, very close to ventral rim of otolith if discernable. Outer face flat in large specimens (Fig. 17a2, b2) to distinctly convex in small specimens (Fig. 17d2), smooth.

Discussion The genus *Centroberyx* is not currently known from the Atlantic; the nearest extant occurrence is *C. spinosus* (Gilchrist, 1903) from eastern South Africa. The current center of distribution of the genus is seas around Australia and New Zealand (four of seven extant species), but this distribution must be regarded as a secondary geographic relict distribution (Schwarzshans & Jagt, 2021). So far, *C. manens* Nolf & Brzobohatý, 2004, from the Early Miocene of Italy and the North Sea Basin represented the last record in the Atlantic, but it is from a different phylogenetic lineage than the specimens from the Pliocene of Morocco. Most extant species of *Centroberyx* grow to large sizes (50 to 65 cm TL; see Froese & Pauly, 2022) and their otoliths grow to sizes of more than 22 mm in length. For comparison, two extant otoliths are figured of *C. affinis* (Günther, 1859) reflecting a large specimen near 45 mm TL (Fig. 17e) and a smaller one of unrecorded fish length (Fig. 17f). Smale et al. (1995) figured two otoliths of *C. spinosus* one 10.6 mm in length from a specimen of 15.2 cm SL, which is near the maximum size of the species (20 cm TL), and the other 7.1 mm in length from a specimen of 12 cm TL. *Centroberyx spinosus* is a relatively small species in the genus. *Centroberyx vonderhochti* resembles *C. spinosus* but differs in having attained at least twice the size of the extant species, the flattened midventral rim, the very intensely lobate dorsal rim, and the ostium being slightly longer than the cauda ($OsL:CaL=1.1-1.17$ vs. $1.0-1.05$). Most likely, *C. vonderhochti* and *C. spinosus* represent vicariant species.

Family Trachichthyidae Bleeker, 1859

Genus *Hoplostethus* Cuvier, 1829

Hoplostethus sp.

Material 1 poorly preserved specimen from Dar bel Hamri, Zanclean, that can only be identified to the genus level.

Order Holocentriformes Patterson, 1993

Family Holocentridae Bonaparte, 1835

Subfamily Holocentrinae Bonaparte, 1835

Genus *Sargocentron* Fowler, 1904

Sargocentron hastatum (Cuvier, 1829)

Figure 17g

Material 1 specimen SMF PO 101.278, Dar bel Hamri, Zanclean.

Discussion The only available specimen is relatively well preserved except for the eroded rostrum, and resembles well the extant specimens figured of *S. hastatum* by Lombarte et al. (2006). Today, *S. hastatum* is the only species of the genus known in the eastern Atlantic from Portugal to Angola (Froese & Pauly, 2022).

Subfamily Myripristinae Nelson, 1955

Genus *Myripristis* Cuvier, 1829

Myripristis ouarredi n. sp.

Figure 17i-l

Holotype SMF PO 101.220 (Fig. 17i), Dar bel Hamri, coquina at river level of Oued Beth, Zanclean.

Paratype 4 specimens SMF PO 101.221, same data as holotype.

Further material 30 specimens, same data as holotype.

Etymology Named in honor of Abdsalam Ouarred (Dar bel Hamri) and his most generous hospitality during the times of my field work in Morocco.

Diagnosis $OL:OH=1.45-1.5$. OL to maximal width of ostium $=2.4-2.5$. Ventral lobe of ostium broadly rounded, moderately deep. Middle part of postventral rim with broad oblate section.

Description Triangular otoliths with deep ventral and nearly horizontal, flat dorsal rim, up to 7.6 mm in length (holotype). Dorsal rim broadly and slightly concave anteriorly up to postdorsal angle, which is positioned far back. Ventral rim very deep, with rounded midventral angle and steep pre- and postventral section. Preventral rim straight to slightly concave at its middle. Postventral

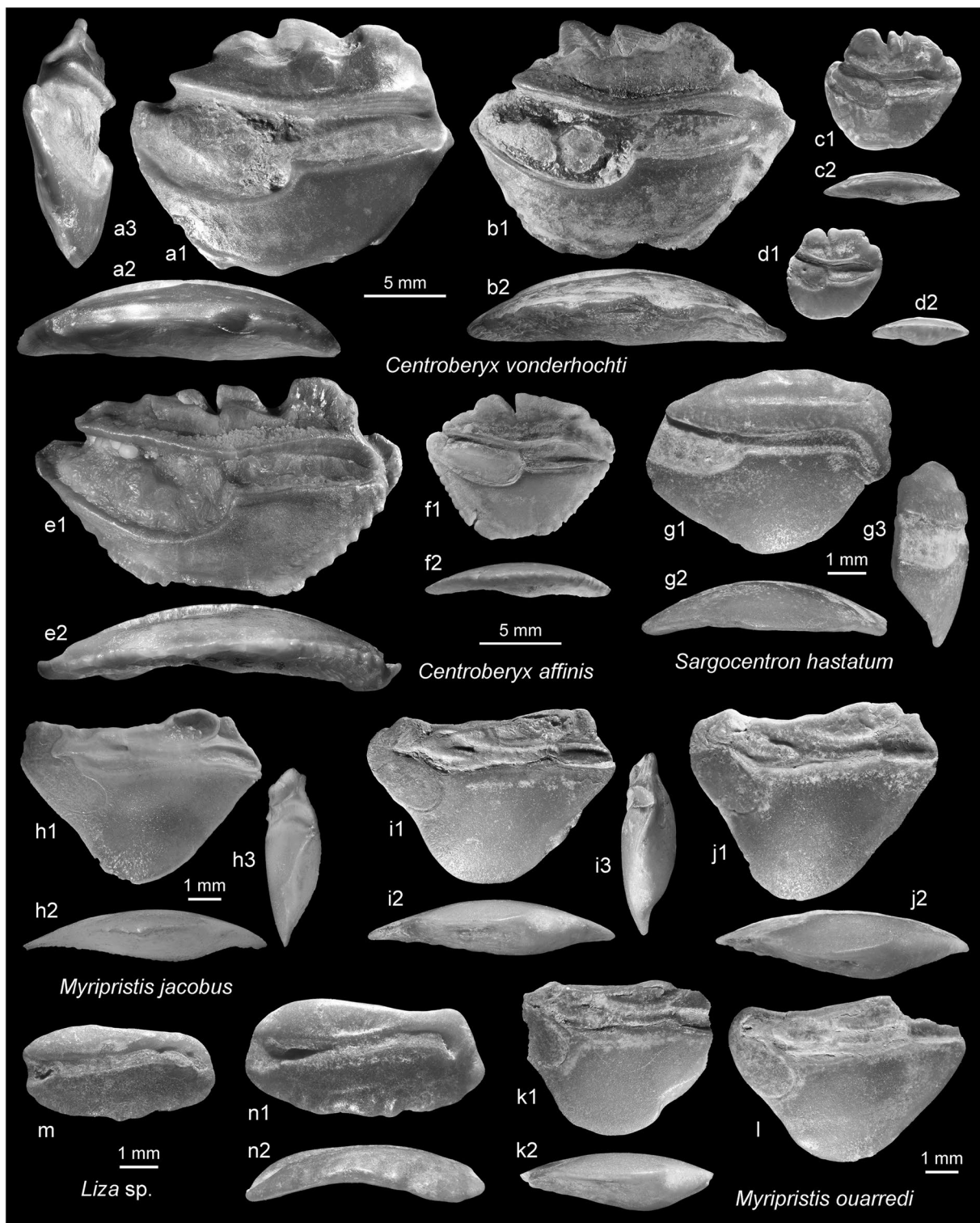


Fig. 17 Beryciformes and Holocentriformes. **a–d** *Centroberyx vonderhochti* n. sp., Dar bel Hamri, Zanclean, **b** holotype, SMF PO 101.219 (reversed), **a, c, d** paratypes, SMF PO 101.277 (**a, c** reversed). **e–f** *Centroberyx affinis* (Günther, 1859), extant, New Zealand (**e** reversed). **g**, *Sargocentron hastatum* (Cuvier, 1829), SMF PO 101.278, Dar bel Hamri. **h**, *Myripristis jacobus* Cuvier, 1829, extant, ZMH, Mona 1891. **i–l**, *Myripristis ouarredi* n. sp., Dar bel Hamri, Zanclean, **i** holotype, SMF PO 101.220 (reversed), **j–k** paratypes, SMF PO 101.221 (**j, l** reversed). **m–n**, *Liza* sp., SMF PO 101.279, Dar bel Hamri

rim nearly straight with broadly oblate section at its middle (see Fig. 17h2, j2). Anterior rim broadly rounded, positioned very high; posterior tip angular, positioned high.

Inner face moderately convex, with strongly supræmedian sulcus. Ostium short, wide, dorsally and ventrally expanded, filled by shallow colliculum; ventral expansion directed backward and rounded. Cauda long, narrow, reaching close to posterior tip of otolith, segmented in three about equally long section; anterior and posterior segment slightly deepened, middle section shallower, with indistinct dorsal margin. CaL (maximal length):OsL (maximal length)=2.4–2.9. Dorsal field very narrow, with small, cup-like expansion of dorsal depression at rear positioned just before postdorsal angle. Ventral field wide, smooth, without ventral furrow. Outer face slightly convex, smooth.

Discussion *Myripristis jacobus* Cuvier, 1829, is the only extant myripristine species occurring in the East Atlantic known from Cape Verde and São Tomé and Príncipe Islands, while its main distribution is in the tropical West Atlantic from Florida to northern Brazil (Ben-Tuvia, in Quérou et al. 1990). Its otoliths (Fig. 17h) are similar to those of *M. ouarredi*, but *M. ouarredi* differs in a less deeply expanded ventral rim of the ostium (OL to maximal width of ostium=2.4–2.5 vs. 2.1–2.2) and the oblate section of the middle part of the postventral rim (vs. slightly indented). Moreover, the postdorsal angle is higher than the rear expansion of the dorsal depression, whereas it is the other way round in *M. jacobus*. While the occurrence of *M. jacobus* in the East Atlantic probably represents a recent geographical expansion from its West Atlantic distribution pattern, the occurrence of *M. ouarredi* may represent a genuine East Atlantic lineage that is not continued into today's fish fauna of the area.

Order Mugiliformes Regan, 1909

Family Mugilidae Risso, 1827

Genus *Liza* Jordan & Swain, 1884

Liza sp.

Figure 17m–n

Material 2 specimens SMF PO 101.279, Dar bel Hamri, Zanclean.

Discussion The otoliths of the many extant species of *Liza* are poorly known and apparently difficult to distinguish depending on relatively few and delicate traits. Otoliths

of the extant west African species *L. grandisquamis* (Valenciennes, 1836) and *L. falcipinnis* (Valenciennes, 1836) are figured in Veen and Hoedemakers (2005) and resemble much the specimens from Dar bel Hamri.

Order Gobiiformes Thacker, 2009

Family Gobiidae Cuvier, 1816

Subfamily Gobiinae Cuvier, 1816

Genus *Hoeseichthys* Schwarzhans, Brzobohatý & Radwańska, 2020

Hoeseichthys brioché (Lin et al., 2015)

Figure 18a–e

2015 “Gobiida” *brioché*—Lin, Girone & Nolf: Fig. 7/16–7/20.

2020 *Hoeseichthys brioché* (Lin et al., 2015)—Schwarzhans, Agiadi & Carnevale: Fig. 6I–N (see there for further references).

2022 *Hoeseichthys brioché* (Lin et al., 2015)—van Hinsbergh & Hoedemakers: pl. 21, Figs. 1, 2.

Material 17 specimens, Zanclean: 13 specimens Dar bel Hamri (figured specimens SMF PO 101.222), 3 specimens Sidi Mohamed ech Chleuh (figured specimen SMF PO 101.223), 1 specimen Asilah.

Discussion *Hoeseichthys brioché* was a widespread and relatively common gobiid species in the Tortonian to Piacenzian of the Mediterranean and adjacent region of Morocco. It is not known from the Pliocene of Portugal (see Nolf & Marques da Silva, 1997).

Genus *Lesueurigobius* Whitley, 1950

Lesueurigobius stazzanensis Schwarzhans et al., 2020

Figure 18f–j

?1997 *Deltentosteus* sp.—Nolf & Marques da Silva: pl. 3, Figs. 7–9.

2010 *Lesueurigobius* sp. 2—Girone, Nolf & Cavallo: Fig. 10c1–4.

2020 *Lesueurigobius stazzanensis*—Schwarzhans, Agiadi & Carnevale: Fig. 6AG–AP.

2022 *Lesueurigobius stazzanensis* Schwarzhans et al., 2020—van Hinsbergh & Hoedemakers: pl. 21, Figs. 7–9.

Material 46 specimens Dar bel Hamri, Zanclean (figured specimens SMF PO 101.224).

Discussion *Lesueurigobius stazzanensis* is known from the Tortonian to Piacenzian of the Mediterranean, the Zanclean of Atlantic Morocco, and possibly the Piacenzian of Portugal. It differs from the otoliths of other extant and fossil *Lesueurigobius* otoliths except *L. heterofasciatus* Maul, 1971, in being more elongate (OL:OH=1.05–1.17 vs. <1.0). The drawing of an extant specimen of *L. heterofasciatus* provided by D. Nolf (Bruges) shows similar proportions (OL:OH=1.22) but with a pronounced pre-ventral projection (vs. blunt anterior rim in *L. stazzanensis*) and a regularly curved dorsal rim (vs. pronounced predorsal and postdorsal angles in *L. stazzanensis*).

Genus *Vanneaugobius* Brownell, 1978

Vanneaugobius? sp.

Figure 18k–m

2013a *Nematogobius maindroni* (Sauvage, 1880)—Schwarzhans: pl. 13, Figs. 1, 2.

Material 2 specimens (SMF PO 101.225), Dar bel Hamri, Zanclean.

Discussion Extant otoliths of *Vanneaugobius* are not well known, and those of other West African gobies such as *Didogobius*, *Ebomegobius*, and *Wheelerigobius* are still unknown. A poorly preserved specimen of *V. canariensis* Van Tassell, Miller & Brito, 1987, extracted from USNM 298,746 and a small specimen of *V. dollfusi* Brownell, 1978, figured in Lombarte et al. (2006) suggest that these otoliths could belong to an unknown species of the genus *Vanneaugobius*. The specimens from the Zanclean of Morocco are characterized by a relatively flat and smooth inner face bearing a small, slightly inclined sulcus with low ostial lobe and no subcaudal iugum. The same otolith morphotype has also been dredged from Holocene sediments of Guinea and Ivory Coast and has been erroneously identified as *Nematogobius maindroni* (Fig. 18m is refigured from Schwarzhans, 2013a) based on small specimens (the only ones then available). New otoliths of both nominal species extracted from larger specimens exhibited a distinctly different morphology reflecting a remarkable ontogenetic allometry possibly accentuated also by different habitats and water chemistry, as the

small otoliths were obtained from freshwater specimens. The true identity of the Pliocene Moroccan and Holocene dredged Gulf of Guinea specimens remains somewhat obscure, since it is not possible to discern from the few extant otoliths known of *Vanneaugobius* whether they have or lack a subcaudal iugum.

Subfamily Gobionellinae Bleeker, 1874

Genus *Buenia* Iljin, 1930

Buenia pulvinus van Hinsbergh & Hoedemakers, 2022

Figure 19a–c

2022 *Buenia pulvinus*—van Hinsbergh & Hoedemakers: pl. 20, Figs. 6–13.

Material 9 specimens, Dar bel Hamri, Zanclean (figured specimens SMF PO 101.226).

Discussion The genus *Buenia* shows a remarkable diversity in otolith-based taxa in the Pliocene of the Mediterranean (Schwarzhans et al., 2020; van Hinsbergh & Hoedemakers, 2022). Two of the extant species (*B. affinis* Iljin, 1930, and *B. massutii* Kovačić, Ordines & Schliwen, 2017) have also been recorded as fossils from the Pliocene, in addition to the two extinct species *B. pisiformis* Schwarzhans et al., 2020, and *B. pulvinus* van Hinsbergh & Hoedemakers, 2022. Van Hinsbergh & Hoedemakers compared *B. pulvinus* with the extant *B. affinis* and mentioned the smaller size of the sulcus as the main distinguishing characteristic. This characteristic is shared by the Moroccan otoliths, which do not, however, exhibit any postdorsal projection as described by van Hinsbergh & Hoedemakers. I attribute the latter difference to the smaller size of the Moroccan otoliths compared to those from Estepona near Málaga.

Genus *Deltentosteus* Gill, 1863

Deltentosteus planus n. sp.

Figure 19f–j

Holotype SMF PO 101.227 (Fig. 19f), Dar bel Hamri, coquina at river level of Oued Beth, Zanclean.

Paratype 4 specimens SMF PO 101.228, same data as holotype.

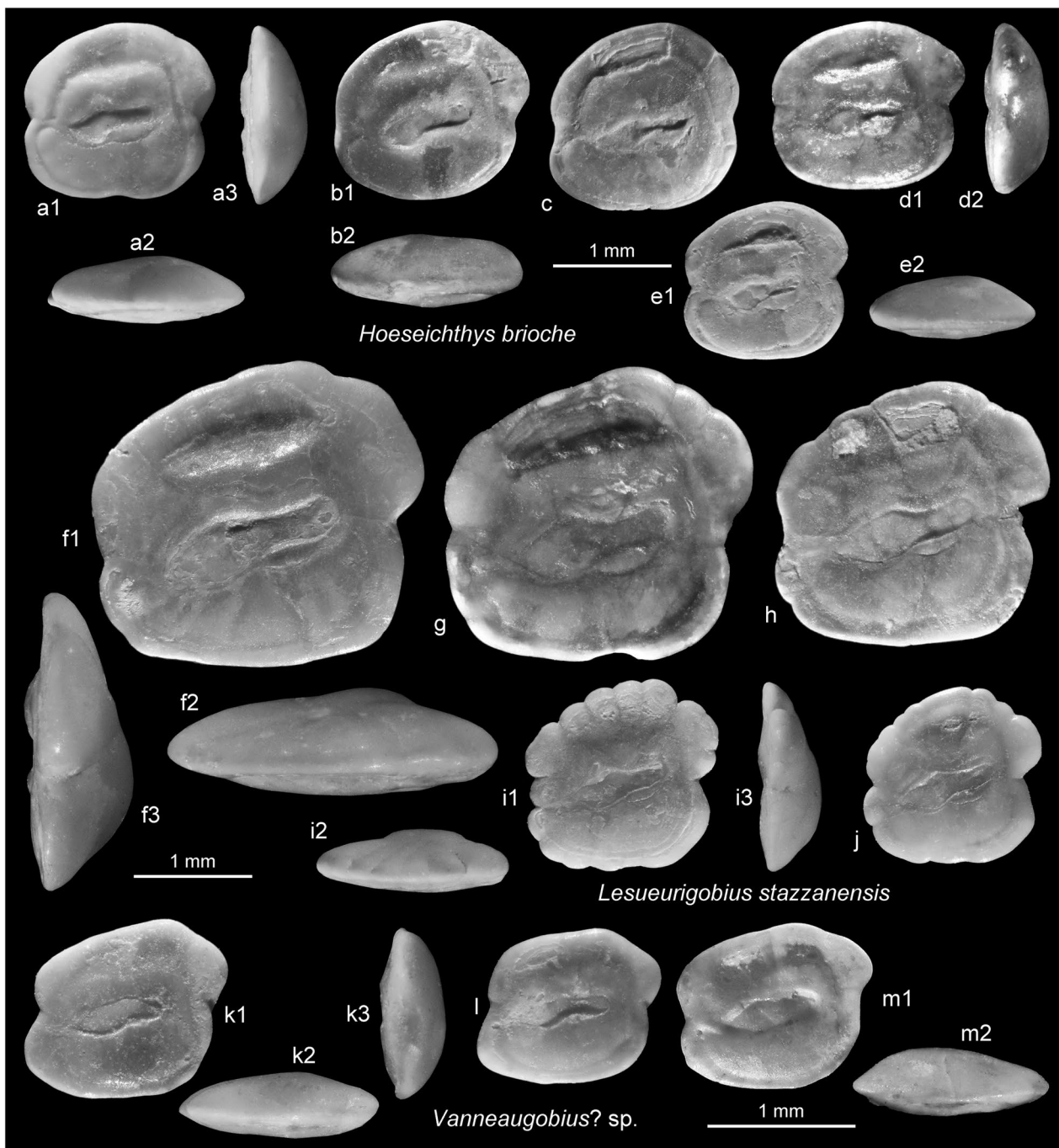


Fig. 18 Gobiiformes. **a–e** *Hoeseichthys brioches* (Lin et al., 2015), **b–e** SMF PO 101.222 (**b, e** reversed), Dar bel Hamri, **a** SMF PO 101.223, Sidi Mohamed ech Chleuh. **f–j** *Lesueurigobius stazzanensis* Schwarzhans, Agiadi & Carnevale, 2020, SMF PO 101.224 (**g–i** reversed), Dar bel Hamri. **k–m** *Vanneaugobius?* sp., **k–l** SMF PO 101.225 (**k** reversed), Dar bel Hamri, **m**, refigured from Schwarzhans (2013a), dredge in the Gulf of Guinea, 04°40'N, 08°54'W

Further material 21 specimens, Zanclean, 20 specimens same data as holotype, 1 specimen Asilah.

Etymology From planus (Latin)=flat, referring to the relatively flat inner face.

Diagnosis OL:OH=1.02–1.1. Dorsal rim regularly curved, smooth. Sulcus shape very asymmetrical with a wide ostium and a narrow, tapering and pointed cauda. Ostium inclined at 22–25°.

Description Small otoliths with rounded shape without prominent angles or projections but resembling a well-rounded rectangle. Size up to 2 mm in length (holotype 1.8 mm). OH:OT=2.7–3.0. Ventral rim shallow, nearly straight; dorsal rim slightly elevated with well-rounded pre- and postdorsal angles at about same level. Anterior and posterior rims nearly vertical. All rims smooth.

Inner face relatively flat, only slightly convex, and rather smooth. Sulcus positioned slightly eccentrically towards anterior and very asymmetrical with a wide ostium and a narrow cauda. Ostium dorsally and ventrally widened, steeply inclined at 22–25°, with angular or rounded anterior tip. Ostial-caudal joint marked by angle on ventral sulcus margin. Cauda narrow and short, with tapering, pointed tip, inclined at 7–12°. OL:SuL=1.85–2.1; OsL:CaL=1.85–2.2; OsH:CaH=2.5–2.8. Subcaudal iugum very feeble and small. Dorsal depression small, cup like, high above sulcus and dorsally open; ventral furrow weak, close to ventral rim of otolith, fading upwards anteriorly and posteriorly. Outer face evenly but relatively faintly convex, smooth.

Discussion *Deltentosteus planus* was apparently a relatively small species with otoliths not exceeding 2 mm in length. The otoliths are nevertheless easily recognized by the nearly flat inner face, the smooth, rounded rectangular outline, and the specific asymmetric sulcus. Of the two extant species, it most resembles *D. collonianus* (Risso, 1820) (Fig. 18e) in the relatively flat inner face and the low OL:OH ratio known from the Mediterranean and adjacent part of the Atlantic. *Deltentosteus planus* differs from *D. collonianus* in the smooth, rounded rectangular outline (vs. bulged dorsal rim and distinct crenulation and undulations), the distinct shape of the sulcus, and the rather steep inclination of the ostium (22–25° vs. 15°). Furthermore, otoliths of *D. planus* do not reach the size of its extant congener.

***Deltentosteus quadrimaculatus* (Valenciennes, 1837)**

Figure 19d, k–m

2020 *Deltentosteus quadrimaculatus* (Valenciennes, 1837)—Schwarzhans, Agiadi & Carnevale: Fig. 12AE–AJ (see there for further references).

2022 *Deltentosteus quadrimaculatus* (Valenciennes, 1837)—van Hinsbergh & Hoedemakers: pl. 20, Figs. 23–26.

Material 43 specimens, Dar bel Hamri, Zanclean (figured specimens SMF PO 101.229).

Discussion Otoliths of *D. quadrimaculatus* have frequently been retrieved from Pliocene rocks from Mediterranean realms. They are easily distinguishable from *D. planus* by the more elongate shape in adults (OL:OH=1.15), while small specimens at a size of about 1.05 are similar in proportions (see extant specimen in Fig. 19d and small fossil specimen in 19 k). The sulcus is larger in *D. quadrimaculatus* than in *D. planus*, with a weaker asymmetry of the ostium to cauda, and the inner face is distinctly convex.

Order Pleuronectiformes Bleeker, 1859

Family Citharidae Hubbs & Hubbs, 1945

Genus *Citharus* Artedi, 1793

***Citharus balearicus* Bauza-Rullan, 1955**

Figure 20a–c

1955 *Eucitharus balearicus*—Bauza-Rullan: pl. 8, Fig. 16.

1999 *Citharus balearicus* Bauza-Rullan, 1955—Schwarzhans: Figs. 74–76 (see there for further references).

Material 8 specimens, Dar bel Hamri, Zanclean (figured specimens SMF PO 101.230).

Discussion *Citharus balearicus* differs from otoliths of the extant *C. linguatula* (Linnaeus, 1758) in the lower expression of the postdorsal angle.

Family Bothidae Schmitt, 1892

Genus *Arnoglossus* Bleeker, 1862

***Arnoglossus kokeni* (Bassoli, 1906)**

Figure 20d–g

1906 *Solea kokeni*—Bassoli: pl. 2, Fig. 3.

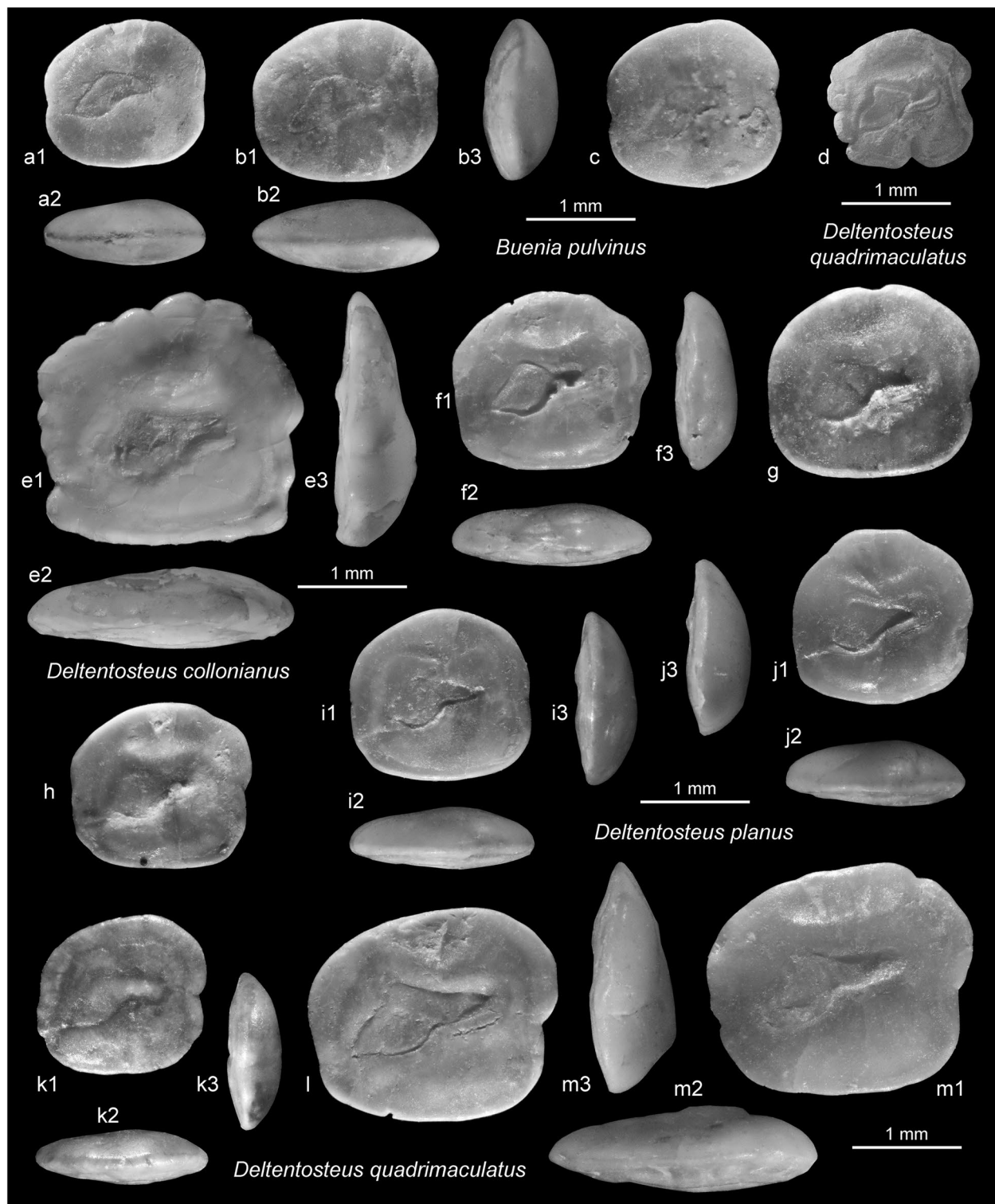


Fig. 19 Gobiiformes. **a–c** *Buenia pulvinus* van Hinsbergh & Hoedemakers, 2022, SMF PO 101.226 (**c** reversed), Dar bel Hamri. **d** *Deltentosteus quadrimaculatus* (Vlenciennes, 1837), extant, ICM-O 132.8 from the Catalanian sea, Spain, TL = 32 mm. **e** *Deltentosteus collonianus* (Risso, 1820), extant, ZMUC 14, Mediterranean 8.12.1891. **f–j** *Deltentosteus planus* n. sp. Dar bel Hamri, Zanclean, **f** holotype, SMF PO 101.227, **g–j** paratypes, SMF PO 101.228 (**h, j** reversed). **k–m**, *Deltentosteus quadrimaculatus* (Vlenciennes, 1837), SMF PO 101.229 (reversed), Dar bel Hamri

1999 *Arnoglossus kokeni* (Bassoli, 1906)—Schwarzahns: Figs. 360–364 (see there for further references).

2022 *Arnoglossus kokeni* (Bassoli, 1906)—van Hinsbergh & Hoedemakers: pl. 27, Figs. 7, 8.

Material 31 specimens, Zanclean, 29 specimens Dar bel Hamri (figured specimens SMF PO 101.231), 1 specimen Sidi Mohamed ech Chleuh, 1 specimen Asilah.

Discussion *Arnoglossus kokeni* is recognized by its nearly perfectly square shape with a ratio OL:OH just slightly above 1.0 (1.1–1.2). *Arnoglossus kokeni* is known in the Mediterranean from the Tortonian to the Piacentian and from Atlantic Morocco from the Zanclean.

***Arnoglossus quadratus* Schwarzahns, 1999**

Figure 20h–k

1999 *Arnoglossus quadratus*—Schwarzahns: Fig. 365–373.

2022 *Arnoglossus quadratus* Schwarzahns, 1999—van Hinsbergh & Hoedemakers: pl. 27, Figs. 4–6.

Material 18 specimens, Dar bel Hamri, Zanclean, photographed holotype (Fig. 20j) SMF P 9317 and paratypes SMF P 9318.

Discussion *Arnoglossus quadratus* differs from the coeval *A. kokeni* in the more elongate, rectangular shape with a ratio OL:OH ranging from 1.25 to 1.3. It has been found also with few specimens in the Pliocene of Estepona near Málaga (van Hinsbergh & Hoedemakers, 2022).

Genus *Laeops* Günther, 1880

***Laeops rharbensis* Schwarzahns, 1999**

Figure 20l–o

1999 *Laeops rharbensis*—Schwarzahns: Fig. 444–447.

Material 7 specimens, Dar bel Hamri, Zanclean, photographed paratypes SMF P 9320.

Discussion *Laeops rharbensis* resembles *Arnoglossus kokeni* in proportions and general appearance, but differs in being more compressed (OL:OH=1.0–1.1 vs. 1.1–1.2), in the more rounded and expanded ventral rim, and in the higher positioned anterior rostrum-like tip of the

otolith. The generic allocation to the genus *Laeops*, which today only lives in the Indo-Pacific, is poorly constrained by means of otolith morphological characters. If verified, it would represent the second taxon in the Zanclean of northwestern Morocco with clear Indo-Pacific affinities, the other being *Brotula multibarbata* (see above).

Family Soleidae Bonaparte, 1835

Genus *Dicologlossa* Chabanaud, 1927

***Dicologlossa hexophthalma* (Bennett, 1831)**

Figure 21e–f

Material 1 specimen SMF PO 101.232, Dar bel Hamri, Zanclean.

Discussion Otoliths of *D. hexophthalma* are relatively thin, oval in shape with a ratio OL:OH of 1.25–1.4 (corrected from Schwarzahns, 1999) and a relatively thin sulcus. A recent specimen is figured for comparison (Fig. 21e). The single fossil specimen from Morocco (Fig. 21f) resembles the extant specimens in all morphological aspects but is distinctly thicker (OH:OT=2.7 vs. 3.5–4.5), and is, therefore, only tentatively placed in the same species.

Genus *Microchirus* Bonaparte, 1833

***Microchirus variegatus* (Donovan, 1808)**

Figure 21i–j

1978 *Microchirus variegatus* (Donovan, 1808)—Nolf: pl. 7, Fig. 18.

1989 *Microchirus variegatus* (Donovan, 1808)—Nolf & Cappetta: pl. 18, Fig. 18.

2019b *Microchirus variegatus* (Donovan, 1808)—Agiadi et al.: Fig. 4l.

2022 *Microchirus variegatus* (Donovan, 1808)—van Hinsbergh & Hoedemakers: pl. 27, Figs. 13–15.

Material 3 specimens SMF PO 101.280, Dar bel Hamri, Zanclean.

Discussion Otoliths of *M. variegatus* are recognized by their rounded trinagular outline with a deep ventral rim and a shallow dorsal rim and the distinctly convex inner face. The species has been regularly recorded from

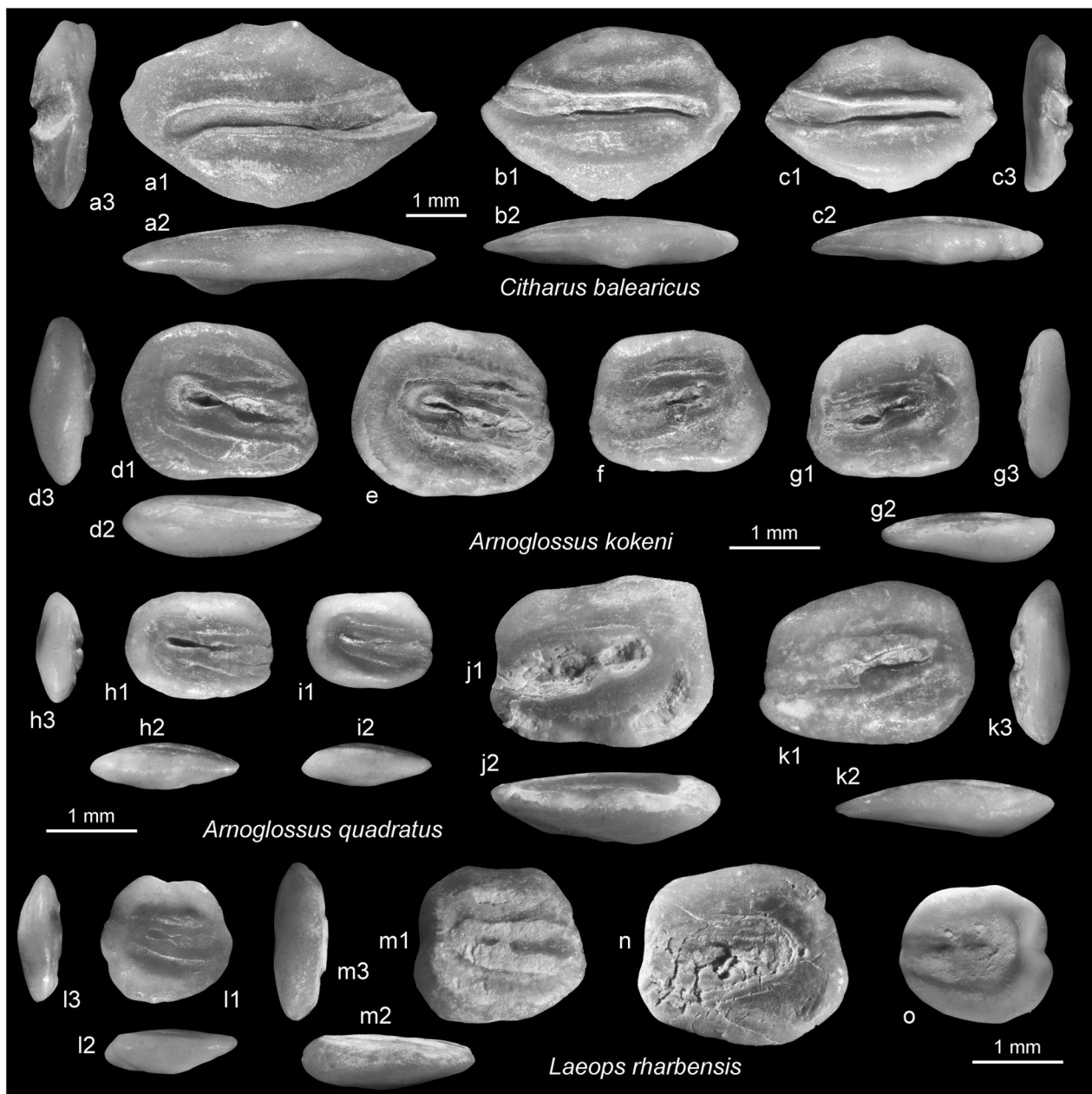


Fig. 20 Citharidae and Bothidae. **a–c** *Citharus balearicus* Bauza-Rullan, 1955, SMF PO 101.230, Dar bel Hamri. **d–g** *Arnoglossus kokeni* (Bassoli, 1906), SMF PO 101.231, Dar bel Hamri. **h–k** *Arnoglossus quadratus* Schwarzhans, 1999, Dar bel Hamri, Zanclean, **j** holotype, SMF P 9317, **h, i, k** paratypes, SMF P 9318. **l–o** *Laeops rharbensis* Schwarzhans, 1999, paratypes, SMF P 9320, Dar bel Hamri, Zanclean

Pliocene and Pleistocene rocks of the North Sea Basin and the Mediterranean. Miocene records may represent a different species (see Schwarzhans, 1999).

Genus *Quenselia* Jordan, 1889

Quenselia cornuta Schwarzhans, 1999

Figure 21a–d

1999 *Quenselia cornuta*—Schwarzhans: Fig. 751–758.

Material 35 specimens, Dar bel Hamri, Zanclean, photographed holotype (Fig. 21b) SMF P 9325 and paratypes SMF P 9326.

Discussion *Quenselia cornuta* is readily recognized by its horn-like predorsal lobe positioned near the anterior end of the otoliths and the fact that the cauda is longer than the ostium. Both are unusual characteristics and the proportions of the sulcus could in fact indicate that *Q. cornuta* could belong to an extinct lineage/genus. *Quenselia cornuta* has only been recorded from the Pliocene of Atlantic Morocco.

Genus *Synaptura* Cantor, 1849

Synaptura sp.

Figure 21g

?2022 *Solea* sp.—van Hinsbergh & Hoedemakers: pl. 27, Fig. 16.

Material 1 specimen SMF PO 101.234, Dar bel Hamri, Zanclean.

Discussion The single, eroded specimen resembles extant otoliths of the genus *Synaptura* in shape and otolith and sulcus proportions but cannot be specifically identified due to its poor preservation.

Genus *Synapturichthys* Chabanaud, 1927

Synapturichthys kleinii (Risso, 1827)

Figure 21h

Material 1 specimen SMF PO 101.235, Dar bel Hamri, Zanclean.

Discussion Otoliths of *S. kleinii* are recognized by their compressed shaped (OL:OH=1.1–1.15) in combination with somewhat undulating otolith rims and a pointed postdorsal projection. *Synapturichthys kleinii* is the only species of the genus occurring today in the Mediterranean and along the East Atlantic coast to South Africa into the western Indian Ocean to off Durban.

Genus *Vanstraelenia* Chabanaud, 1950

Vanstraelenia chirophthalma (Regan, 1915)

Figure 21k

Material 1 specimen SMF PO 101.236, Dar bel Hamri, Zanclean.

Discussion Otoliths of *V. chirophthalma* are recognized by their compressed, high-bodied shape (OL:OH=1.0–1.15) combined with a flat inner face, a convex outer face and a small, morphologically much reduced sulcus. Today, *V. chirophthalma* occurs only along the tropical coast of West Africa from Guinea-Bissau to Angola.

Family Cynoglossidae Jordan & Goss, 1889

Genus *Cynoglossus* Hamilton-Buchanan, 1832

Cynoglossus obliqueventralis Schwarzzhans, 1999

Figure 21l–o

1999 *Cynoglossus obliqueventralis*—Schwarzzhans: Fig. 905–906.

2006 *Cynoglossus obliqueventralis* Schwarzzhans, 1999—Nolf & Girone: pl. 2, Fig. 16.

2019b *Cynoglossus obliqueventralis* Schwarzzhans, 1999—Agiadi et al.: Fig. 4m–n.

Material 7 specimens, Dar bel Hamri, Zanclean, photographed holotype (Fig. 21j) SMF P 9327 and paratype SMF P 9328, and 5 newly collected specimens (figured specimens SMF PO 101.281).

Order Xiphiiformes Rafinesque, 1810 (for Istiophoriformes Betancur R. et al. 2013)

Family Sphyraenidae Rafinesque, 1815

Genus *Sphyraena* Artedi, 1793

Sphyraena sp.

Figure 22a

Material 3 specimens, Dar bel Hamri, Zanclean, figured specimen SMF PO 101.237.

Discussion All specimens of this morphotype lack the rostrum and the anterior part of the ostium. Therefore, the otoliths cannot be identified to the species level but despite of the fragmentation are clearly recognizable as *Sphyraena* otoliths. A similar but much less bent *Sphyraena* otolith was described in open nomenclature from the Zanclean of Piedmont, Italy, by Nolf and Girone (2006).

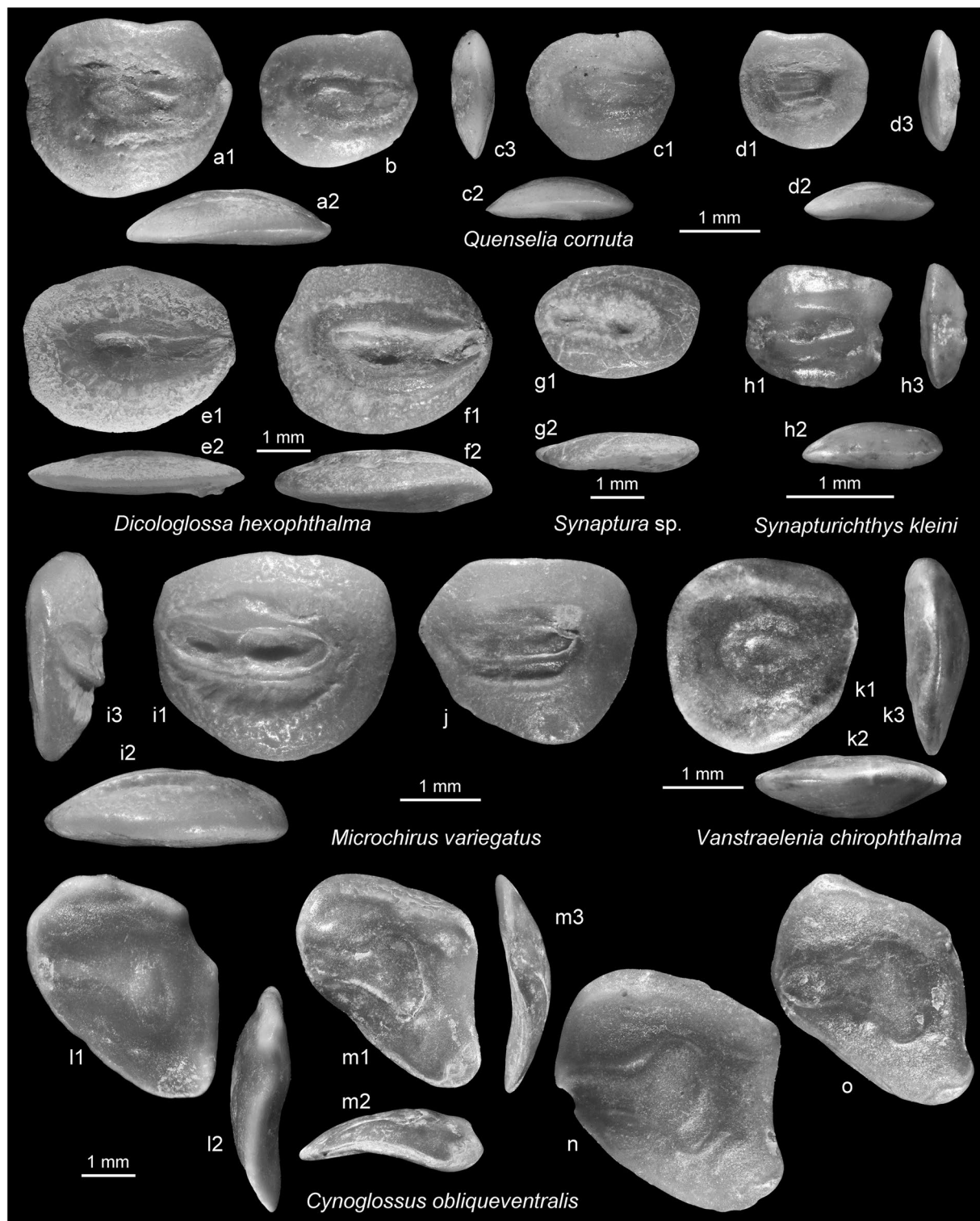


Fig. 21 Soleidae and Cynoglossidae. **a–d** *Quenselia cornuta* Schwarzhans, 1999, Dar bel Hamri, Zanclean, **b** holotype, SMF P 9325, **a, c–d** paratypes, SMF P 9326. **e–f** *Dicologlossa hexophthalma* (Bennett, 1831), **f** SMF PO 101.232, Dar bel Hamri, **e** extant, Lagos fish market, Portugal. **g** *Synaptura* sp. SMF PO 101.234, Dar bel Hamri. **h** *Synapturichthys kleini* (Risso, 1827), SMF PO 101.235, Dar bel Hamri. **j–j** *Microchirus variegatus* (Donovan, 1808), SMF PO 101.280, Dar bel Hamri. **k** *Vanstraelenia chirophthalma* (Regan, 1915), SMF PO 101.236, Dar bel Hamri. **l–o** *Cynoglossus obliqueventralis* Schwarzhans, 1999, Dar bel Hamri, 21 **l** holotype, SMF P 9327, **m** paratype, SMF P 9328, **n–o** newly collected specimens, SMF PO 101.281

Order Carangiformes Patterson, 1993

Family Carangidae Rafinesque, 1815

Genus *Caranx* Lacepède, 1801

Caranx rharbensis n. sp.

Figure 22e–g

Holotype SMF PO 101.238 (Fig. 22e), Dar bel Hamri, coquina at river level of Oued Beth, Zanclean.

Paratype 8 specimens SMF PO 101.282, same data as holotype.

Etymology From Rharb, the geographical region in north-west Morocco where Dar bel Hamri is located.

Diagnosis OL:OH=1.95–2.1. Ventral rim shallow, smooth; dorsal rim shallow, coarsely crenulated. Rostrum relatively short, 20–25% OL. Ostium short, CaL:OsL=2.9–3.3. Curvature of caudal tip 40–50°, terminating very close to postventral rim, caudal tip rounded and slightly widened.

Description Relatively large and slender otoliths up to 9 mm in length (holotype 8.25 mm). OH:OT=3.0–3.4. Ventral rim very shallow, regularly curved, smooth; dorsal rim shallow as well but intensely and irregularly crenulated, without discernable pre- or mediodorsal angles and variably developed postdorsal angle. Rostrum relatively short (completely preserved only in specimens of Fig. 22f, g); antirostrum and excisura weak. Posterior rim blunt (Fig. 22e) or oblique (Fig. 22f, g).

Inner face slightly convex with slightly supramedian positioned, deep, relatively wide and long sulcus. Ostium short, narrow, only slightly widened ventrally. Cauda long, straight, its tip bend downward with the downward oriented section nearly straight; caudal tip broadly rounded, slightly widened, terminating very close to postventral otolith rim. Dorsal depression narrow, ventrally marked by crista superior, dorsal margin indistinct; ventral field smooth, with feeble ventral furrow close to ventral rim of otolith. Outer face flat to slightly concave, relatively smooth.

Discussion These otoliths are placed in the genus *Caranx* because of their resemblance with otoliths of the extant *C. hippos* (Linnaeus, 1766) and *C. rhonchus* Geoffroy Saint-Hilaire, 1817 as figured in Lombarte et al. (2006). It differs from extant and coeval *Trachurus* otoliths in the low ventral and dorsal rims. *Caranx rharbensis* is

distinguished from said extant *Caranx* species in the short rostrum and rounded and widened caudal tip, and from parallel occurring *Trachurus* species (see below) in the slender shape (OL:OH=1.95–2.1 vs. 1.55–1.9), the shallow dorsal and ventral rims and the rounded and widened caudal tip.

Genus *Trachurus* Rafinesque, 1810

Trachurus insectus n. sp.

Figure 22b–d

Holotype SMF PO 101.283 (Fig. 22b), Dar bel Hamri, coquina at river level of Oued Beth, Zanclean.

Paratype 11 specimens SMF PO 101.284, same data as holotype.

Etymology From *insectus* (Latin)=notched, referring to the characteristic postdorsal notch.

Diagnosis OL:OH=1.55–1.7. Ventral rim with obtuse, rounded midventral angle; dorsal rim with broad lobe behind its middle followed by distinct notch. Rostrum relatively short, 15% OL. Ostium short, CaL:OsL=2.9–3.6. Curvature of caudal tip 37–45°, terminating close to postventral rim.

Description Moderately large and thin otoliths up to 6.9 mm in length (holotype). OH:OT=4.0–4.5. Ventral rim moderately deep, anterior and posterior regions nearly straight, inclined, with rounded midventral angle, smooth or finely crenulated; dorsal rim anteriorly depressed, rising to broad lobe slightly behind middle followed by deep and distinct notch and slightly expanded postdorsal section, irregularly undulating. Rostrum relatively short (completely preserved only in specimens of Fig. 22b, d); antirostrum and excisura very weak. Posterior rim angular.

Inner face slightly convex with distinctly supramedian positioned, deep, relatively narrow and long sulcus. Ostium short, narrow, only slightly widened ventrally. Cauda long, straight, its tip bend downward; caudal tip not widened, terminating close to postventral otolith rim. Dorsal depression narrow, ventrally marked by crista superior, dorsal margin indistinct; ventral field with feeble ventral furrow distant from ventral rim of otolith, smooth above ventral furrow, slightly plicated below. Outer face flat to slightly concave, relatively smooth.

Discussion This species is recognized as a member of the genus *Trachurus* by the otolith shape with the midventral

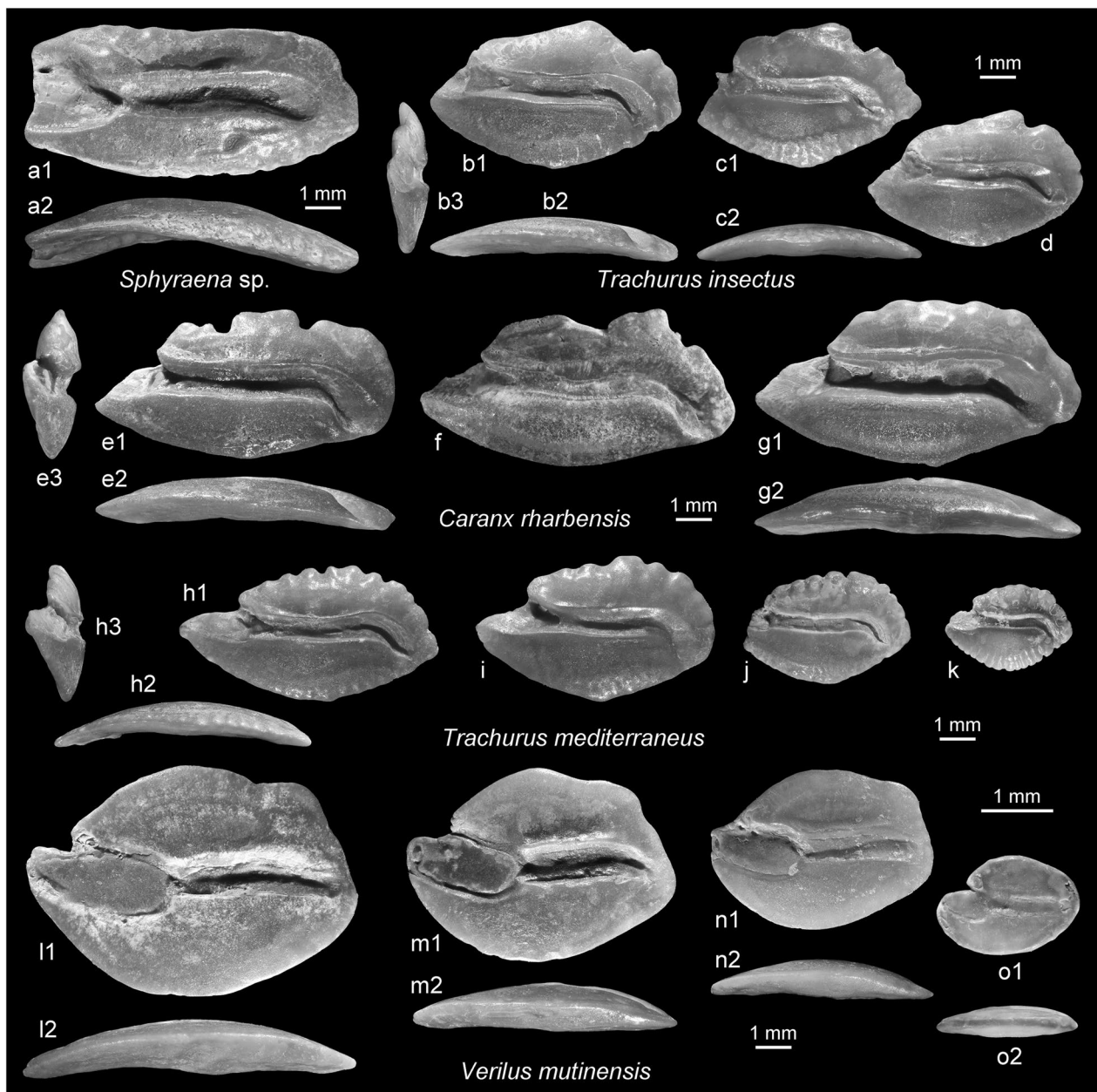


Fig. 22 Sphyraenidae, Carangidae and Acropomatidae. **a** *Sphyraena* sp., SMF PO 101.237, Dar bel Hamri. **b–d** *Trachurus insectus* n. sp., Dar bel Hamri, Zanclean, **b** holotype, SMF PO 101.283, **c–d** paratypes, SMF PO 101.284 (reversed). **e–g** *Caranx rhabdus* n. sp., Dar bel Hamri, Zanclean, **e** holotype, SMF PO 101.238, **f–g** paratypes, SMF PO 101.282 (reversed). **h–k** *Trachurus mediterraneus* (Steindachner, 1868), SMF PO 101.239 (**h, j** reversed), Dar bel Hamri. **l–o** *Verilus mutinensis* (Bassoli, 1906), SMF PO 101.240 (**m, n** reversed), Dar bel Hamri

angle and the shape and proportions of the sulcus. It differs from the four extant congeners occurring in the eastern Atlantic in the short rostrum and the peculiar shape of the dorsal rim with the broad lobe behind the middle and the postdorsal notch. Otoliths of the parallel occurring *T. mediterraneus* are further distinguished by the regularly rounded and intensely crenulated dorsal rim.

Trachurus mediterraneus (Steindachner, 1868)

Figure 22h–k

Material 32 specimens, figured specimens SMF PO 101.239, Dar bel Hamri, Zanclean.

Discussion Otoliths of *T. mediterraneus* differ from otoliths of *T. trachurus* in being slightly more compressed, showing a much stronger and finer crenulation of the dorsal and ventral rims and a more rounded postdorsal angle. Both species have been commonly recorded from Pliocene and Pleistocene sediments in the Mediterranean (e.g., Agiadi et al., 2019a).

Order Perciformes (sensu Nelson et al., 2016)

Family Acropomatidae Gill, 1891

Genus *Verilus* Poey, 1860

Verilus mutinensis (Bassoli, 1906)

Figure 22l–o

1906 Ot. (Sparidarum) *mutinensis*. Bassoli: pl. 2, Fig. 36.

2017 *Verilus mutinensis* (Bassoli, 1906)—Schwarzahans & Prokofiev: pl. 33, fig. L, M.

2018 *Verilus mutinensis* (Bassoli, 1906)—Agiadi et al.: Fig. 5/49–51.

2022 *Verilus mutinensis* (Bassoli, 1906)—van Hinsbergh & Hoedemakers: pl. 29, Figs. 1–4 (see there for further references).

Material 101 specimens, Zanclean, 99 specimens, Dar bel Hamri (figured specimens SMF PO 101.240), 2 specimens Jebel Zebbouj.

Discussion *Verilus mutinensis* is a long ranging and rather common species in the Mediterranean from the Tortonian (Bassoli, 1906) well into the Pleistocene (Agiadi et al., 2018). Today, the genus *Verilus* is not present anymore in the East Atlantic or Mediterranean.

Family Haemulidae Gill, 1885

Genus *Parapristipoma* Bleeker, 1873

Parapristipoma bethensis n. sp.

Figure 23a–c

Holotype SMF PO 101.285 (Fig. 23a), Dar bel Hamri, coquina at river level of Oued Beth, Zanclean.

Paratype 3 specimens SMF PO 101.286, same data as holotype.

Etymology Named after the Oued Beth along which the outcrops occur from which the otoliths were obtained.

Diagnosis OL:OH = 1.5–1.6. Dorsal rim irregularly undulating, highest anteriorly; ventral rim regularly curved. Cauda distinctly inclined at angle of 50–65°.

Description Relatively large and elongate otoliths with overall oval shape reaching 9.5 mm in length (holotype). OH:OT = 3.0. Dorsal rim gently curved and irregularly undulating, highest anteriorly, with rounded postdorsal region. Ventral rim relatively shallow, gently and regularly curved. Rostrum short, blunt to broadly rounded; no or very weak excisura or antirostrum. Posterior tip broadly rounded, slightly inferior.

Inner face distinctly convex, with slightly supramedian positioned, moderately deepened sulcus. Ostium short, its ventral rim box-shaped, the dorsal rim short and upward directed. Cauda long, narrow, reaching close to posterior tip of otolith, distinctly curved toward its tip. CaL:OsL = 1.75–1.85; OsH:CaH = 1.8–2.0. Dorsal field narrow, with indistinct, narrow depression; ventral field smooth without ventral furrow. Outer face concave, with small central umbo, smooth.

Discussion These otoliths readily differ from the more common haemulid otoliths at Dar bel Hamri (*Pomadasys incisus* and *P. zemmourensis* n. sp.) in the more slender shape, the shallower and more gently curved ventral rim and the more strongly bent caudal tip. *Parapristipoma bethensis* is characterized through its relatively elongate shape and the gently curved ventral rim as a member of the genus *Parapristipoma*. Three of four extant species of *Parapristipoma* are known from the east Atlantic. Otoliths are known from all of them (see Lombarte et al., 2006 and Nolf et al., 2009 for figures). Otoliths of *Parapristipoma bethensis* are less slender than those of *P. humile* (Bowdich, 1825) and the inner and outer faces are less strongly curved than in *P. humile* and *P. octolineatum* (Valenciennes, 1833) and the ostium is relatively shorter and wider. *Parapristipoma bethensis* resembles most *P. macrops* (Pellegrin, 1912) but differs in the rounded posterior rim (vs. tapering) and the broadly undulating anterior dorsal rim (vs. finely crenulated; see Lombarte et al., 2006 for figures of otoliths of *P. macrops*).

Genus *Pomadasys* Lacepède, 1802

***Pomadasys incisus* (Bowdich, 1825)**

Figure 23d–h

2010 *Pomadasys incisus* (Bowdich, 1825)—Schwarzahns: pl. 78, Figs. 1–6 (see there for further references).

2022 *Pomadasys incisus* (Bowdich, 1825)—van Hinsbergh & Hoedemakers: pl. 31, Fig. 1.

Material 518 specimens, Dar bel Hamri, Zanclean (figured specimens SMF PO 101.241).

Discussion *Pomadasys incisus* is one of the most common species in Dar bel Hamri. It is also a long-ranging species that has been recorded since the late Early Miocene (Schwarzahns, 2010, and references therein). The otoliths of *P. incisus* are also remarkable for a pronounced late ontogenetic morphological change whereby large otoliths (14 mm in length, Fig. 23d) become increasingly more elongate than smaller ones (8.7–11.8 mm in length, Fig. 23e–h) (see Lombarte et al., 2006, for figures of extant otoliths). This effect is also documented in the ontogenetic sequence depicted in Lombarte et al. (2006). Today, *P. incisus* is distributed from the Strait of Gibraltar to Angola and is also known from the western Mediterranean (Froese & Pauly, 2022).

***Pomadasys zemmourensis* n. sp.**

Figure 23j–l

Holotype SMF PO 101.242 (Fig. 23j), Dar bel Hamri, coquina at river level of Oued Beth, Zanclean.

Paratype 6 specimens SMF PO 101.243, same data as holotype.

Further material 15 specimens, same data as holotype.

Etymology Named after Zemmours, the region in Maroc of the origin of the described otoliths and the name of the Berber people native to this region.

Diagnosis OL:OH=1.4–1.5. Dorsal rim shallow, with depressed postdorsal region. Cauda only slightly inclined at angle of 25–40°.

Description Relatively large, moderately elongate and robust otoliths with overall oval shape reaching 9 mm in length (holotype 8.9 mm). OH:OT=2.5–3.0. Dorsal rim shallow, highest anteriorly, with depressed

postdorsal region, broadly undulating, often with small, broad postdorsal denticle. Ventral rim deep, regularly curved. Rostrum short, blunt; very weak excisura and antirostrum. Posterior tip pointed, more distinctly so than rostrum.

Inner face distinctly convex, with distinctly suprmedian positioned, moderately deepened sulcus. Ostium short, its ventral rim box-shaped, the dorsal rim short and upward directed. Cauda long, narrow, reaching close to posterior tip of otolith, only slightly inclined. CaL:OsL=2.2–2.35; OsH:CaH=1.5–1.6. Dorsal field narrow, with indistinct, narrow depression; ventral field smooth without ventral furrow. Outer face flat to slightly concave, smooth.

Discussion *Pomadasys zemmourensis* is one of the species of the genus *Pomadasys* with otoliths that exhibit only a mild inclination of the caudal tip; in most species of the genus, the inclination is much stronger, almost 90°. It differs from the coeval *P. incisus* in the specific shape of the dorsal rim and the lesser degree of the curvature of the caudal tip (25–40° vs. 45–55°).

***Pomadasys* sp.**

Figure 23i

Material 7 specimens, SMF PO 101.244, Dar bel Hamri, Zanclean.

Discussion These smaller and incomplete specimens differ from the *P. incisus* in the more strongly bent cauda, the dorsal rim with a broad mediodorsal bulge, and the posterior rim that is broad, blunt, and extending somewhat behind the caudal tip. Figure 23i shows the largest and best preserved specimen of 7.5 mm in length, which lacks the rostrum (reconstructed about 8.2 mm in length). These specimens probably represent a further species of *Pomadasys*, although they cannot be identified to species level.

Family Cepolidae Rafinesque, 1810**Genus *Cepola* Linnaeus, 1764*****Cepola lombartei* n. sp.**

Figure 24i–n

1989 *Cepola rubescens* Linnaeus, 1766—Nolf & Capetta: pl. 16, Fig. 4.

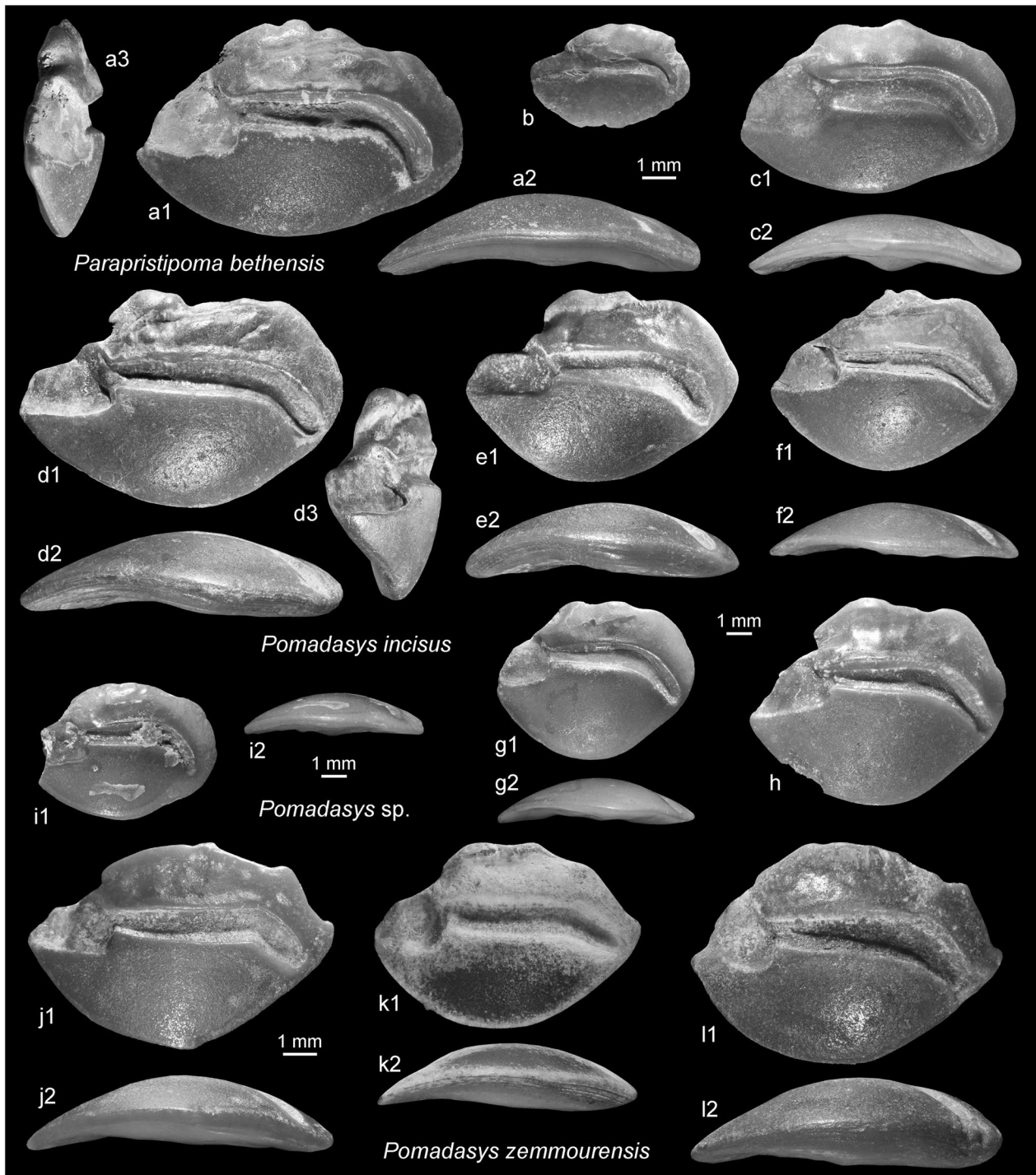


Fig. 23 Haemulidae. **a–c** *Parapristipoma bethensis* n. sp., Dar bel Hamri, Zanclean, **a** holotype, SMF PO 101.285, **b–c** paratypes, SMF PO 101.286. **d–h** *Pomadasys incisus* (Bowdich, 1825), SMF PO 101.241 (**d–g** reversed), Dar bel Hamri. **i**, *Pomadasys* sp. SMF PO 101.244, Dar bel Hamri. **j–l**, *Pomadasys zemmourensis* n. sp., Dar bel Hamri, Zanclean, **j** holotype, SMF PO 101.242 (reversed), **k–l** paratypes, SMF PO 101.243 (**k** reversed)

?2000 *Cepola rubescens* Linnaeus, 1766—Nolf & Girone: pl. 4, Fig. 22.

Holotype SMF PO 101.245 (Fig. 24i), Dar bel Hamri, coquina at river level of Oued Beth, Zanclean.

Paratype 5 specimens SMF PO 101.246, same data as holotype.

Further material 16 specimens, Zanclean, 5 specimens same data as holotype, 2 specimens Sidi Mohamed ech Chleuh, 1 specimen Asilah.

Etymology Named in honor of Antoni Lombarte (Barcelona) in recognition of his contribution to the knowledge of extant otoliths.

Diagnosis OL:OH=2.03–2.1. Dorsal and ventral rims shallow. Cauda very narrow. Ostial colliculum terminating at some distance from anterior opening. Collum narrow.

Description Slender, thin otoliths up to 4.2 mm in length (holotype). OH:OT=2.8–3.0. Dorsal and ventral rims shallow. Dorsal rim nearly straight in central section, with weak or indiscernible postdorsal angle and broadly rounded predorsal angle. Ventral rim regularly curved, sometimes flattened at its center. Anterior tip pointed in large specimens, less in smaller ones; posterior tip rounded in small specimens, becoming more pointed in large ones but less pointed than anterior tip. All rims smooth or slightly undulating.

Inner face distinctly convex, with slightly supramedian positioned narrow sulcus. OL:SuL=1.4–1.5. Sulcus anteriorly open, but ostial colliculum not reaching anterior rim of otolith but terminating at some distance from it. Cauda very small and narrow, slightly shifted upwards. OsL:CaL=2.1–2.5; OsH:CaH=1.6–2.0. Cauda somewhat deepened with caudal colliculum less well defined than ostial colliculum. Dorsal depression indistinct; ventral furrow moderately developed, distant from ventral rim of otolith, anteriorly departing from ventral rim and leading to anterior tip of ostial colliculum. Outer face flat to slightly concave, smooth.

Discussion The genus *Cepola* currently contains five recognized valid recent species. Otoliths are known from four of those (except *C. australis* Ogilby, 1899) and are figured here for comparison: *Cepola macrophthalma* (Linnaeus, 1758), known from the northeastern Atlantic and the Mediterranean (Fig. 24a); *C. pauciradiata* Cadenat, 1950, known from West Africa from Mauritania to Angola (Fig. 24e–f); *C. schlegelii* Bleeker, 1854, known from Indonesia and the West Pacific (Fig. 24g); and *C. haastii* (Hector, 1881) from New Zealand (Fig. 24h). The differences between the otoliths of these species are subtle and concern otolith proportions, course of the dorsal rim, and details of the sulcus. One important characteristic is the position of the ostial colliculum, which usually

terminates at some distance from the anterior rim of the otolith in all species except *C. macrophthalma*, where it reaches the anterior rim of the otolith or approaches very closely.

Cepola lombartei resembles the extant West African *C. pauciradiata* in otolith shape, but is more slender (OL:OH=2.03–2.1 vs. 1.85–1.9) and has a narrower cauda. It also lacks the well-developed postdorsal angle of *C. pauciradiata*. The Indo-West Pacific species (*C. schlegelii* and *C. haastii*) show a distinctly shorter ostial colliculum. It appears that *C. lombartei* has also been found in the Pliocene and possibly Pleistocene of the Mediterranean. These interpretations are based on published drawings (see synonymy listing) showing likewise slender otoliths with the ostial colliculum detached from the anterior rim of the otolith and are to be regarded tentative at present until revision.

Cepola macrophthalma (Linnaeus, 1758)

Figure 24a–d

1980 *Cepola macrophthalma* (Linnaeus, 1758) —Nolf & Martinell: pl. 4, Figs. 25, 26.

1994 *Cepola rubescens* Linnaeus, 1766—Nolf & Cavallo: pl. 7, Fig. 7.

1998 *Cepola rubescens* Linnaeus, 1766—Nolf, Mané & Lopez: pl. 7, Fig. 12.

2019a *Cepola macrophthalma* (Linnaeus, 1758)—Agiadi et al.: Fig. 5G.

2022 *Cepola macrophthalma* (Linnaeus, 1758)—van Hinsbergh & Hoedemakers: pl. 30, Figs. 3–5.

Material 27 specimens, Zanclean, 25 specimens Dar bel Hamri (figured specimens SMF PO 101.247), 1 specimen Sidi Mohamed ech Chleuh, 1 specimen Asilah.

Discussion For differentiation of *C. macrophthalma* otoliths from *C. lombartei*, see above. *Cepola macrophthalma* otoliths have been referred to since Early Miocene from the North Sea Basin and the Mediterranean but are in much need of revision. Most or all of the Miocene specimens probably represent different species for which at least three nominal species names are available: *C. praerubescens* Bassoli, 1906 (Tortonian of Italy), *C. voeslauensis* Schubert, 1907 (Badenian of Austria), and *C. multicrenata* Radwańska, 1984 (Badenian of Poland). For further discussion, see Schwarzhans (2014). Therefore, I

have accepted only Pliocene and younger otoliths as valid references here.

Genus *Owstonia* Tanaka, 1908

Owstonia sp.

Figure 24o

Material 1 specimen, SMF PO 101.248, Dar bel Hamri, Zanclean.

Discussion A single, relatively large otolith of 5.35 mm in length that is well preserved except for some slightly damaged section of the posterior rim. The otolith is characterized by the dorsal rim rising towards a pronounced postdorsal angle and the sulcus fading anteriorly with a small ostial colliculum positioned very far from the anterior rim of the otolith. The position of the ostial colliculum is considered typical for otoliths of the genus *Owstonia*.

Order Scorpaeniformes Garman, 1899

Family Triglidae Rafinesque, 1810

Genus *Peristedion* Lacepède, 1801

Peristedion cataphractum (Linnaeus, 1758)

Figure 24p

Material 1 specimen, SMF PO 101.249, Dar bel Hamri, Zanclean.

Suborder Trachiniformes Bertin & Aambourg, 1958

Family Trachinidae Rafinesque, 1810

Genus *Trachinus* Linnaeus, 1758

Trachinus armatus Bleeker, 1861

Figure 25a

2022 *Trachinus* sp.—van Hinsbergh & Hoedemakers: pl. 28, Figs. 7, 8.

Material 3 specimens, Dar bel Hamri, Zanclean (figured specimen SMF PO 101.250).

Discussion *Trachinus armatus* today lives along the shores of West Africa from Senegal to Angola (Schwarzhans & Kovalchuk, 2022) but has also been tentatively

recorded from the Middle Miocene of the Aquitaine Basin (Steurbaut, 1984). See Schwarzhans (2019c) for figures of extant trachinid otoliths.

Trachinus maroccanus n. sp.

Figure 25b–d

Holotype SMF PO 101.251 (Fig. 25b), Dar bel Hamri, coquina at river level of Oued Beth, Zanclean.

Paratype 4 specimens SMF PO 101.252, same data as holotype.

Further material 10 specimens, same data as holotype.

Etymology Named after Morocco, the country of origin of the specimens.

Diagnosis OL:OH = 1.8–1.9; OH:OT = 2.0–2.2. Otolith shape oval; otolith size up to 3 mm in length. Ostium slightly longer than cauda and of equal width (OsL:CaL = 1.15–1.3).

Description Small, robust, oval otoliths up to 3 mm in length (holotype). Dorsal and ventral rims regularly curved without marked angles. Anterior tip rounded, without distinct rostrum; posterior tip bluntly rounded. All rims smooth except dorsal rim sometimes somewhat undulating.

Inner face distinctly convex, smooth, with suprasedian positioned, narrow, slightly oscillating sulcus. Sulcus opening to anterior rim, posteriorly terminating far from posterior rim of otolith. Ostium not wider than cauda and only slightly longer. Dorsal depression very indistinct, above anterior part of sulcus and narrow, sometimes with few radial furrows from otolith rim; ventral furrow mostly distinct, close to ventral rim of otoliths, posteriorly curving upwards and inwards towards tip of cauda. Outer face slightly convex, less than inner face, smooth.

Discussion *Trachinus maroccanus* resembles otoliths of *T. armatus* (see above) and the Oligocene–Miocene *Echiichthys biscissus* (Koken, 1884). *Trachinus maroccanus* shares with both species the relatively small size, biconvex inner and outer faces, and the regular oval shape. It differs from *T. armatus* in being thinner, with the outer face being distinctly less convex than the inner face, being more elongate (OL:OH = 1.8–1.9 vs. 1.6–1.7), and the ostium not being wider than the cauda. From *E. biscissus* (figures in, e.g., Schwarzhans, 1994, 2008), it differs in being less elongate (OL:OH = 1.8–1.9 vs. 2.0–2.2),

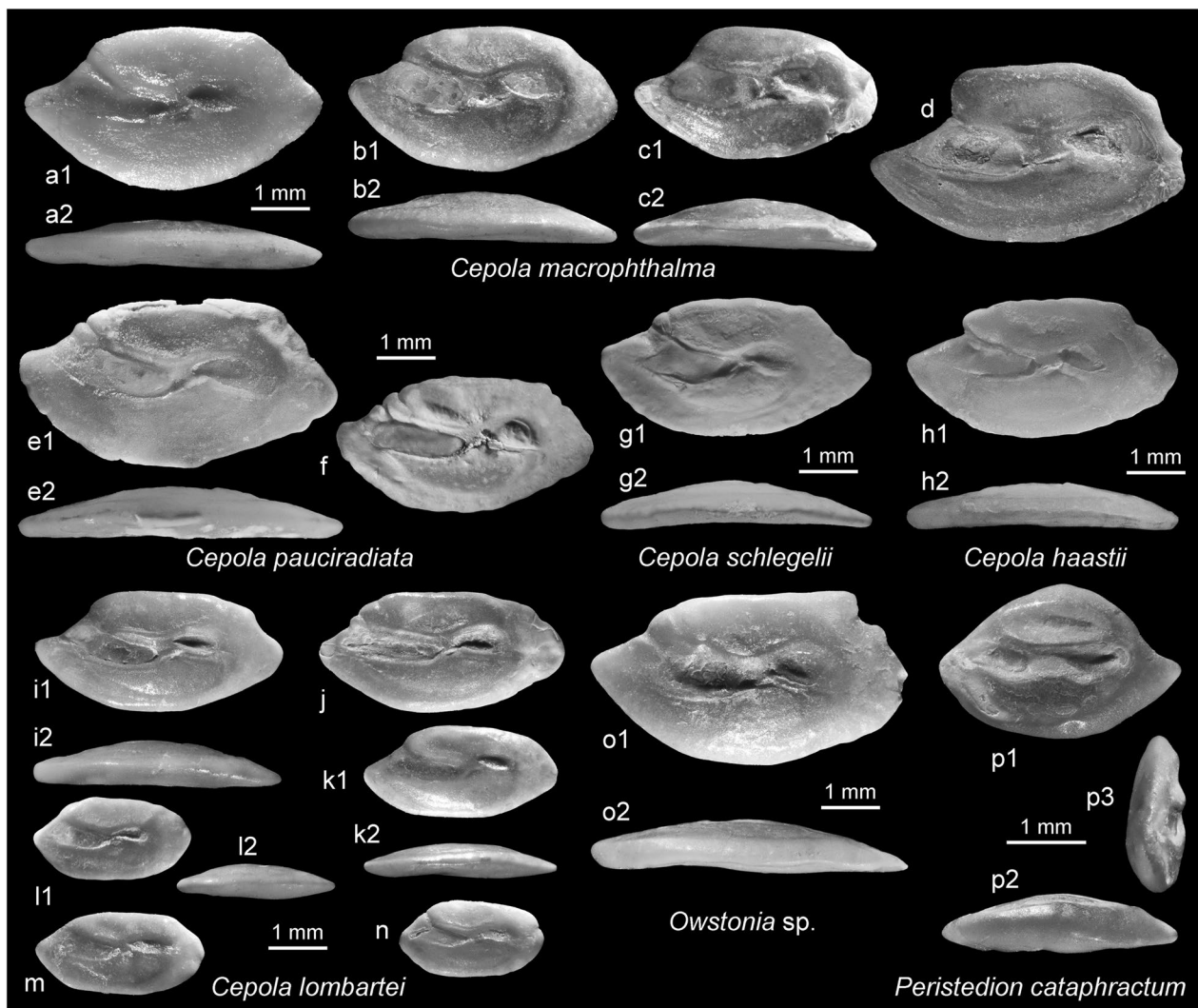


Fig. 24 Cepolidae and Triglidae. **a–d** *Cepola macrophthalmia* (Linnaeus, 1758), **a** extant, southwestern France (reversed), **b–d** Dar bel Hamri, Zanclean, SMF PO 101.247. **e–f** *Cepola pauciradiata* Cadenat, 1950, extant, **e**, CAS 235490, 14°11'N, 17°22'W, **f** refigured from Schwarzhans (2013a), dredge in the Gulf of Guinea, 04°39'N, 01°08'W. **g**, *Cepola schlegelii* Bleeker, 1854, NSMT 110130, Taiwan. **h** *Cepola haastii* (Hector, 1881), New Zealand (reversed). **i–n** *Cepola lombartei* n. sp., Dar bel Hamri, Zanclean, **i** holotype, SMF PO 101.245, **j–n** paratypes, SMF PO 101.246. **o** *Owstonia* sp. SMF PO 101.248, Dar bel Hamri. **p** *Peristedion cataphractum* (Linnaeus, 1758), SMF PO 101.249, Dar bel Hamri

showing different proportions of the ostium to cauda ($OsL:CaL = 1.15–1.3$ vs. $1.6–1.9$), and in the rounded anterior tip (vs. pointed). *Trachinus biscissus* has recently been placed in the *Echiichthys* (see Schwarzhans & Kovalchuk, 2022). Otoliths of the only extant species, *E. vipera* (Cuvier, 1829), have been figured in Nolf (2018) (as *Trachinus vipera*) and Lombarte et al. (2006). I maintain the view that *E. biscissus* and possibly the coeval related *E. verus* (Koken, 1891) should be placed in the clade with the extant *E. vipera*. However, *T. maroccanus* bears more resemblance to the clade with *T. armatus* (see Schwarzhans & Kovalchuk, 2022) and, therefore, is allocated to *Trachinus*. Several small *Trachinus* specimens from the

Pliocene of the Mediterranean and from Portugal have been allocated to *T. draco*, *T. radiatus*, or *T. sp.* (see Nolf & Martinell, 1980; Nolf & Cappetta, 1989; Nolf & Cavallo, 1994; Nolf & Marques da Silva, 1997; van Hinsbergh & Hoedemakers, 2022) and require review.

Trachinus wernlii n. sp.

Figure 25e–h

Holotype SMF PO 101.253 (Fig. 25g), Dar bel Hamri, coquina at river level of Oued Beth, Zanclean.

Paratype 7 specimens SMF PO 101.254, same data as holotype.

Further material 50 specimens, same data as holotype.

Etymology Named in honor of the late Roland Wernli (Genf) who laid the foundation for the Neogene biostratigraphy of Morocco.

Diagnosis OL:OH=2.35–2.5; OH:OT=2.6–3.1. Dorsal rim low; posterior rim with angular ventral tip. Sulcus narrow, ostium not wider than cauda and only slightly longer (OsL:CaL=1.1–1.4).

Description Large, elongate, thin otoliths up to 7 mm in length (holotype 6.4 mm). Dorsal rim low, shallower than ventral rim, both regularly curved without marked angles. Anterior tip moderately pointed but distinct rostrum; posterior rim slanted, straight to slightly concave, posterior tip with angular ventral projection. All rims smooth.

Inner face slightly convex, smooth, with supramedian positioned, narrow, distinctly oscillating sulcus. Sulcus opening to anterior rim, posteriorly terminating relatively close to dorsal part of posterior rim of otolith. Ostium not wider than cauda and only slightly longer. Dorsal field very narrow without discernable dorsal depression; ventral furrow feeble, very close to ventral rim of otoliths, posteriorly curving upwards and inwards towards tip of cauda. Outer face flat to slightly concave, smooth.

Discussion *Trachinus wernlii* belongs to the group comprising the extant *T. araneus* Cuvier, 1829, *T. collignoni* Roux, 1957, and *T. pellegrini* Cadenat, 1937, and the fossil *T. acutus* Weiler, 1942, from the Miocene of the North Sea Basin, *T. meridianus* Schwarzhans & Kovalchuk, 2022, from the Miocene of the Paratethys, and *T. unus* Müller, 1999, from the Miocene of Northeast America and the North Sea Basin (see Schwarzhans, 2019c, for figures of the extant species). This group is characterized by elongate and relatively thin otoliths (but not as elongate and thin as in the *Trachinus draco* group) and an ostium that is about 1.1 to 1.8 (mostly <1.6) the length of the cauda (vs. 1.5–2.0 in the *Trachinus draco* group). *Trachinus wernlii* is similar to the fossil Miocene species in appearance, but is more elongate (OL:OH=2.35–2.5 vs. 1.9–2.3), differs in the ratio OsL:CaL (1.1–1.4 vs. 1.4–1.8), and shows a lower dorsal rim, resulting in a narrower dorsal field. It further differs from *T. acutus* in the distinctly narrower sulcus. *Trachinus wernlii* shares the proportions of the sulcus (OsL:CaL=1.1–1.4 vs. 1.2–1.4) with *T. unus* Müller, 1999, but differs in the longer sulcus reaching closer to the posterior rim of the otolith and the

low dorsal rim. The low dorsal rim and the slender proportions also distinguish *T. wernlii* from the three mentioned extant species.

Family Uranoscopidae Bonaparte, 1831

Genus *Uranoscopus* Linnaeus, 1758

Uranoscopus ciabatta Girone, Nolf & Cavallo, 2010

Figure 25i

2010 *Uranoscopus ciabatta*—Girone, Nolf & Cavallo: Fig. 12b1–12b2.

2022 *Uranoscopus* sp.—van Hinsbergh & Hoedemakers: pl. 28, Fig. 11.

Material 2 specimens SMF PO 101.287, Dar bel Hamri, Zanclean.

Discussion *Uranoscopus ciabatta* was established based on two compact and thick otoliths from the pre-evaporitic Messinian of Piedmont, Italy, which fall out of the variation breadth observed in the extant *U. scaber* (see Girone et al., 2010). Van Hinsbergh and Hoedemakers (2022) described a unique very compressed otolith from the Piacenzian of Estepona as *Uranoscopus* sp. because of uncertainties in respect to the degree of variability known from the extant *U. scaber*. Now, with two more specimens of such compressed shape from the Zanclean of Morocco, these together with the Messinian and Piacenzian specimens are regarded as representing a single species, i.e., *U. ciabatta*.

Uranoscopus hoedemakersi n. sp.

Figure 25p–q

Holotype SMF PO 101.258 (Fig. 25p), Dar bel Hamri, coquina at river level of Oued Beth, Zanclean.

Paratypes 3 specimens SMF PO 101.288, same data as holotype.

Etymology Named in honor of Kristiaan Hoedemakers (Mortsel, Belgium) for his contribution to the knowledge of fossil otoliths.

Diagnosis OL:OH=1.8–1.9; OH:OT=2.45. Dorsal rim with broad middorsal expansion. Sulcus deepened, anteriorly closed, with clearly distinct ostium and cauda. Anterior and posterior tips symmetrical, moderately

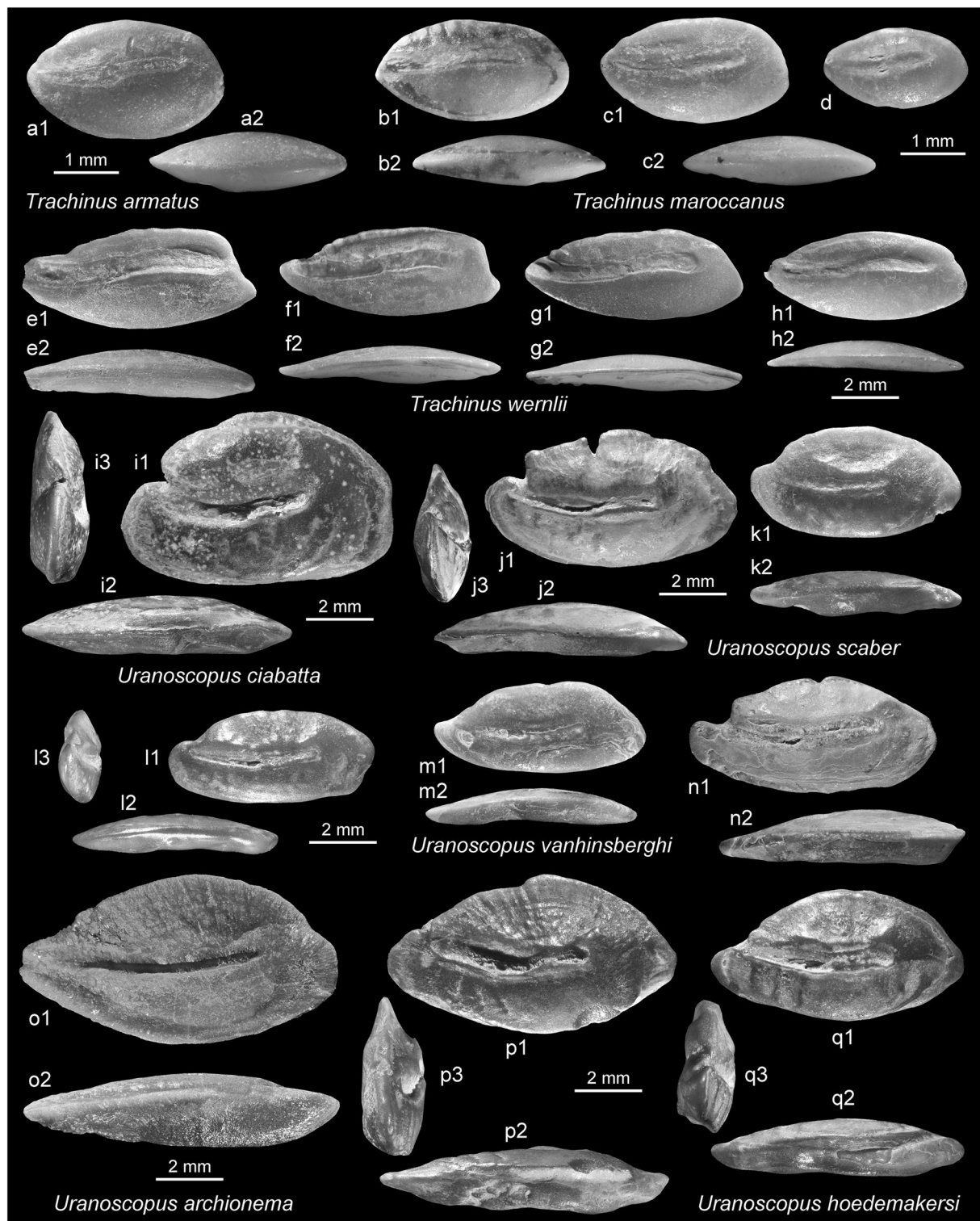


Fig. 25 Trachinidae and Uranoscopidae. **a** *Trachinus armatus* Bleeker, 1861, SMF PO 101.250, Dar bel Hamri. **b–d** *Trachinus maroccanus* n. sp., Dar bel Hamri, Zanclean, **b** holotype, SMF PO 101.251, **c–d** paratypes, SMF PO 101.252 (25c reversed). **e–h** *Trachinus wernlii* n. sp., Dar bel Hamri, Zanclean, 25 g holotype, SMF PO 101.253 (reversed), **e–f, h** paratypes, SMF PO 101.254 (**e, h** reversed). **i** *Uranoscopus ciabatta* Giron et al., 2010, SMF PO 101.287, Dar bel Hamri. **j–k** *Uranoscopus scaber* Linnaeus, 1758, Dar bel Hamri, SMF PO 101.255 (reversed). **l–n** *Uranoscopus vanhinsberghi* n. sp., Dar bel Hamri, Zanclean, **l** holotype, SMF PO 101.256 (reversed), **m–n** paratypes, SMF PO 101.257 (**n** reversed). **o** *Uranoscopus archionema* Regan, 1921, Madagascar (reversed). **p–q** *Uranoscopus hoedemakersi* n. sp., Dar bel Hamri, Zanclean, **p** holotype, SMF PO 101.258, **q** paratype, SMF PO 101.288

pointed. OL:SuL = 1.75–1.9; OsL:CaL = 1.8–2.2. Broad dorsal field with many radial furrows.

Description Robust, large otoliths up to 8.5 mm in length (holotype). Dorsal rim high, with broad medi-odorsal expansion and with flat predorsal and slightly curved postdorsal regions, almost triangular in shape, somewhat irregular. Ventral rim shallower than dorsal rim, regularly curved. Anterior tip inferior, strongly projecting, rounded. Posterior tip at level with anterior tip, symmetrical in expression but slightly less projecting.

Inner face mildly convex, with short, deepened, anteriorly closed sulcus. Ostium about twice as long as cauda and slightly wider, somewhat downward inclined towards collum. Cauda terminating far from posterior tip of otolith, slightly upward shifted against ostium. Dorsal depression very wide, dorsally open, with many radial furrows. Ventral field with three transverse furrows below central part of ostium. Ventral furrow running on ventral rim of otolith except somewhat turning inwards posteriorly. Outer face flat to slightly convex, somewhat irregularly shaped.

Discussion *Uranoscopus hoedemakersi* represents a different morphotype in the highly diverse genus *Uranoscopus* from the other species described here. The otoliths of the three tropical West African species—*U. albesca* Regan, 1915, *U. cadenati* Poll, 1959, and *U. polli* Cadenat, 1951—are known (Schwarzahans, 2019c) and also represent different morphotypes. Otoliths of *U. albesca* and *U. cadenati* are somewhat similar in otolith shape and in the reduced sulcus morphology, but show much further separation of the sulcus from the anterior rim and a small, completely unstructured sulcus. The closest morphotype is found in *U. archionema* Regan, 1921 (Fig. 25o), a species distributed in the southeastern Indian Ocean along East Africa from Kenya to South Africa, Madagascar, and Mauritius and Reunion (Froese & Pauly, 2022). Otolith shape, proportions, and robustness and the wide dorsal depression with radial furrows are all shared characteristics. *Uranoscopus hoedemakersi* differs from *U. archionema* in the shorter sulcus (OL:SuL = 1.75–1.9 vs. 1.4) and the clearly structured sulcus with well-defined ostium and cauda (vs. contiguous ostium and cauda). Both species are thought to represent a vicariant species pair.

Uranoscopus scaber Linnaeus, 1758

Figure 25j–k

2022 *Uranoscopus scaber* Linnaeus, 1758—van Hinsbergh & Hoedemakers: pl. 28, Fig. 10 (see there for further references).

Material 20 specimens, Dar bel Hamri, Zanclean (figured specimens SMF PO 101.255).

Discussion *Uranoscopus scaber* is known for its large range in variability (see figures and discussion in Girone et al., 2010 and figures in Lombarte et al., 2006). Most *Uranoscopus* otoliths found in Dar bel Hamri can be convincingly placed within the morphological limits depicted by Lombarte et al. (2006) for *U. scaber*.

Uranoscopus vanhinsberghi n. sp.

Figure 25l–n

Holotype SMF PO 101.256 (Fig. 25m), Dar bel Hamri, coquina at river level of Oued Beth, Zanclean.

Paratype 4 specimens SMF PO 101.257, same data as holotype.

Etymology Named in honor of Victor van Hinsbergh (Leiden, the Netherlands) for his contribution to the knowledge of fossil otoliths.

Diagnosis OL:OH = 2.15–2.35; OH:OT = 2.2–2.8. Rostrum massive, moderately long, 13–17% OL. OsL:CaL = 1.1–1.4. Outer face flat to concave.

Description Elongate, thin and rather large otoliths reaching 7.3 mm in length (holotype 6.05 mm). Dorsal rim relatively shallow, irregular, slightly undulating, highest at its middle, without prominent angles; ventral rim shallow, gently curved. Rostrum well developed, relatively long and massive, with rounded tip. Excisura wide, broadly concave; no or very feeble antirostrum. Posterior rim blunt, with central or inferior rounded tip.

Inner face distinctly convex, with moderately long, slightly bent, shallow sulcus. Ostium slightly longer than cauda and slightly wider, its anterior opening indistinct. OL:SuL = 1.5–1.7. Distinction of ostium and cauda and of colliculi feeble. Dorsal depression wide, dorsally open, with indistinct margins. Ventral furrow rarely visible, then very close to ventral margin of otolith. Outer face flat to concave, smooth.

Discussion *Uranoscopus vanhinsberghi* is closely related to *U. scaber* and differs in being more slender and thinner

and showing a more massive rostrum. The species thus falls outside the range of variations shown in Lombarte et al. (2006) for *U. scaber*. *Uranoscopus vanhinsbergi* may represent a sympatric vicariant species to the extant *U. scaber*, known in parallel from Dar bel Hamri and today from the Mediterranean and in the adjacent Atlantic from the British Isles to Mauritania.

Order Spariformes Akazaki, 1962

Family Sparidae Rafinesque, 1810

Remarks The Sparidae represent the family with the largest diversity in Dar bel Hamri with 15 species. The distinction of the otoliths of the many species often depends on rather subtle traits such as proportions of the otolith or the sulcus, curvature of inner and outer face, details of the otolith outline particularly of the dorsal rim and curvature of the caudal tip. Many small or poorly preserved specimens in the collection from Dar bel Hamri cannot be identified to species level and therefore are omitted from the description. Fortunately, many large and well preserved sparid otoliths exist as well from Dar bel Hamri and allow recognition of taxa. The allocation of the otoliths to genera of the Sparidae is also a delicate task and often depends on direct comparison with extant species since no useful traits have been identified for a definition of genera by means of otoliths. Some genera contain rather different otolith morphological patterns, for instance *Pagellus* or *Dentex*. In the case of *Dentex*, the highly diverse otolith patterns strongly support the separation of the formal genus in independent clades as depicted in Chiba et al. (2009) and Santini et al. (2014). However, a character analysis of sparid otoliths has not yet been done, but see also comment to *Dentex*.

Genus *Boops* Cuvier, 1814

Boops boops (Linnaeus, 1758)

Figure 26a–b

1997 *Boops boops* (Linnaeus, 1758) —Nolf & Marques da Silva: pl. 1, Fig. 13.

2022 *Boops boops* (Linnaeus, 1758) —van Hinsbergh & Hoedemakers: pl. 33, Figs. 1–4.

Material 3 specimens, Zanclean, 2 specimens SMF PO 101.259, Dar bel Hamri, 1 specimen SMF PO 101. 260, Asilah.

Discussion Otoliths of *Boops boops* are recognized by the highly characteristic dorsal rim with the sharply bordered, flat, box-shaped postdorsal expansion (see Nolf et al., 2009 for extant otoliths). Today, the species occurs in the Mediterranean and the East Atlantic from Norway to Angola. It has also been recorded as fossil from the Piacenzian of Portugal (Nolf & Marques da Silva, 1997).

Genus *Diplodus* Rafinesque, 1810

Diplodus bellottii (Steindachner, 1882)

Figure 26d–f

1997 *Diplodus* aff. *bellottii* (Steindachner, 1882) —Nolf & Marques da Silva: pl. 2, Figs. 13, 14.

Material 20 specimens (figured specimens SMF PO 101.261), Dar bel Hamri, Zanclean.

Discussion Otoliths of *Diplodus bellottii* differ from those of its congeners by the relatively straight and distinctly inclined cauda (see Lombarte et al., 2006, for figures of extant otoliths). Nolf and Marques da Silva (1997) reported this species tentatively because of incomplete preservation from the Piacenzian of Portugal, which, following the new specimens from Morocco, can now be allocated with more certainty. Today, *Diplodus bellottii* occurs from southern Spain (Malaga, Cadiz) to the Cape Verde islands (Froese & Pauly, 2022). Its occurrence in the Alboran Sea is considered to represent a recent immigration through the Strait of Gibraltar (Golani et al., 2021).

Genus *Oblada* Cuvier, 1829

Oblada melanura (Linnaeus, 1758)

Figure 26c

2022 *Oblada melanura* (Linnaeus, 1758)—van Hinsbergh & Hoedemakers: pl. 33, Figs. 12, 13.

Material 7 specimens, Dar bel Hamri, Zanclean (figured specimen SMF PO 101.262).

Genus *Pagellus* Valenciennes, 1830

Pagellus acarne (Risso, 1827)

Figure 26j

1980 *Pagellus* cf. *acarne* (Risso, 1827)—Nolf & Martinell: pl. 4, Fig. 13.

2022 *Pagellus acarne* (Risso, 1827)—van Hinsbergh & Hoedemakers: pl. 34, Figs. 3–8.

Material 7 specimens, Dar bel Hamri, Zanclean (figured specimen SMF PO 101.289).

Discussion Otoliths of *Pagellus acarne* resemble those of *Diplodus bellottii* in shape and proportions but differ in the relatively longer cauda (CaL:OsL = 1.4–1.5 vs. 1.1–1.3) and the fine crenulation of all otolith rims.

***Pagellus bellottii* Steindachner, 1882**

Figure 26k

1997 *Pagellus* aff. *bellottii* Steindachner, 1882—Nolf & Marques da Silva: pl. 2, Figs. 3, 4.

2022 *Pagellus* cf. *bellottii* Steindachner, 1882—van Hinsbergh & Hoedemakers: pl. 36, Fig. 7.

Material 13 specimens, Dar bel Hamri, Zanclean (figured specimen SMF PO 101.263).

Discussion Otoliths of *Pagellus bellottii* are characterized by a relatively high body and pronounced mid- and postdorsal angles (see Lombarte et al., 2006 for figures of extant otoliths). They resemble *P. erythrinus* but are more compressed. Today, *Pagellus bellottii* occurs from the Strait of Gibraltar to Angola (Froese & Pauly, 2022). Its occurrence in the Mediterranean is considered to represent a recent immigration through the Strait of Gibraltar (Golani et al., 2021).

***Pagellus bogaraveo* (Brünnich, 1768)**

Figure 26g–i

1979 *Pagellus* aff. *bogaraveo* (Brünnich, 1768)—Lanckneus & Nolf: pl. 3, Fig. 2.

2022 *Pagellus bogaraveo* (Brünnich, 1768)—van Hinsbergh & Hoedemakers: pl. 34, Fig. 9 (?11–13, non 10).

Material 26 specimens, Dar bel Hamri, Zanclean (figured specimens SMF PO 101.264).

Discussion Large specimens of *P. bogaraveo* are characterized by a slender shape, rough crenulation of the

dorsal rim, and a distinctive twist of the otolith along the long axis (Fig. 26g2). The rostrum is sometimes bent downward at its tip (Fig. 26h). However, otoliths of *P. bogaraveo* show a pronounced ontogenetic allometry, and smaller specimens are sometimes difficult to distinguish from other *Pagellus* species, notably *P. erythrinus*. A large ontogenetic series of extant otoliths is depicted by Lombarte et al. (2006). Today, *P. bogaraveo* is distributed from Norway to Mauritania and in the western Mediterranean (Froese & Pauly, 2022).

***Pagellus erythrinus* (Linnaeus, 1758)**

Figure 26l

1979 *Pagellus* aff. *erythrinus* (Linnaeus, 1758)—Lanckneus & Nolf: pl. 3, Fig. 4.

1980 *Pagellus* aff. *erythrinus* (Linnaeus, 1758)—Nolf & Martinell: pl. 4, Figs. 14, 15.

1988 *Pagellus* aff. *erythrinus* (Linnaeus, 1758)—Nolf & Cappetta: pl. 15, Fig. 10.

1994 *Pagellus erythrinus* (Linnaeus, 1758)—Nolf & Cavallo: pl. 7, Fig. 5.

1997 *Pagellus erythrinus* (Linnaeus, 1758)—Nolf & Marques da Silva: pl. 2, Figs. 6, 7.

2022 *Pagellus erythrinus* (Linnaeus, 1758)—van Hinsbergh & Hoedemakers: pl. 36, Figs. 4–6.

?2022 *Pagellus bogaraveo* (Brünnich, 1768)—van Hinsbergh & Hoedemakers: pl. 34, Fig. 10 non 9, 11–13).

Material 41 specimens, Dar bel Hamri, Zanclean (figured specimen SMF PO 101.265).

Discussion Otoliths of *P. erythrinus* are amongst the most common sparids recorded from the European Pliocene. They differ from otoliths of *P. bellottii* primarily in being slightly more elongate (OL:OH = 1.4 vs. 1.3). Today, the species is distributed from Norway to Guinea Bissau and in the Mediterranean (Froese & Pauly, 2022).

Genus *Pagrus* Cuvier, 1816

***Pagrus pagrus* (Linnaeus, 1758)**

Figure 26m–o

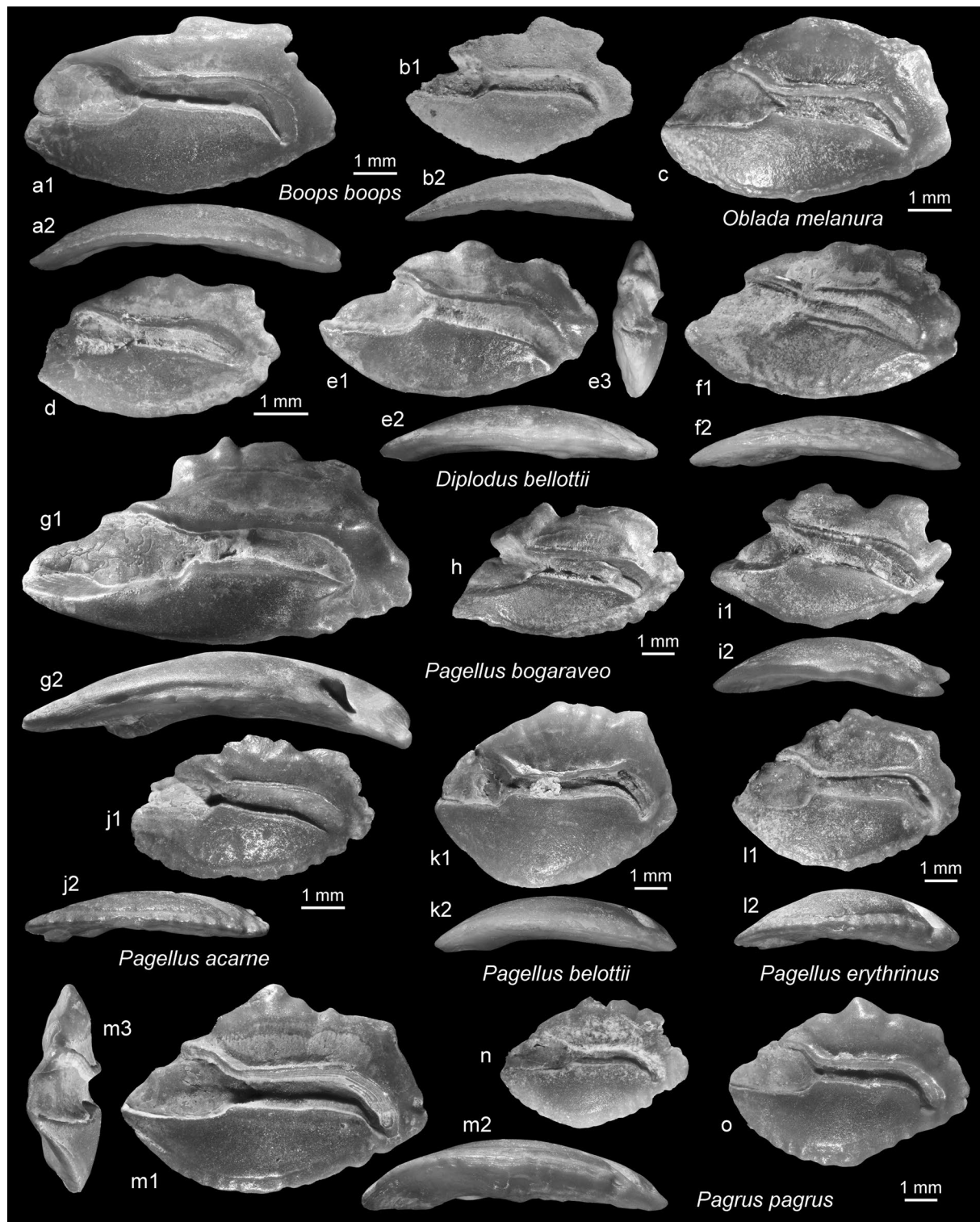


Fig. 26 Sparidae. **a–b** *Boops boops* (Linnaeus, 1758), **a** SMF PO 101.259 (reversed), Dar bel Hamri, **b** SMF PO 101.260 (reversed), Asilah. **c** *Oblada melanura* (Linnaeus, 1758), SMF PO 101.262 (reversed), Dar bel Hamri. **d–f** *Diplodus bellottii* (Steindachner, 1882), SMF PO 101.261 (**e–f** reversed), Dar bel Hamri. **g–i** *Pagellus bogaraveo* (Brünnich, 1768), SMF PO 101.264 (reversed), Dar bel Hamri. **j** *Pagellus acarne* (Risso, 1827), SMF PO 101.289 (reversed), Dar bel Hamri. **k** *Pagellus bellottii* Steindachner, 1882, SMF PO 101.263 (reversed), Dar bel Hamri. **l** *Pagellus erythrinus* (Linnaeus, 1758), SMF PO 101.265, Dar bel Hamri. **m–o** *Pagrus pagrus* (Linnaeus, 1758), SMF PO 101.290, Dar bel Hamri

Material 39 specimens, Dar bel Hamri, Zanclean (figured specimen SMF PO 101.290).

Discussion Otoliths of *Pagrus pagrus* are very similar to those of *Pagellus erythrinus* differing mainly in being slightly more elongate (OL:OH = 1.45–1.5 vs 1.4), which is partly counterbalanced by a more pronounced middorsal projection (Fig. 26m). *Pagrus pagrus*, *Pagellus erythrinus* and *Pagellus bellottii* are resolved in one clade in the molecular phylogenetic studies in Chiba et al. (2009) and Santini et al. (2014). Otolith morphology confirms such interrelationships.

Genus *Spicara* Rafinesque, 1810

Spicara alta (Osório, 1917)

Figure 27d

2022 *Spicara alta* (Osório, 1917)—van Hinsbergh & Hoedemakers: pl. 36, Figs. 8, 9.

Material 24 specimens, Dar bel Hamri, Zanclean (figured specimen SMF PO 101.291).

Discussion Fossil otoliths of *S. alta* were first described by van Hinsbergh and Hoedemakers (2022) from the Piacenzian of Estepona, Spain. It is relatively common in the Zanclean of Dar bel Hamri, and as commented by van Hinsbergh & Hoedemakers can be easily confused with small specimens of species of *Opsodentex*. They differ from *O. angolensis* in the lesser curvature of the inner face and the lesser curvature of the caudal tip. In the molecular phylogenetic analysis of Chiba et al. (2009), *Spicara alta* resolves in a clade also containing species of *Dentex* which are here placed in *Opsodentex*. Such a relationship of *Spicara alta* would be consistent with its otolith morphology. *Spicara alta* today lives along the tropical west African coast from Senegal to southern Angola (Froese & Pauly, 2022).

Spicara smarís (Linnaeus, 1758)

Figure 27a

2022 *Spicara smarís* (Linnaeus, 1758)—van Hinsbergh & Hoedemakers: pl. 35, Figs. 3–6.

Material 2 specimens SMF PO 101.292, Dar bel Hamri, Zanclean.

Discussion Two relatively small (4.5 mm in length) and slender otoliths (OL:OH = 1.75) are interpreted to

represent *S. smarís*. They are further characterized by a low curvature of the inner face and a nearly straight caudal tip. For figures of extant otoliths of *Spicara* otoliths see Nolf et al. (2009). *Spicara smarís* occurs today in the Mediterranean and adjacent region of the northeast Atlantic.

Genus *Spondyliosoma* Cantor, 1849

Spondyliosoma tingitana n. sp.

Figure 27b–c

Holotype SMF PO 101.293 (Fig. 27c), Dar bel Hamri, coquina at river level of Oued Beth, Zanclean.

Paratype 4 specimens SMF PO 101.294, same data as holotype.

Etymology From “Mauretania tingitana” (Latin) = the Roman name for the northwestern Moroccan region, deduced from Tingis (Latin), the ancient name of Tanger.

Diagnosis OL:OH = 1.75 to approximately 2.0. Ventral rim very shallow, regularly curved; dorsal rim with low predorsal and distinct postdorsal angle; posterior rim slanted, concave. Rostrum relatively short, 15% OL. CaL:OsL = 1.6. Curvature of caudal tip 45–55°, terminating moderately close to postventral rim.

Description Moderately large, elongate and thin otoliths up to at least 8 mm in length judging from the incomplete specimen of Fig. 27b (holotype 5.7 mm). OH:OT = 3.4–3.7. Ventral rim shallow, regularly curved, smooth; dorsal rim with low predorsal angle, more pronounced postdorsal angle, slightly to irregularly undulating. Rostrum relatively short (completely preserved only in specimens of Fig. 27c); no antirostrum or excisura. Posterior rim slanted, concave below postdorsal angle, with rounded or projecting inferior tip.

Inner face slightly convex with distinctly supramedian positioned, moderately deep, long sulcus. Ostium short, wide. Cauda long, anteriorly straight, its tip bend downward at 45 to 55°; caudal tip tapering or rounded, terminating moderately close to postventral otolith rim. Dorsal depression narrow, short, ventrally marked by crista superior, dorsal margin indistinct; ventral field with feeble ventral furrow close to ventral rim of otolith. Outer face distinctly concave, relatively smooth.

Discussion The genus *Spondyliosoma* contains two species today, *S. cantharus* (Linnaeus, 1758) in the Mediterranean and northeast Atlantic from the British Isles

to Namibia (Froese & Pauly, 2022; for extant otoliths see Lombarte et al., 2006 and Nolf et al., 2009) and *S. emarginatum* (Valenciennes, 1830) in the southwestern Indian Ocean along the shores of South Africa and Madagascar (Froese & Pauly, 2022; for extant otoliths see Smale et al. 1995). *Spondyliosoma tingeana* resembles the otoliths of both extant species, but differ in the relatively strongly developed postdorsal angle, concave posterior rim and in being less strongly bent.

Genus *Dentex* Cuvier, 1814

Remarks The genus *Dentex* has been subdivided into several subgenera, most of which are regarded as valid genera in the recent literature (Fricke et al., 2022). Molecular studies (Chiba et al., 2009 and Santini et al., 2014) have consistently shown the genus *Dentex* to be polyphyletic. The species currently allocated to *Dentex* (Froese & Pauly, 2022) contain two distinct otolith morphologies, one with more elongate otoliths and the other with more compressed otoliths (Nolf, 1979). As far as their otoliths are known, the distinction of the two otolith morphotypes reflects the clustering of the molecular phylogeny. The type species, *Dentex dentex*, belongs to the elongate otolith morphotype. The compressed otolith morphotype is found in the species *D. angolensis*, *D. congoensis*, *D. macrophthalmus* and *D. maroccanus* (see Nolf, 1979). *Dentex macrophthalmus* is the type species of *Opsodentex*, established as subgenus of *Dentex* by Fowler (1925). In the light of the congruence of molecular and otolith morphology data I, therefore, propose to use *Opsodentex* as a valid genus for the above mentioned four nominal *Dentex* species, the fossil otolith-based *Dentex gregarius* (Koken, 1891) and *Opsodentex mordax* n. sp. described in the following. Fossil otolith-based evidence shows that these two morphotypes belong to lineages that have been separate since at least the Late Oligocene (Schwarzhan, 1994, 2010). It should be noted, however, that distinction of *Opsodentex*, *Polysteganus* and *Evynnis* by means of otoliths is complex and requires further investigation.

Dentex canariensis Steindachner, 1881

Figure 27e–f

Material 12 specimens, Dar bel Hamri, Zanclean (figured specimens SMF PO 101.266).

Discussion Otoliths of *D. canariensis* are similar to those of *D. dentex* and differ in only a few subtle features: OL:OH ratio (1.5–1.6 vs. 1.65–1.7; *D. canariensis* first),

being more strongly bent along the long axis of the otolith, a blunter posterior tip, and a more strongly bent caudal tip. However, many of these characteristics appear to be considerably variable and thus may only be useful for distinction in combination (see Lombarte et al., 2006, for extant otoliths of both species). *Dentex canariensis* occurs in the tropical East Atlantic from Cabo Bojador to Angola (Froese & Pauly, 2022).

Dentex dentex (Linnaeus, 1758)

Figure 27h–i

Material 19 specimens, Dar bel Hamri, Zanclean (figured specimens SMF PO 101.267).

Discussion For distinction from otoliths of *D. canariensis*, see above. *Dentex dentex* is distributed in the Mediterranean and northeastern Atlantic from the British Isles to Mauritania (Froese & Pauly, 2022); today, it has only a small area of overlap with the vicariant *D. canariensis* (see above).

Genus *Opsodentex* Fowler, 1925

Opsodentex angolensis (Poll & Maul, 1953)

Figure 27g

Material 14 specimens, Dar bel Hamri, Zanclean (figured specimen SMF PO 101.268).

Discussion The distinction of the four extant species in *Opsodentex* (*O. angolensis*, *O. congoensis*, *O. macrophthalmus*, *O. maroccanus*) is difficult and may not be possible in many cases. Veen and Hoedemakers (2005) commented that these species could not be distinguished and combined their otoliths in a “group de *Dentex maroccanus*.” Van Hinsbergh and Hoedemakers (2022), however, distinguish otoliths of *O. macrophthalmus* and *O. maroccanus* in the Pliocene of Estepona near Málaga without giving a rationale. It appears that they concluded that *O. macrophthalmus* has more stretched otoliths than *O. maroccanus*, a view that I follow. *Opsodentex angolensis* is similar to the otoliths of *O. macrophthalmus* but differs in a more strongly bent caudal tip (up to 60°), although this is not evident in all cases studied by me or figured in the literature (see Veen & Hoedemakers, 2005, and Lombarte et al., 2006). Today, *O. angolensis* is distributed from Mauritania to Angola (Froese & Pauly, 2022).

Opsodentex mordax n. sp.

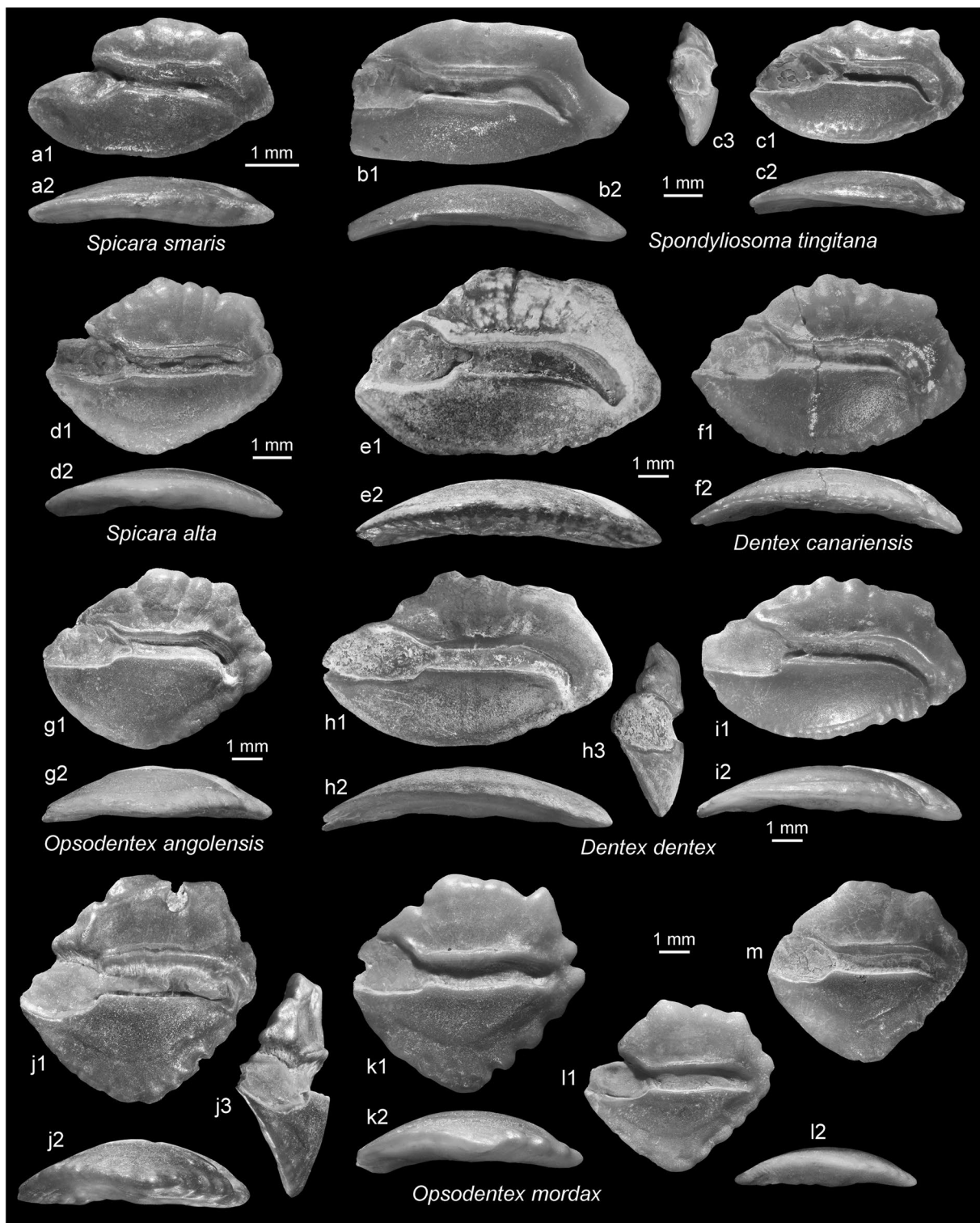


Fig. 27 Sparidae. **a** *Spicara smaris* (Linnaeus, 1758), SMF PO 101.292, Dar bel Hamri. **b–c** *Spondyllosoma tingitana* n. sp., Dar bel Hamri, Zanclean, **c** holotype, SMF PO 101.293 (reversed), **b** paratype, SMF PO 101.294 (reversed). **d**, *Spicara alta* (Osório, 1917), SMF PO 101.291, Dar bel Hamri. **e–f** *Dentex canariensis* Steindachner, 1881, SMF PO 101.266 (**f** reversed), Dar bel Hamri. **g** *Opsodentex angolensis* Poll & Maul, 1953, SMF PO 101.268. **h–i** *Dentex dentex* (Linnaeus, 1758), SMF PO 101.267 (**h** reversed). **j–m** *Opsodentex mordax* n. sp., Dar bel Hamri, Zanclean, **j** holotype, SMF PO 101.269 (reversed), **k–m** paratypes, SMF PO 101.295 (**k–l** reversed)

Figure 27j–m

Holotype SMF PO 101.269 (Fig. 27j), Dar bel Hamri, coquina at river level of Oued Beth, Zanclean.

Paratype 6 specimens SMF PO 101.295, same data as holotype.

Further material 23 specimens, same data as holotype.

Etymology From *mordax* (Latin) = cynical, referring to the presence of a further species of *Opsodentex* in North Africa.

Diagnosis OL:OH = 1.02–1.1. Ventral rim deep, with distinct midventral angle; dorsal rim high, coarsely lobate. Rostrum short, blunt, 15–20% OL. CaL:OsL = 1.6–1.7. Curvature of caudal tip 10–20°, terminating close to posterior rim. Ventral furrow distant from ventral rim of otolith.

Description Moderately large, high-bodied and compact otoliths up to at least 9 mm in length (holotype 7.2 mm). OH:OT = 3.5–4.5, decreasing with size. Ventral rim deep, with prominent midventral angle, preventral section nearly smooth, postventral section undulating; dorsal rim high, with narrow placed predorsal and postdorsal angles, predorsal angle higher, predorsal and postdorsal rims steeply inclined, nearly straight; dorsal rim coarsely and irregularly lobate. Rostrum relatively short; weak antirostrum and excisura. Posterior tip angular, positioned slightly higher than rostral tip.

Inner face distinctly convex with distinctly suprmedian positioned, moderately deep, long sulcus reaching close to posterior tip of otolith. Ostium short, wide. Cauda long, its tip very slightly bend at 10 to 20°, mostly less than 15°; caudal tip rounded. Dorsal depression broad, large, ventrally marked by crista superior, dorsally fading. Ventral furrow mostly distinct, positioned distantly from ventral rim of otolith and less strongly bend, thus leaving widest space between them at middle of section; ventral field smooth above ventral furrow, irregularly sculptured or plicated below. Outer face flat to slightly concave, with some irregular radial furrows.

Discussion *Opsodentex mordax* is clearly distinguished from its extant congeners by two distinct traits: the compressed shape with the ratio OL:OH not exceeding 1.1 (vs. > 1.25) and the position of the ventral furrow distant from the ventral rim of the otolith (vs. parallel and close to ventral rim of otolith). The latter character can become obliterated when the otolith is slightly eroded or the

ventral rim of the otolith has become abraded. It is also less clearly developed in specimens smaller than 5 mm in length.

Order Acanthuriformes Berg, 1930

Family Sciaenidae Cuvier, 1828

Genus *Afroscion* Trewavas, 1977

Afroscion trewavasae Schwarzhans, 1993

Figure 28a–d

1993 *Afroscion trewavasae*—Schwarzhans: Fig. 246–250.

1997 *Afroscion trewavasae* Schwarzhans, 1993—Nolf & Marques da Silva: pl. 3, Figs. 1–6.

Material 1564 specimens, Dar bel Hamri, Zanclean, figured specimens are photographs of holotype, SMF P 8226 (Fig. 28b) and paratypes, SMF P 8227 (Fig. 28a, c–d).

Discussion *Afroscion trewavasae* is the most common species at Dar bel Hamri. I know of no other fossil otolith location where a sciaenid species represents the most common species. Furthermore, the majority of specimens are large, in the size category of 8 to 14 mm in length, while specimens 5 mm in length (Fig. 28d) or smaller are rare. At Vale de Freixo (Portugal, Piacenzian) Nolf and Marques da Silva (1997) recorded *A. trewavasae* as one of the most common species in their assemblage, trailing only a goby (*Deltentosteus* sp.) and an ophidiid (*Ophidion rochei*), but they described a more continuous ontogenetic sequence starting with specimens slightly over 1 mm in length. *Afroscion* contains a single extant species, *A. thorpei* (Smith, 1977), distributed in south-eastern Africa from Mozambique to Algoa Bay, where juveniles are found on sand and mud and adults predominantly on reefs (Sasaki in Heemstra et al. 2022). Even though obviously not reef-associated, it appears likely that the fossil northeastern Atlantic *A. trewavasae* lived in different environments during its ontogeny. *Afroscion* is often placed as a junior synonym of *Argyrosomus* de La Pylaie, 1835, since Sasaki and Kailola (1988), but in the light of its distinct lineage and disjunctive distribution pattern, I consider it valid.

Genus *Atractoscion* Gill, 1862

Atractoscion cf. *macrolepis* Song, Kim & Kim, 2017

Figure 28e

Material 1 specimen, SMF PO 101.296, Dar bel Hamri, Zanclean.

Discussion In a recent analysis of Song et al. (2017) the hitherto widely distributed East Atlantic/Indo-West Pacific species *A. aequidens* (Cuvier, 1830) has been subdivided into four geographically separated species. Specimens from West Africa are placed in *A. macrolepis*, while *A. aequidens* is restricted to South Africa. Therefore, specimens figured from South Africa in Schwarzhans (1993) and Smale et al. (1995) would represent *A. aequidens* and specimens figured in Lombarte et al. (2006) from Mauritania may represent *A. macrolepis*. However, Song et al. only studied *A. macrolepis* specimens from Angola and Namibia and, therefore, the identity of further northerly specimens remains tentative. The unique specimen from Dar bel Hamri is consistent with the morphology of the extant specimens from Mauritania figured by Lombarte et al. and should represent the same species. Song et al. figured an otolith of *A. microlepis* Song et al., 2017, but a comprehensive analysis of the otoliths of the various extant species of the genus is still outstanding.

Genus *Pseudotolithus* Bleeker, 1863

Pseudotolithus cf. *typus* Bleeker, 1863

Figure 28g

Material 1 specimen, SMF PO 101.270, Dar bel Hamri, Zanclean.

Discussion The single, relatively large otolith of 8.6 mm in length is very similar in all morphological aspects to the extant *P. typus* known from Mauritania to Angola (see Schwarzhans, 1993 for figures of extant specimens). The identification, however, is only tentative because of some abrasion of the anterior otolith rim and in the area of the caudal tip.

Pseudotolithus sp.

Figure 28h

2003 *Pteroscion* sp. 2—Mendiola & Martínez: pl. 12, Figs. 17–19, pl. 17, Figs. 1–8.

Material 1 specimen, SMF PO 101.271, Dar bel Hamri, Zanclean.

Discussion An otolith of 9.5 mm in length represents a second species of the genus *Pseudotolithus*. It differs

from *P. cf. typus* (see above) in the slightly more compressed shape (OL:OH=1.6 vs. at least 1.75), the much thicker outer face with a massive postcentral umbo (OH:OT=1.35 vs. 1.6), the much less pronounced twist of the ventral margin of the otolith, and the small expansion of the outer face over the postdorsal rim (vs. significant overlap). The otolith resembles the extant *P. elongatus* (Bowdich, 1825) and *P. epipercis* Bleeker, 1863 (see Schwarzhans, 1993, for figures of extant specimens) in proportions but differs in the ostium reaching close to the anterior rim of the otoliths (vs. distant from anterior rim), the massive postcentral umbo on the outer face, and the postdorsal rim. It may represent an extinct species, but I refrain from formal action, because it is not clear how much the thin anterior rim of the otolith could have been affected by erosion and the features of the dorsal rim and outer face could be reflecting aspects of variability. Otoliths figured by Mendiola and Martínez (2003) as *Pteroscion* sp. 2 from the lower Pliocene of southern Spain may represent the same species, but judging from their drawings appear to be mostly eroded. The six extant species of the genus *Pseudotolithus* are known today from tropical West Africa south of Morocco to Angola.

Genus *Pteroscion* Fowler, 1925

Pteroscion peli (Bleeker, 1863)

Figure 28i–l

1993 *Pteroscion maroccanus*—Schwarzhans: Fig. 289–292.

2003 *Pteroscion peli* (Bleeker, 1863)—Mendiola & Martínez: Fig. 9:4–6, pl. 13, Fig. 289–291.

2003 *Pteroscion guardamarensis*—Mendiola & Martínez: Fig. 9:7–9, pl. 12, Figs. 1–8, pl. 15, Figs. 1–8, pl. 16, Figs. 1–2.

2003 *Pteroscion* sp. 1—Mendiola & Martínez: pl. 12, Figs. 9–16, pl. 16, Figs. 3, 4.

Material 46 specimens, Dar bel Hamri, Zanclean, figured specimens are photographs of holotype of *P. maroccanus*, SMF P 8599 (Fig. 28h) and paratypes, SMF P 8600 (Fig. 28i–k).

Discussion I agree with Mendiola and Martínez (2003) and in the light of the many extant and fossil species they figured that *P. maroccanus* is synonymous with the extant *P. peli*. However, I also agree with the view of the reviewer of their manuscript, D. Nolf (as mentioned in

their acknowledgements), that the species they described from the Pliocene of Spain as *P. guardamarensis* represent a further synonym of *P. peli*. The species was found to be by far the most common sciaenid in the lower Pliocene rocks of Guardamar in southern Spain (Mendiola & Martínez, 2003). Today, *Pteroscion peli* is distributed from Senegal to Namibia.

Genus *Umbrina* Cuvier, 1817

Umbrina canariensis Valenciennes, 1843

Figure 28f

1993 *Umbrina* aff. *canariensis* Valenciennes, 1843—Schwarzahns: Fig. 88–90.

2003 *Umbrina canariensis* Valenciennes, 1843—Mendiola & Martínez: pl. 2, Figs. 3–7, pl. 3, Figs. 1, 2.

2003 *Umbrina* aff. *canariensis* Valenciennes, 1843—Mendiola & Martínez: pl. 4, Figs. 1–4.

Material 43 specimens, Dar bel Hamri, Zanclean (figured specimen SMF PO 101.272).

Discussion Several large and well preserved specimens have now been obtained from Dar bel Hamri confirming the identity of these otoliths, which previously have been only tentatively allocated as *U.* aff. *canariensis* (see Schwarzahns, 1993).

Diversification level and environmental assessment

Ninety-six otolith-based species have been identified based on 4375 specimens collected from four locations along the Oued Beth and one location near Asilah (Table 1), whereby 4250 otoliths were obtained from a single location, the coquina at the base of section 1, approximately 1.5 km south of Dar bel Hamri, with 95 species. Therefore, only location 1 near Dar bel Hamri qualifies for a quantitative assessment of the bony fish fauna. However, only subsample 1 with 1202 specimens can be quantitatively evaluated because subsample 2 was screened off at 2 mm mesh diameter and thus small species are not adequately represented in it. Percentages in the following therefore reflect only subsample 1 (Table 1). The two most common species are *Afroscion trewavasae* (19.55%) and *Diaphus maghrebensis* (16.39%), together accounting for 35.94% of the entire assemblage (Table 1). The diversification index is 31 of the most common species to reach the threshold of 90% of all identified species. This is an exceptionally high diversification index and in fact the highest ever recorded in any otolith assemblage.

This high diversity is probably a result of several inter-relating effects, such as environment, sedimentary facies, water depth, rich and diverse food supply at various trophic levels, and the biogeographic situation (see below).

The coquina of Dar bel Hamri, from where the otoliths were obtained, has been deposited in a subaqueous environment, probably at moderate depth on the middle to lower shelf. Coquina accumulations observed in Late Miocene/Early Pliocene sediments of Portugal, the Huelva Basin in Spain, and the Rharb Basin in Morocco have been interpreted by Gonzales Delgado et al. (1994) as caused by winnowing from storm activities in shallow marine environments below the wave base. However, the composition of the otolith assemblage points to a deeper environment in a middle to lower shelf position that would be below the storm wave base. The majority of the 43 extant fishes occurring as fossils in Dar bel Hamri occur at water depth of 50 to 100 m (55.8%), another 18.6% in water shallower than 50 m and the remainder in water deeper than 100 m (Table 2). About 58% of the 43 extant fishes occurring as fossils in Dar bel Hamri have a demersal life habitat (Table 2) making them relatively reliable depth indicators. The winnowing responsible for the formation of the coquina and the accumulation of fossils in the sediment at Dar bel Hamri instead could have been caused by subaqueous currents, possibly as a result of tidal reflux. Such explanation is supported by the report of a Late Miocene/Early Pliocene channel observed on seismic sections due east of Dar bel Hamri (Capella et al., 2017). The current and winnowing at the base of the early Zanclean may also have been responsible for some reworking and erosion of directly underlying sediments of (late) Messinian age in the area. Furthermore, the current activity could have led to an increase in the availability of food in the trophic chain. In combination with the water activity this in turn could have led to an unusually high percentage of large, adult fishes as expressed in the high percentage of relatively large otoliths in the coquina. The most abundant species, *Afroscion trewavasae*, is a sciaenid of a group that today feeds primarily on small, mostly nektonic fishes and large invertebrates. The abundance of such a fish, particularly with adult specimens, is unusual and supports the hypothesis of an increased food supply in the depositional environment. The abundance of large otoliths also increases the potential for their identification, which is somewhat counterbalanced by a nearly ubiquitous mild to moderate mechanical erosion, which one would expect in such a facies. The other, stratigraphically comparable locations at Sidi Mohamed ech Chleuh, Kef Nsour and Jebel Zebbouj have yielded much fewer otoliths and are dominated by myctophids. The myctophid otoliths in

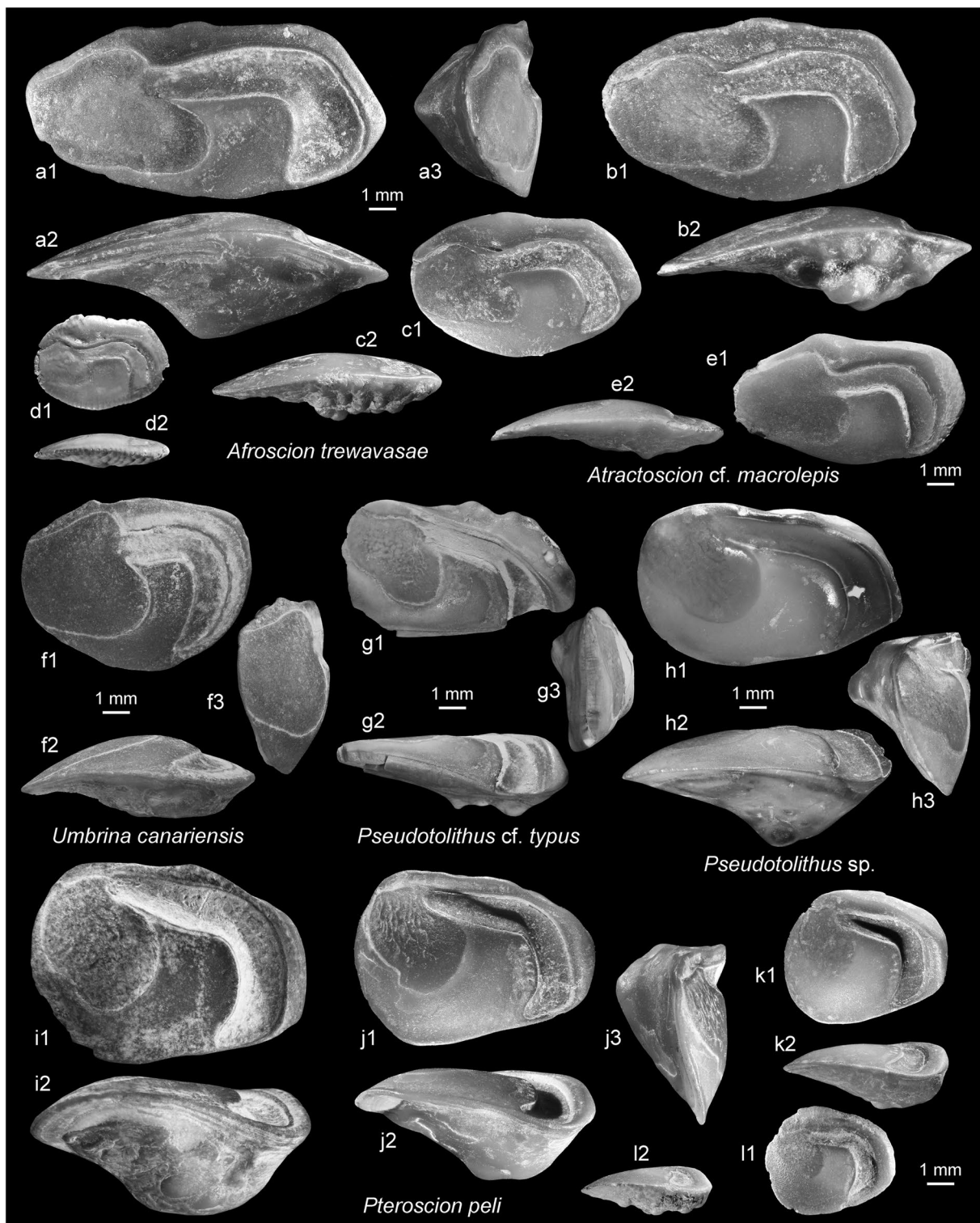


Fig. 28 Sciaenidae. **a–d**, *Afroscion trewavasae* Schwarzzhans, 1993, Dar bel Hamri, Zanclean, **b** holotype, SMF P8226, **a, c–d** paratypes, SMF P 8227 (reversed). **e** *Atractoscion cf. macrolepis* Song, Kim & Kim, 2017, SMF PO 101.296, Dar bel Hamri. **f** *Umbrina canariensis* Valenciennes, 1843, SMF PO 101.272 (reversed), Dar bel Hamri. **g** *Pseudotolithus cf. typus* Bleeker, 1863, SMF PO 101.270, Dar bel Hamri. **h** *Pseudotolithus* sp., SMF PO 101.271 (reversed), Dar bel Hamri. **i–l** *Pteroscion peli* (Bleeker, 1863), types of *Pteroscion maroccanus* Schwarzzhans, 1993, Dar bel Hamri, Zanclean, **h** holotype, SMF P 8599, **i–k** paratypes, SMF P 8600 (**k–l** reversed)

these locations were mostly well preserved including the frail denticles along the ventral rim of *Diaphus* otoliths, and thus indicate no or very little erosion in a more calm and possibly also deeper environment. Asilah has yielded even fewer otoliths, which are often somewhat leached hampering identification. This small assemblage contains only species also known from Dar bel Hamri.

Lyellian percentage

Forty-three species identified by means of otoliths in the Early Pliocene of Dar bel Hamri are also known from today. This compares to 39 fossil species and 14 that cannot be identified to species level. Disregarding the latter which could either represent extant or extinct species, the Lyellian percentage thus amounts to 52.4%. A calculation on the same basis for the otolith assemblage recently described from the Pliocene of Estepona near Málaga, southern Spain, by van Hinsbergh and Hoedemakers (2022) arrives at a Lyellian ratio of about 67%. An evaluation of the Lyellian percentage for goby otoliths in the Mediterranean arrived at 70% (Schwarzhans et al., 2020). Overall, the Lyellian percentage of otolith associations in the Zanclean of the Mediterranean is in the order of 72% and for the Piacenzian 78%. However, articulated skeletons exhibit a lower Lyellian percentage in the Early Pliocene of the Mediterranean than otoliths (Landini & Sorbini, 1992, 2005), which may be regarded as an expression of the generally more conservative approach in otolith research. Overall, the Lyellian percentages of Early Pliocene otolith associations vary between about 50% (tropical West Atlantic Sciaenidae, Morocco) and about 75% (New Zealand) (see Schwarzhans, 2019a). Thus, the Moroccan otolith-based fauna described here is remarkable for a comparably low Lyellian percentage, which will be discussed further in the chapter below about a potential “Maghrebian bioprovince” during the Pliocene.

The ratio of extant versus extinct species is unevenly distributed among the families represented. Considering families with at least three identifiable species, one can note that extinct taxa prevail in the Myctophidae (5 extinct species in a total of 8 species), Gobiidae (4 in 5), Bothidae (3 extinct species), Trachinidae (with 2 extinct species in 3) and Uranoscopidae (3 extinct species in 4). I interpret the low yield of extant species in the Early Pliocene of these families as an indication of a dynamic speciation in the recent geologic past. The dynamic recent speciation is matched with observations made about Pliocene myctophid otoliths from tropical America (Schwarzhans & Aguilera, 2013). In respect to gobies, the extant–extinct ratio is somewhat mixed. Schwarzhans et al. (2020) calculated a Lyellian percentage of about 70% for the Gobiidae in the Early Pliocene of the Mediterranean. A calculation from the

species list provided by van Hinsbergh and Hoedemakers (2022) for the Pliocene of Estepona near Málaga, southern Spain, arrived at about 62%. Thus, the yield of extinct gobiid species in Dar bel Hamri is distinctly higher than in Mediterranean locations, even though all except one of the species (*Deltentosteus planus*) found in Morocco are also known from the Mediterranean. I find no ready explanation for this discrepancy. Conversely, the yield of extinct species is low in the Congridae (1 extinct species in 4), Carapidae (1 extinct species in 3), Soleidae, and Sciaenidae (1 extinct species in 5) and particularly in the Sparidae (2 extinct species in 15). The high percentage of extant species in the Early Pliocene record of these families could indicate that much of the speciation that led to the extant fauna occurred earlier. However, the low yield of extinct taxa in the family with the most species in Dar bel Hamri, the Sparidae, could have a different cause. Otoliths of the Myctophidae (Brzobohatý & Nolf, 1996, 2000; Schwarzhans, 2013b; Schwarzhans & Aguilera, 2013) and of the Gobiidae (Schwarzhans et al., 2020; Bratishko et al., 2023 ms, and literature cited in both studies) have been studied extensively and have in part been calibrated by finds of otoliths in situ (Bedini et al., 1986; Reichenbacher & Bannikov, 2021, 2022; Schwarzhans et al., 2017). As a result, the character analysis of otoliths of these two groups is more advanced than in Sparidae and aids the recognition of species. Comparable studies of otoliths are lacking in the case of the Sparidae, and it is, therefore, possible that the species identification is not as accurate as in the Myctophidae and Gobiidae and could in fact be too conservative.

Comparison with Mediterranean assemblages from the Pliocene: implications for fish remigration from the Northeast Atlantic into the Mediterranean after the Messinian Crisis

The terminal Miocene in the Mediterranean is well known for the late Messinian Salinity Crisis (MSC) that was caused by the closure of the Mediterranean Sea to the northeastern Atlantic in the West during that time. Both seas became fully reconnected again beginning with the Pliocene. Since the first article on the MSC (“When the Mediterranean dried up” by Hsü, 1972), a large body of research has been published on the subject, and what precisely happened—whether marine life was extinguished in the Mediterranean during the event, the water budget, base level drop, and so on—is still very much under discussion (e.g., Roveri et al., 2014, 2016; Ben-Mosche et al., 2020; Gvirtzman et al., 2022; and literature cited in these articles). Recently, Carnevale and Schwarzhans (2022) showed that stenohaline marine fishes lived in the Mediterranean through the MSC, at least

Table 1 Species list of otoliths from the NW Moroccan Early Pliocene and Late Miocene, correlation with Estepona, Spain (from van Hinsbergh & Hoedemakers, 2022), and entire Mediterranean (compiled from cited literature)

	Messinian/Tortonian			Zanclean		Sidi Mohamed Chleuh	Jebel Zebbouj	Asilah	Total	Percentage at Dar bel Hamri subsample 1	Estepona	Mediterranean
	Kef Nsour + Chaba Kadiat el Mogen	Dar bel Hamri subsample 1	Dar bel Hamri subsample 2	Dar bel Hamri subsample 1	Dar bel Hamri subsample 2							
Pterothrissidae												
<i>Pterothrissus darbelhamiensis</i>		11	68				1	1	80	0.92		
Heterenchelyidae												
<i>Panturichthys cf. fowleri</i>		4							4	0.33	X	X
Ophichthidae												
<i>Echelus myrus</i>			1						1		X	X
Nettastomatidae												
<i>Saurenhelys silex</i>		2	2						4	0.17	X	X
Congridae												
<i>Conger</i> sp. juv		3	2						5	0.25		
<i>Gnathophis mystax</i>		1	1						2	0.08	X	X
<i>Japonoconger africanus</i>		1							1	0.08	X	X
<i>Paraxenomystax cf. bidentatus</i>			2						2			
<i>Rhynchoconger pantanellii</i>		18	99					1	118	1.50	X	X
Clupeidae												
<i>Clupeidae</i> indet. frag		3							3	0.25		
Ariidae												
<i>Carliarius cf. latiscutatus</i>		1	1						2	0.08		
Myctophidae												
<i>Hygophum cf. hygomi</i>		2							2	0.17	X	X
<i>Myctophum firchi</i>		2					1	1	4	0.17	X	X
<i>Ceratoscopelus maderensis</i>		1							1	0.08	X	X
<i>Lampanyctus</i> sp.		2							2	0.17		
<i>Diaphus adenomus</i>			4						4		X	X
<i>Diaphus cavallonis</i>		20	126						146	1.66	X	X
<i>Diaphus dirknolli</i>		81	3			4		2	90	6.74	X	X
<i>Diaphus draconis</i>	3					5			8		X	X
<i>Diaphus maghrebiensis</i>	24	197	21			40	17		299	16.39	X	X
Moridae												
<i>Physiculus</i> sp.		20				1			21	1.66		
Bregmacerotidae												
<i>Bregmaceros</i> sp.		1							1	0.08		

Table 1 (continued)

	Messinian/Tortonien		Zanclean		Kef Nsour + Chaba Kadiat el Mogen		Dar bel Hamri subsample 1		Dar bel Hamri subsample 2		Sidi Mohamed ech Chleuh	Jebel Zebbouj		Asilah	Total	Percentage at Dar bel Hamri subsample 1	Estepona	Mediterranean
Macrouridae																		
<i>Coelrinchus cf. arthaberoideis</i>			1												1	0.08	X	X
<i>Nezumia ornata</i>			2				8								10	0.17	X	X
<i>Trachyrincus scabratus</i>							1								1			X
Merlucciidae																		
<i>Merluccius polli</i>	1		2				6								9	0.17		
Gadidae																		
<i>Paratrisopterus glaber</i>	2		64						2			3	1		72	5.32	X	X
Carapidae																		
<i>Carapus acus</i>			1												1	0.08		X
<i>Echiodon dentatus</i>			3				20		1						24	0.25		X
<i>Echiodon praeimberbis</i>			6				73								79	0.50	X	X
Brotulidae																		
<i>Brotula aff. multibarbata</i>			2				3								5	0.17	X	X
Ophidiidae																		
<i>Ophidion tuseri</i>			22				222								244	1.83		
Ogcocephalidae																		
Ogcocephalidae indet							1								1			
Berycidae																		
<i>Centroberyx vanderhocti</i>			3				8								11	0.25		
Trachichthyidae																		
<i>Hoplostethus</i> sp.			1												1	0.08		
Holocentridae																		
<i>Myripristis ouarredi</i>			13				22								35	1.08		
<i>Sargocentron hastatum</i>							1								1			
Mulgilidae																		
<i>Liza</i> sp.							2								2			
Gobiidae																		
<i>Hoeseichthys brioche</i>			13						3			1			17	1.08	X	X
<i>Lesueurigobius stazzanensis</i>			46				11								57	3.83	X	X
<i>Vanneaugobius?</i> sp.			2												2	0.17		

Table 1 (continued)

	Messinian/Tortonian			Zanclean			Sidi Mohamed ech Chleuh	Jebel Zebbouj	Asilah	Total	Percentage at Dar bel Hamri subsample 1	Estepona	Mediterranean
	Kef Nsour + Chaba Kadiat el Mogen	Dar bel Hamri subsample 1	Dar bel Hamri subsample 2	Dar bel Hamri subsample 1	Dar bel Hamri subsample 2	Dar bel Hamri subsample 1							
<i>Buenia pulvinus</i>		9								9	0.75	X	X
<i>Deltentosteus planus</i>		25						1		26	2.08		
<i>Deltentosteus quadrimaculatus</i>		43			5					48	3.58	X	X
Citharidae													
<i>Citharus balearicus</i>		8			14					22	0.67		X
Bothidae													
<i>Arnoglossus kokeni</i>		29					1		1	31	2.41	X	X
<i>Arnoglossus quadratus</i>		18			7					25	1.50	X	X
<i>Laeops rharbensis</i>		7								7	0.58		
Soleidae													
<i>Dicoglossa hexophthalma</i>		1								1	0.08		
<i>Microchirus variegatus</i>					3					3		X	X
<i>Quenselia cornuta</i>		35								35	2.91		
<i>Synaptura</i> sp.		1								1	0.08		
<i>Synapturichthys kleinii</i>		1								1	0.08		
<i>Vanstraelenia chirophthalma</i>		1								1	0.08		
Cynoglossidae													
<i>Cynoglossus obliqueventralis</i>		2			5					7	0.17		X
Sphyraenidae													
<i>Sphyraena</i> sp.					3					3			
Carangidae													
<i>Caranx rharbensis</i>					9					9			
<i>Trachurus insectus</i>		3			9					12	0.25		
<i>Trachurus mediterraneus</i>		9			23					32	0.75		X
Acropomatidae													
<i>Verilus mutinensis</i>		16			83			2		101	1.33	X	X
Haemulidae													
<i>Parapristipoma bethensis</i>					4					4			
<i>Pomadasyx incisus</i>		67			451					518	5.57	X	X
<i>Pomadasyx zemmouriensis</i>		5			17					22	0.42		
<i>Pomadasyx</i> sp.		3			4					7	0.25		

Table 1 (continued)

	Messinian/Tortonian		Zanclean						Percentage at Dar bel Hamri subsample 1	Estepona	Mediterranean
	Kef Nsour + Chaba Kaudiat el Mogen	Dar bel Hamri subsample 1	Dar bel Hamri subsample 2	Sidi Mohamed ech Chleuh	Jebel Zebbouj	Asilah	Total				
Cepolidae											
<i>Cepola lombartei</i>		11	8	2		1	22	0.92			
<i>Cepola macrophthalma</i>		5	20	1		1	27	0.42	X		X
<i>Owstonia</i> sp.		1					1	0.08			
Triglidae											
<i>Peristedion cataphractum</i>		1	1				2	0.08			X
Trachinidae											
<i>Trachinus armatus</i>		3					3	0.25	X		X
<i>Trachinus maroccanus</i>		11	4				15	0.92			
<i>Trachinus wernlii</i>		12	46				58	1.00			
Uranoscopidae											
<i>Uranoscopus ciabatta</i>			2				2		X		X
<i>Uranoscopus hoedemakersi</i>		1	3				4	0.08			
<i>Uranoscopus scaber</i>		5	15				20	0.42	X		X
<i>Uranoscopus vanhinsbergi</i>		3	2				5	0.25			
Sparidae											
<i>Boops boops</i>		1	1			1	3	0.08	X		X
<i>Diplodus bellottii</i>		4	16				20	0.33			
<i>Oblada melanura</i>		4	3				7	0.33	X		X
<i>Pagellus acarne</i>			7				7		X		X
<i>Pagellus bellottii</i>		7	6				13	0.58	X		X
<i>Pagellus bogaraveo</i>		5	21				26	0.42	X		X
<i>Pagellus erythrinus</i>		16	25				41	1.33	X		X
<i>Pagrus pagrus</i>			39				39				X
<i>Spicara alta</i>			24				24		X		X
<i>Spicara smaris</i>			2				2		X		X
<i>Spondylusoma tingitana</i>			5				5				
<i>Dentex canariensis</i>		4	8				12	0.33			
<i>Dentex dentex</i>		7	12				19	0.58			
<i>Opsodentex angolensis</i>		5	9				14	0.42			
<i>Opsodentex mordax</i>		6	24				30	0.55			

Table 1 (continued)

	Messinian/Tortonian		Zanclean		Sidi Mohamed Chleuh	Jebel Zebbouj	Asilah	Total	Percentage at Dar bel Hamri subsample 1	Estepona	Mediterranean
	Kef Nsour + Chabab Kaudiat el Mogen	Dar bel Hamri subsample 1	Dar bel Hamri subsample 2	Dar bel Hamri subsample 1							
Sciaenidae											
<i>Afroscion trewavasae</i>		235	1329				1564	19.55			
<i>Atractoscion</i> cf. <i>macrolepis</i>			1				1				
<i>Pseudotolithus</i> cf. <i>typus</i>		1					1	0.08			
<i>Pseudotolithus</i> sp.		1					1	0.08			
<i>Pteroscion peli</i>		15	31				46	1.25		X	
<i>Umbrina canariensis</i>		5	38				43	0.42		X	
Number of specimens	30	1202	3047		60	23	12	4375			
Number of species	4		95		10	4	11	96	39		50



Fig. 29 Paleogeographic situation in northern Morocco and southern Spain during Messinian prior to the closure of the Mediterranean (a) and the Zanclean after opening of the Strait of Gibraltar (b), after Martin et al. (2014) and Pérez-Asensio (2021). Otolith-bearing localities are indicated by asterisks (Estepona from van Hinsbergh & Hoedemakers, 2022). Number of species at location in black printing; number of shared species on correlation arrows

periodically, as evidenced by articulated fish skeletons and otoliths, which is in contrast to a study by Andreetto et al. (2021), who postulated that all marine fossils found in sediments of the MSC interval resulted from reworking of pre-MSC rocks. The reworking hypothesis cannot be maintained for the explanation of the presence of articulated skeletons of marine fishes in MSC rocks. Another subject of continued dispute is the role of re-flooding of the Mediterranean with the onset of the Early Pliocene (Zanclean) (Bache et al., 2012; Garcia-Castellanos et al., 2009; Micallef et al., 2018; and literature cited in these articles).

During the Pliocene, the Rharb Basin was a funnel-shaped embayment that represented the relict of the last connection of the Atlantic with the Mediterranean (Fig. 29) (Achalhi et al., 2016; Capella et al., 2017; de Weger et al., 2020a, 2020b, 2020c; Flecker et al., 2015; Flinch, 1993; Martin et al., 2014; Pérez-Asensio, 2021). The Rharb Basin is ideally situated to investigate the composition of the fauna during the late stage of the Atlantic–Mediterranean connection and the fauna during the re-flooding when the Rharb Basin represented the reservoir from which a proportion of the remigration must have been recruited. Little is known so far about the Late Miocene fish fauna of the Rharb Basin from the few otoliths collected from outcrops at Kef Nsour and Chaba Kaudiat el Mogen, which are all known in the Early Pliocene as well, except for *Diaphus draconis*. The Early Pliocene fish fauna from Dar bel Hamri and the other studied

locations is significant and allows for a correlation with time-equivalent assemblages from the Mediterranean. Indeed, there have been many studies about Pliocene otolith associations in the Mediterranean realm (Fig. 30): from Italy for example Dieni (1968), Weiler (1971), Schwarzhans (1978a), Anfossi and Mosna (1979), Nolf and Cappetta (1988), Girone (2006), Nolf and Girone (2006); from Greece Agiadi et al., (2013, 2017, 2019a, 2019b); from southern France Schwarzhans (1986), Nolf and Cappetta (1988); from southern Spain Nolf and Martinell (1980), Nolf et al. (1988), Mendiola and Martínez (2003), van Hinsbergh and Hoedemakers (2022). These many articles contrast with only two otolith associations described from the adjacent Atlantic: one from the Piacenzian of central Portugal described by Nolf and da Silva (1997) and the other this study from Morocco. Many of the Zanclean otolith assemblages described from the Mediterranean realms originate from deep marine settings with predominant meso- to bathypelagic and bathydemersal fishes, while the Portuguese and Moroccan faunas are characterized by middle to lower shelf fishes associated with a few upper slope elements. The assemblage described from Estepona in southern Spain by van Hinsbergh and Hoedemakers (2022) is the most important for comparison, because it is rich (209 species, 107 thereof in the Zanclean), includes faunal elements of the lower shelf similar to Morocco, and is located just about 50 km to the east of the Strait of Gibraltar. The nearest location studied in Morocco is Asilah, about

Table 2 Ecology chart of extant species found as fossils in Dar bel Hamri. Ecology data from Froese and Pauly (2022); depth ranges reflect “usual ranges” where given

	Habitat	Temperature	Water depth
Heterenchelyidae			
<i>Panturichthys fowleri</i>	Demersal	Subtropical	27–120 m
Ophichthidae			
<i>Echlus myrus</i>	Demersal	Subtropical	3–550 m
Congridae			
<i>Gnathopis mystax</i>	Demersal	Subtropical	75–800 m
<i>Japonoconger africanus</i>	Demersal	Tropical	250–650 m
<i>Paraxenomystax bidentatus</i>	Demersal	Tropical	494–604 m
Ariidae			
<i>Carlarius laticutatus</i>	Demersal	Tropical	to 30–70 m
Myctophidae			
<i>Hygophum hygomi</i>	Oceanic-mesopelagic	Temperate-tropical	600–800 m (day)
<i>Ceratoscopelus maderensis</i>	Mesopelagic, high oceanic	Temperate-subtropical	460–1082 m (day)
<i>Diaphus adenomus</i>	Mesopelagic, pseudoceanic	Subtropical-tropical	500–686 m (day)
Macrouridae			
<i>Trachyrinchus scabrus</i>	Demersal	Temperate-tropical	395–1700 m
Merlucciidae			
<i>Merluccius polli</i>	Demersal	Subtropical-tropical	50–1000 m
Carapidae			
<i>Carapus acus</i>	Demersal	Subtropical	1–150 m
<i>Echiodon dentatus</i>	Demersal	Subtropical	120–3250 m
Brotulidae			
<i>Brotula multibarata</i>	Benthopelagic	Tropical	100–650 m (adult)
Holocentridae			
<i>Sargocentron hastatum</i>	Neritic, reef-associated	Subtropical-tropical	50–100 m
Gobiidae			
<i>Deltentosteus quadrimaculatus</i>	Demersal	Subtropical	10–90 m
Soleidae			
<i>Dicologlossa hexophthalma</i>	Demersal	Subtropical-tropical	shallow water
<i>Microchirus variegatus</i>	Demersal	Temperate-subtropical	20–40 m
<i>Synapturichthys kleinii</i>	Demersal	Subtropical / antitropical	20–460 m
<i>Vanstraelenia chirophthalma</i>	Demersal	Tropical	8–100 m
Carangidae			
<i>Trachurus mediterraneus</i>	Pelagic	Subtropical	5–250 m
Haemulidae			
<i>Pomadasys incisus</i>	Demersal	Subtropical-tropical	10–100 m
Cepolidae			
<i>Cepola macrophthalma</i>	Demersal	Temperate-subtropical	15–400 m
Triglidae			
<i>Peristedion cataphractum</i>	Demersal	Subtropical-tropical	50–600 m
Trachinidae			
<i>Trachinus armatus</i>	Demersal	Tropical	15–150 m
Uranoscopidae			
<i>Uranoscopus scaber</i>	Demersal	Subtropical	15–400 m
Sparidae			
<i>Boops boops</i>	Pelagic	Temperate-tropical	0–100 m
<i>Diplodus bellottii</i>	Benthopelagic	Subtropical	30–50 m
<i>Oblada melanura</i>	Benthopelagic	Subtropical-tropical	0–30 m

Table 2 (continued)

	Habitat	Temperature	Water depth
<i>Pagellus acarne</i>	Benthopelagic	Subtropical	40–100 m
<i>Pagellus bellottii</i>	Demersal	Subtropical-tropical	10–50 m
<i>Pagellus bogaraveo</i>	Benthopelagic	Temperate-subtropical	150–300 m
<i>Pagellus erythrinus</i>	Benthopelagic	Temperate-subtropical	20–100 m
<i>Pagrus pagrus</i>	Benthopelagic	Temperate-subtropical	10–80 m
<i>Spicara alta</i>	Benthopelagic	Tropical	100–300 m
<i>Spicara smaris</i>	Benthopelagic	Subtropical	15–328 m
<i>Dentex canariensis</i>	Demersal	Tropical	to 150 m
<i>Dentex dentex</i>	Benthopelagic	Subtropical	15–50 m
<i>Opsodentex angolensis</i>	Demersal	Tropical	15–300 m
Sciaenidae			
<i>Atractoscion macrolepis</i>	Benthopelagic	Subtropical-tropical	100–200 m
<i>Pseudotolithus typus</i>	Demersal	Tropical	0–60 m
<i>Pteroscion peli</i>	Benthopelagic	Tropical	0–50 m
<i>Umbrina canariensis</i>	Demersal	Subtropical-tropical	50–200 m
Percentages	Demersal 58.1%	Temper.-subtrop. 20.9%	to 50 m 18.6%
	Benthopelagic 30.2%	Subtropical 30.2%	to 100 m 55.8%
	Pelagic 4.7%	Subtrop.-tropical 23.2%	from 100 m 25.6%
	Mesopelagic 7.0%	Tropical 25.6%	

50 km to the west of the Strait of Gibraltar and about 130 km from Estepona. Dar bel Hamri is 190 km south of the Strait of Gibraltar and about 260 km from Estepona. However, Dar bel Hamri is much closer to Estepona than the other nearest Mediterranean locations (450 km to Guardamar, described by Mendiola & Martínez, 2003, and 850 km to Papiol near Barcelona, described by Nolf et al., 1998).

Fifty of the 82 identified species in the Early Pliocene of the Rharb Basin have also been recorded from time-equivalent strata of the Mediterranean (Table 1; 61%), thereof 39 species in the Zanclean and/or Piacenzian of Estepona (Fig. 29). This ratio is consistent with the similarity coefficient calculated by Ben Moussa (1994) for Pliocene bivalves of Morocco in comparison with Mediterranean localities. Nevertheless, the fish fauna shows a lower correlation than one might expect over such a small distance and under the consideration of the recruitment of the Mediterranean fauna from the adjacent Northeast Atlantic during the Early Pliocene re-flooding event. It appears that not all species of the Northeast Atlantic were actually able to migrate into the Mediterranean, and furthermore there could be environmental differences at play in the locations that could mask faunal exchange. However, it is worth elucidating those 32 species that have not been found in the Mediterranean. Thirteen of those represent extant species, of which today 5 occur in the Atlantic off Morocco, 7 primarily south of the Mauritanian upwelling zone in the tropical East Atlantic and 1 in the tropical West Atlantic. Another

19 species, including all of the new species, could be considered potentially endemic to the area (a “Maghrebian bioprovince”, see below). *Pterothrissus darbelhamriensis* of those potentially endemic species may in fact represent an allopatric vicariant species of the Mediterranean *P. compactus* at the time. *Pterothrissus darbelhamriensis* was already considered by Schwarzhans (1981) as vicariant to *P. compactus* from the Mediterranean (known from the Tortonian [Fig. 9 h, j] until Zanclean [Fig. 9f–g, i]). It has now also been identified from the Piacenzian of Estepona (van Hinsbergh & Hoedemakers, 2022), but this is not considered contradictory to the interpretation, since it could represent a late immigrant from the Northeast Atlantic into the adjacent region of the Mediterranean. The recognition of a vicariant species in the Northeast Atlantic and the Mediterranean in the Zanclean (and ideally since the Late Miocene) supports the hypothesis of in situ survival of marine fish taxa in the Mediterranean, but it is so far restricted to a single conclusive case. The more important outcome of the correlation of Northeast Atlantic and Mediterranean fishes of the Early Pliocene times is that a substantial number of Atlantic fish taxa apparently did not migrate into the Mediterranean during the re-flooding. This non-migratory effect could be caused by a warmer climate in the Rharb Basin than at the Strait of Gibraltar, as can be inferred from the presence of some southern elements then present in Morocco and putative endemic species. They are primarily the species with tropical East Atlantic affinities that have not been found in the Mediterranean.

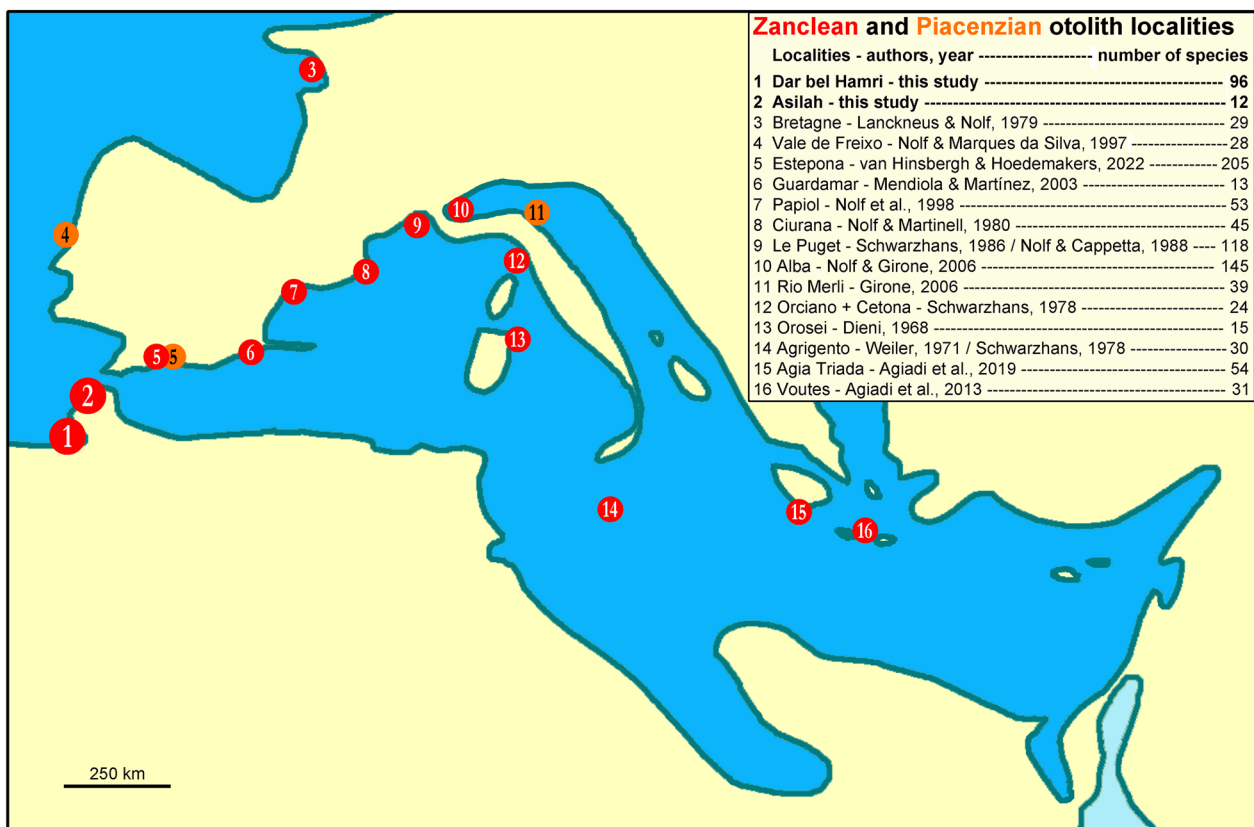


Fig. 30 Early Pliocene paleogeography of the Mediterranean and adjacent northeastern Atlantic. Paleogeographic configuration based on Popov et al., (2004; middle Pliocene map) and Pérez-Asensio (2021). Zanclean locations with otoliths marked by white numbers with red frame, Piacenzian locations with otoliths marked by black numbers with orange frame. Number of species and authors annotated

Comparison with extant fish faunas and its implications

The otolith association of the Early Pliocene of Dar bel Hamri and nearby locations contains 43 species that still exist today. The majority of them are distributed over the subtropical to temperate zones (74.4%), 30.2% thereof exclusively in the subtropical zone (Table 2). The distribution of only 20.9% of the species range into the temperate zone, and 25.6% are exclusively tropical (Table 2). Thirty-two species (74.4%) of the extant fishes occurring as fossils in Dar bel Hamri live today in the same general area (i.e., in the Northeast Atlantic off the coasts of Morocco) (Table 3); and 9 species (20.9%) live today in the tropical East Atlantic, chiefly south of Mauritania.

Clearly, the high content of persistent species indicates a high degree of continuity in the faunal composition of species occurring today and during the Early Pliocene in the region, but tropical West African species, which do not live off Morocco anymore or occur rarely as stray specimens, also contributed a significant component. Their presence indicates that the water temperatures in the sea off northwestern Morocco were significantly warmer in the Early Pliocene than they are today. Similar

conclusions were drawn by Avila et al. (2016) on the basis of molluscs found in Late Miocene and Early Pliocene sediments on the Azores and many previous studies of molluscs cited therein. If the sea off northwestern Africa was warmer in the Early Pliocene than it is today, this must have had consequences for the paleo-currents in the region. Today's faunal provinces along the northwestern coast of Africa are driven by the cool Canary Current, the permanent coastal upwelling between Cape Yubi and Cape Blanc, and further offshore by the position of the Intertropical Convergence Zone (Matsuzaki et al., 2011; Michel et al., 2011). The change from a tropical sea off Morocco to the current subtropical situation dominated by the cool Canary Current and separation from the tropical West African sea by the coastal upwelling system probably occurred during the Late Pliocene. Studies of the mollusc faunas from the Mediterranean, the Azores and the Canary Islands have revealed the disappearance of tropical taxa between 4.2 and 3.0 Ma (i.e., latest during the mid-Piacenzian cooling event) (Avila et al., 2016, and literature cited therein). Even though indications for upwelling along the Northwestern African

coast appear to have been present since the Early to Middle Miocene (Diester-Haas & Schrader, 1979), one has to assume that during the Late Miocene and Early Pliocene its intensity was insufficient to keep (some) tropical West African fishes from living in the Rharb Basin. However, some degree of separation still must have been effective, since most Early Pliocene fishes exhibit a clear subtropical Northeast Atlanto-Mediterranean relationship. In respect to the total of 74 biogeographically interpretable species (excluding fossil mesopelagic and bathydemersal fishes of uncertain biogeographic affinities), 42 species corresponding to 56.8% are identical or related to extant species in the same area (Table 3). Twenty-three species (31.1%) are identical or related to tropical East Atlantic species (Table 3). Nineteen species (25.6% of above 74 species) are putative endemics during the Early Pliocene of Dar bel Hamri; they are mostly related to extant Mediterranean, tropical East Atlantic and South African species (Table 3). Of about 600 marine bony fish species recorded from Morocco, the Canary Islands, Madeira and the Azores today, only about 30 (5%) represent northward extensions of species with primarily tropical East Atlantic distribution patterns (calculated from Froese & Pauly, 2022). The relationships of the 31 extinct otolith-based fish species at Dar bel Hamri (of the 74 biogeographically interpretable species) on a stand-alone basis are naturally less certain. The largest group among them is 19 species (25.6%) that have not been recorded from Mediterranean localities and hence are considered of potentially endemic nature (Table 3).

When investigating the probable provenances of the more exotic species (Table 3; Fig. 31), some more remote relationships are notable. *Paratrisopterus glaber* shows the closest relationship with northern Atlantic/North Sea Basin taxa. Three species (4.1%) exhibit affinities to the tropical West Atlantic (*Paraxenomystax* cf. *bidentatus*, *Myripristis ouarredi* and *Verilus mutinensis*), three (4.1%) to South Africa (*Centroberyx vonderhochti*, *Uranoscopus hoedemakersi* and *Afrosicion trewavasae*), and two (2.6%), namely *Brotula* aff. *multibarbata* and *Laeops rharbensis*, to the Indo-West Pacific (Table 3). A somewhat special case is that of the genus *Rhynchoconger* which has had a long history in Europe since Eocene times. Its latest representatives are *R. carnevalei* in the Early Pliocene of the Mediterranean and *R. pantanellii* in the Pliocene of the Mediterranean and Northeast Atlantic. The nearest occurrence of the genus today is in the central West Atlantic, but otoliths found in Holocene dredge samples in the Gulf of Guinea (Schwarzhans, 2013a) indicate that the disappearance of the genus from the East Atlantic is either very recent or false. The occurrence of another species with a West Atlantic relationship, *Verilus mutinensis*, is of a different nature, as it probably represents a

vicariant East Atlantic/Mediterranean species ranging from the Late Miocene Tortonian (Bassoli, 1906) to the middle Pleistocene Calabrian (Agiadi et al., 2018) before the lineage became extinct in the East Atlantic. As for the Indo-West Pacific affinity, *Brotula* aff. *multibarbata* could possibly represent a fossil species (subject to further material becoming available) and in any case represents a clade not present anymore in the Atlantic (Froese & Pauly, 2022).

The South African link is particularly interesting and perhaps unexpected, as it also contains the most common otolith-based species (*Afrosicion trewavasae*) of the entire assemblage. The extant *A. thorpei* is geographically restricted to a rather small area in southeast Africa (Sasaki in Heemstra et al. 2022). The occurrence of *A. trewavasae* in Morocco and Portugal clearly represented a vicariant species, and the distribution of *Afrosicion* in southeast Africa must thus be considered a relict occurrence. This coincides with South Africa representing a classical region for (secondary) endemism (<http://Intreasures.com/rsa.html>). The same explanation may hold for *Uranoscopus hoedemakersi*, which is thought to represent a vicariant species to the extant *U. archionema* off southeastern Africa. *Centroberyx* is a slightly different case as it is today known from seven species with a disjunctive distribution pattern, richest in Australia and New Zealand with an outlier species each in Japan, Taiwan, and South Africa (Froese & Pauly, 2022). *Centroberyx* is a genus with a long history reaching back into Cretaceous times and is well known from European basins until the Eocene, after which it becomes rather sparse (e.g., Schwarzhans & Jagt, 2021). Its current distribution is clearly a relict of a formerly much wider pattern. In Europe, the last record so far was *C. manens* Nolf & Brzobohatý, 2004, from the Middle Miocene. The large specimens of *Centroberyx vonderhochti* in the Pliocene of the Rharb Basin represent a different lineage from *C. manens*, that is probably related to the extant *C. spinosus* (Gilchrist, 1903) from South Africa (see Schwarzhans & Jagt, 2021).

Was there a “Maghrebian bioprovince” during the Early Pliocene?

Today's fish fauna in the seas around Morocco and the Macaronesian archipelago (Canary Islands, Madeira, Azores) includes about 600 species, of which about 30 species (5%) can be considered endemic and another 5% as primarily tropical West African fishes that also occur rarely to the north of the Mauritanian upwelling system (calculated from Froese & Pauly, 2022). This bioprovince has been named the subtropical Mediterranean–Moroccan Province by Avila et al. (2016). Most of the 560 or so non-endemic indigenous fishes have distribution ranges

Table 3 Biogeographic relationships of extant and interpretable fossil species for. Asterisk indicates that non-interpretable species (extinct myctophid and macrourid species) are excluded from the calculations because of their uncertain biogeographic affinities

	Persistent extant	Extinct	Nearest extant relationship					Potentially endemic
			Northeast- Atlantic	Mediterranean +/ adjacent Atlantic	Tropical East Atlantic	Tropical West Atlantic	South Africa Indo- West Pacific	
Pterothrissidae								
<i>Pterothrissus dar- belhamriensis</i>		80			80			80
Heterenchelyidae								
<i>Panturichthys</i> cf. <i>fowleri</i>	4			4				
Ophichtidae								
<i>Echelus myrus</i>	1			1				
Nettastomatidae								
<i>Saurechelys silex</i>		4			4			
Congridae								
<i>Gnathophis mystax</i>	2			2				
<i>Japonoconger</i> <i>africanus</i>	1				1			
<i>Paraxenomystax</i> cf. <i>bidentatus</i>	2					2		
<i>Rhynchoconger</i> <i>pantanelii</i>		118			118			
Ariidae								
<i>Carlarius</i> cf. <i>latis- cutatus</i>	2				2			
Myctophidae								
<i>Hygophum</i> cf. <i>hygomi</i>	2			2				
<i>Ceratoscopelus</i> <i>maderensis</i>	1			1				
<i>Diaphus adenomus</i>	4			4				
Macrouridae								
<i>Trachyrincus</i> <i>scabrus</i>	1			1				
Merlucciidae								
<i>Merluccius polli</i>	9				9			
Gadidae								
<i>Paratrisopterus</i> <i>glaber</i>		72	72					
Carapidae								
<i>Carapus acus</i>	1			1				
<i>Echiodon dentatus</i>	24			24				
<i>Echiodon praeim- berbis</i>		79			79			
Brotulidae								
<i>Brotula</i> aff. <i>multi- barbata</i>	5						5	
Ophidiidae								
<i>Ophidion tuseti</i>		244			244			244
Berycidae								
<i>Centroberyx von- derhohti</i>		11					11	11
Holocentridae								

Table 3 (continued)

	Persistent extant	Extinct	Nearest extant relationship					Potentially endemic
			Northeast- Atlantic	Mediterranean + / adjacent Atlantic	Tropical East Atlantic	Tropical West Atlantic	South Africa Indo- West Pacific	
<i>Myripristis ouarredi</i>		13				13		13
<i>Sargocentron hastatum</i>	1			1				
Gobiidae								
<i>Lesueurigobius stazzanensis</i>		57		57				
<i>Buenia pulvinus</i>		9		9				
<i>Deltentosteus planus</i>		26		26				26
<i>Deltentosteus quadrifasciatus</i>	48			48				
Citharidae								
<i>Citharus balearicus</i>		22		22				
Bothidae								
<i>Arnoglossus kokeni</i>		31		31				
<i>Arnoglossus quad- ratus</i>		25		25				
<i>Laeops rhabdensis</i>		7					7	7
Soleidae								
<i>Dicologlossa hexophthalma</i>	1			1				
<i>Microchirus var- iegatus</i>	3			3				
<i>Quenselia cornuta</i>		35		35				35
<i>Synapturichthys kleinii</i>	1			1				
<i>Vanstraelenia chirophthalma</i>	1				1			
Cynoglossidae								
<i>Cynoglossus obliqueventralis</i>		7			7			
Carangidae								
<i>Caranx rhabdensis</i>		9		9				9
<i>Trachurus insectus</i>		12		12				12
<i>Trachurus mediter- raneanus</i>	32			32				
Acropomatidae								
<i>Verilus mutinensis</i>		101				101		
Haemulidae								
<i>Parapristipoma bethensis</i>		4		4				4
<i>Pomadasys incisus</i>	518			518				
<i>Pomadasys zem- mouriensis</i>		22			22			22
Cepolidae								
<i>Cepola lombartei</i>		22			22			22
<i>Cepola macroph- thalma</i>	27			27				
Triglidae								

Table 3 (continued)

	Persistent extant	Extinct	Nearest extant relationship						Potentially endemic
			Northeast- Atlantic	Mediterranean +/ adjacent Atlantic	Tropical East Atlantic	Tropical West Atlantic	South Africa	Indo- West Pacific	
<i>Peristedion cata- phractum</i>	2			2					
Trachinidae									
<i>Trachinus armatus</i>	3				3				
<i>Trachinus maroc- canus</i>		15			15				15
<i>Trachinus wernlii</i>		58			58				58
Uranoscopidae									
<i>Uranoscopus ciabatta</i>		2			2				
<i>Uranoscopus hoedemakersi</i>		4					4		4
<i>Uranoscopus scaber</i>	20			20					
<i>Uranoscopus vanhinsberghi</i>		5		5					5
Sparidae									
<i>Boops boops</i>	3			3					
<i>Diplodus bellottii</i>	20			20					
<i>Oblada melanura</i>	7			7					
<i>Pagellus acarne</i>	7			7					
<i>Pagellus bellottii</i>	13			13					
<i>Pagellus bogaraveo</i>	26			26					
<i>Pagellus erythrinus</i>	41			41					
<i>Pagrus pagrus</i>	39			39					
<i>Spicara alta</i>	24				24				
<i>Spicara smaris</i>	2			2					
<i>Spondylusoma tingitana</i>		5		5					5
<i>Dentex canariensis</i>	12				12				
<i>Dentex dentex</i>	19			19					
<i>Opsodentex angol- ensis</i>	14				14				
<i>Opsodentex mordax</i>		30			30				30
Sciaenidae									
<i>Afroscion trewavasae</i>		1564					1564		1564
<i>Afroscion cf. mac- rolepis</i>	1				1				
<i>Pseudotolithus cf. typus</i>	1				1				
<i>Pteroscion peli</i>	15				15				
<i>Umbrina canar- iensis</i>	43			43					
Total species*	43	31	1	42	23	3	3	2	19
Percentage of spe- cies*	58.1	41.9	1.3	56.8	31.1	4.1	4.1	2.6	25.6
Total specimens*	1003	2693	72	1153	764	116	1579	12	2086
Percentage of speci- mens*	27.1	72.9	1.9	31.2	20.7	3.1	42.8	0.3	56.5

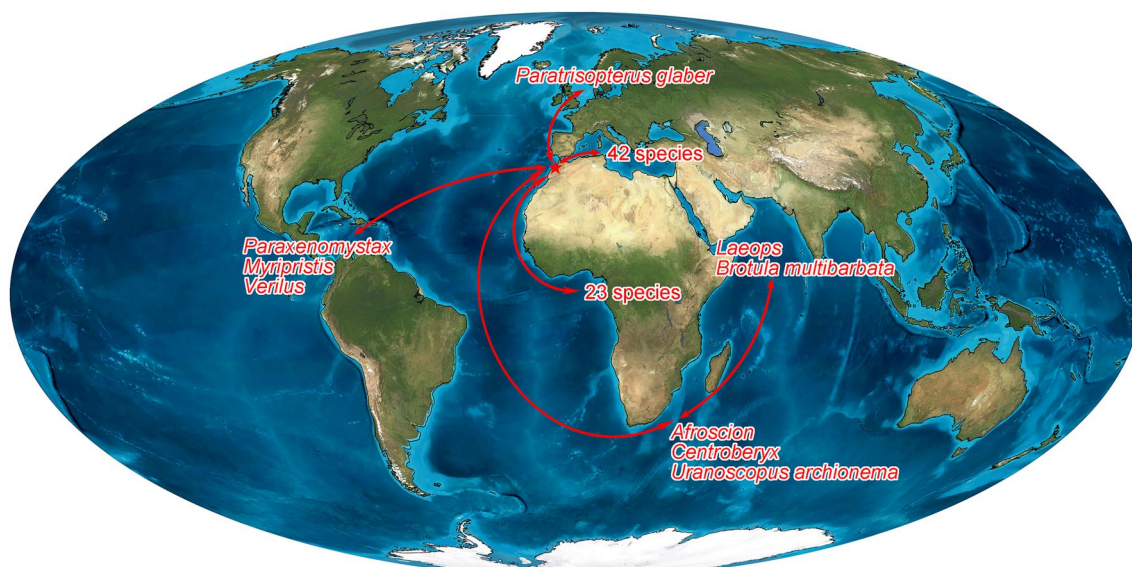


Fig. 31 Biogeographic correlation map showing nearest relationships of Early Pliocene otolith-based taxa from Dar bel Hamri. Red arrows and annotations indicate correlations to extant species also known as fossils from the Rharb Basin and relationships of extinct taxa from the Rharb Basin. Map from Blakey, 2020

northward to the Bay of Biscay or the British Isles, into the Mediterranean, and/or southward to various extents.

The situation was quite different in the Early Pliocene (and Late Miocene), when the Moroccan coast was under warmer climatic conditions and the Transition Zone was located further north. Based on analysis of the molluscan fauna, Avila et al. (2016) postulated a Pliocene Mediterranean–West African Province that stretched from the Azores to the southern tip of Portugal and incorporated the entire Mediterranean and the Gulf of Guinea. The fish fauna from the Rharb Basin, however, indicates that some degree of differentiation existed in this large area at least toward the Mediterranean, and is also inferred toward tropical West Africa (Fig. 32). The Early Pliocene otolith-based fish fauna of the Mediterranean is exceptionally well known and includes more than 200 identified taxa. The recent monograph of the otolith assemblage from Estepona in southwest Spain not far from the Strait of Gibraltar is particularly important for correlation. Only half (52%) of the otolith taxa identified in the Rharb Basin were also identified from the Pliocene in the Mediterranean. Nineteen species in the Rharb Basin are potential endemics, which is much higher than endemic species in the region today (25.6% vs. 5%), even taking into account uncertainties in the fossil data coverage. There is no comparable Early Pliocene otolith assemblage known from the Gulf of Guinea realms, the nearest being from the Middle Miocene of Gabon (Schwarzahans, 2013c). However, it can be stated that the tropical West African influence in the Early Pliocene fish fauna of the Rharb Basin

is significant at about 31.1% (species also occurring today and those related to extant West African species). This compares to about 5% of species off Morocco today shared with tropical West Africa.

Thus, the assessment of the otolith-based fish fauna in the Rharb Basin does not justify combining it with the Early Pliocene Mediterranean nor with tropical West African fauna, the latter deduced from the extant faunal composition. I therefore postulate the presence of an Atlantic Moroccan bioprovince during the Early Pliocene, and potentially Late Miocene, which I propose to name the “Maghrebian bioprovince.”

Conclusions and outlook

The otolith assemblage from the Early Pliocene of the Rharb Basin is the first Northwest African otolith-based fish fauna described, but a few elements have been described previously (Schwarzahans, 1981, 1993, 1999). It is a rich fauna, with 96 species recognized, 82 thereof identifiable to species level, including 16 new species. The geology and stratigraphy of the sampled area are outlined and discussed in the light of recent geological research in the region.

1. The main sampled section on the river Beth section about 1.5 km south of Dar bel Hamri is interpreted to be of Early Pliocene (Zanclean) age based on planktonic foraminifer assessment, which is in agreement

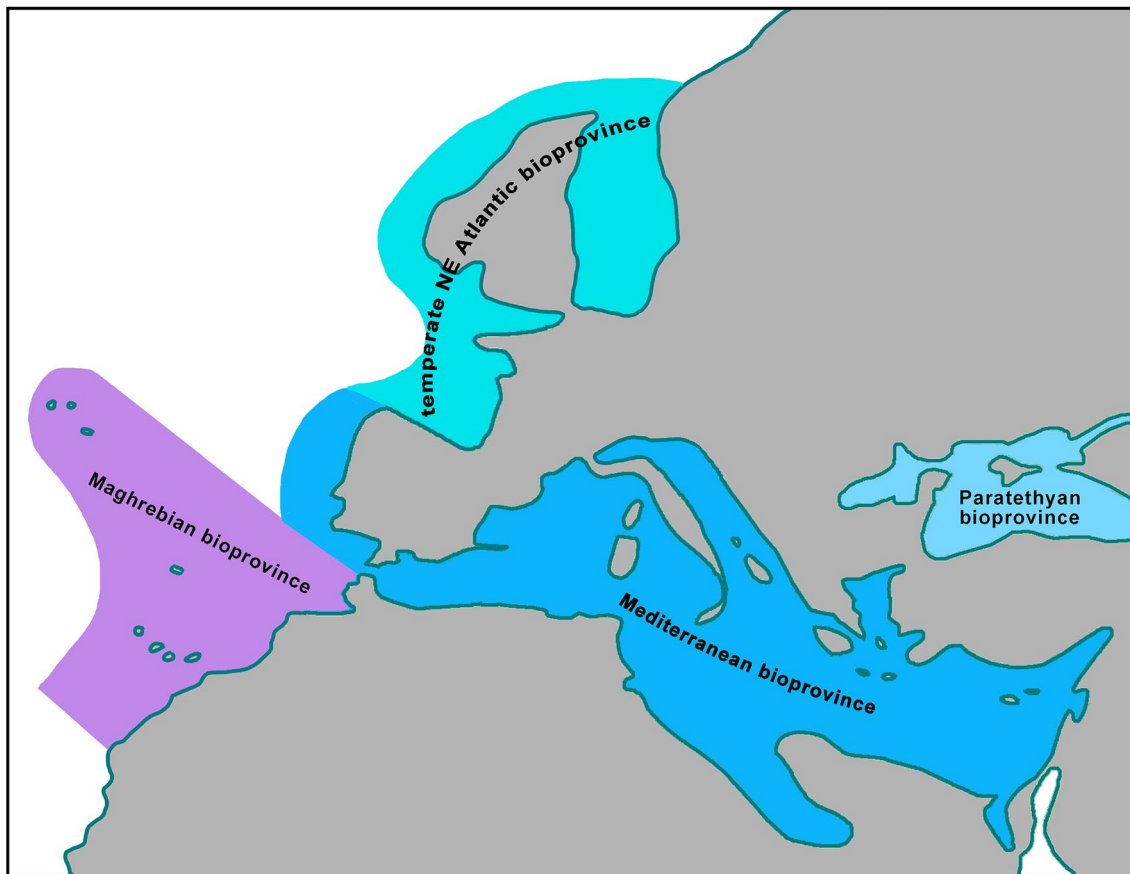


Fig. 32 Conceptual map of marine fish bioprovinces during the Early Pliocene. From west to east: transitional tropical Maghrebian bioprovince; subtropical Mediterranean bioprovince; temperate northeastern Atlantic bioprovince; Paratethyan bioprovince. Paleogeographic configuration based on Popov et al. (2004); delimitation of bioprovinces altered from Avila et al. (2016)

with Lecointre and Roger (1943) and in partial agreement with Wernli (1988).

2. The diversification of the fish fauna is exceptionally high and dominated by otoliths from adult specimens, which probably indicates a high food supply at moderate depth on a middle to lower shelf position during the deposition of the coquina near Dar bel Hamri.
3. The otolith-based fish fauna from the Early Pliocene of the Rharrb Basin shows a good resemblance not only to the coeval fauna of the Mediterranean, but also exhibits a notable proportion of putative endemic species and species related to today's tropical West African fauna.
4. The faunal composition thus exhibits a unique character that is sufficiently different from known or deduced neighboring bioprovinces, and thus a "Maghrebian bioprovince" is proposed for the Early Pliocene NW African region.

The Rharrb Basin also offers opportunities to sample Late Miocene otolith assemblages, which are important in the evaluation of the interaction with well-known Late Miocene fish faunas from the Mediterranean. It is hoped that such samples will eventually be made and worked up for otoliths. Further prospects for older fish faunas and knowledge about West African fossil otolith assemblages further to the south will depend on offshore drilling samples becoming available, since Cenozoic onshore outcrops are scarce.

Abbreviations

OL	Otolith length
OH	Otolith height
OT	Otolith thickness
SuL	Sulcus length
SuH	Sulcus height
OsL	Ostium length
OsH	Ostium height
CaL	Cauda length

CaH Cauda height
TL Total length of fish

Acknowledgements

I would like to cordially thank F. von der Hocht (Kerpen), who alerted me to the location near Dar bel Hamri and collected many of the otoliths studied. Further, I would like to thank A. Ouarred (Dar bel Hamri) and his family for the most generous hospitality during my field work sessions. I thank L. Kubig (Berlin) and T. Schlüter (Eswatini) for their great help and friendship during the field work. Further I would like to thank A. Boudda (Rabat), ministry of geology of Morocco during the time of my field work, for his support and granting allowances. My late supervisors B. Krebs and S. Henkel (Berlin) supported me during the preparation of the field work and thesis. Ms C. Franz and R. Brocke (Senckenberg, Frankfurt) are thanked for making the earlier types of otoliths available for review. Ms L. Kraus (Senckenberg, Frankfurt) helped in registering of material for SMF. This study would have been impossible without the help of many colleagues and institutions allowing to access fishes for otolith extractions. For this study, I am particularly thankful to J. Paxton and M. McGrowther (AMS, Sydney), O. Crimmen and J. MacLaine (BMNH, London), H. Endo (BSKU, Kochi), D. Catania (CAS, San Francisco), A. Lombarte (CSIC, Barcelona), D. Nolf (IRSNB, Brussels), A. Williston (MCZ, Cambridge, Boston), C. Struthers (NMNZ, Wellington), G. Shinohara (NSMT, Tsukuba, Tokyo), W. Schmidt (Hamburg), J. Williams and D. Pitassy (USNM, Washington), R. Thiel (ZMH, Hamburg), P. Möller and J. Nielsen (ZMUC, Copenhagen). Ms C. Kahlfeld and H. Keupp (Berlin) supported me to locate important old geological literature pertinent for this study. V. van Hinsbergh (Leiden) and K. Hoedemakers (Mortsel) are thanked for information about the otolith assemblage from Estepona and fruitful discussions. Finally, I would like to thank the two anonymous reviewers for their constructive reviews.

Author contributions

Not applicable.

Funding

No funding.

Availability of data and materials

All materials studied, described and figured in this manuscript has been registered and deposited in public institutional scientific collections in Germany. All other data are contained in the text.

Author details

¹Zoological Museum, Natural History Museum of Denmark, Universitetsparken 15, 2100 Copenhagen, Denmark. ²Ahrensburger Weg 103, Hamburg, 22359, Germany.

Received: 5 December 2022 Accepted: 8 March 2023

Published online: 13 April 2023

References

- Achalhi, M., Münch, P., Cornée, J.-J., Azdimousa, A., Melinte-Dobrinescu, M., Quillévéré, F., Drinia, H., Fauquette, S., Jiménez-Moreno, G., Merzeraud, G., Ben Moussa, A., El Kharim, Y., & Feddi, N. (2016). The Late Miocene Mediterranean-Atlantic connections through the North Rifian Corridor: New insights from the Boudinar and Arbaa Taourirt basins (northeastern Rif, Morocco). *Palaeogeography, Palaeoclimatology, Palaeoecology*, 459, 131–152.
- Agathangelou, A., Agiadi, K., Tsiolakis, E., Sfenthourakis, S., & Iliopoulos, G. (2022). The Eastern Mediterranean fish fauna from the Piacenzian deposits of Polis Graben (Cyprus Island). *Geobios*, 71, 1–12.
- Agiadi, A., Koskeridou, E., Triantaphyllou, M., Girone, A., & Karakitsios, V. (2013). Fish otoliths from the Pliocene Heraklion Basin (Crete Island, eastern Mediterranean). *Geobios*, 46, 461–472.
- Agiadi, K., & Albano, P. G. (2020). Holocene fish assemblages provide baseline data for the rapidly changing eastern Mediterranean. *The Holocene*, 30, 1438–1450.
- Agiadi, K., Antonarakou, A., Kontakiotis, G., Kafousia, N., Moissette, P., Cornée, J.-J., Manoutsoglou, E., & Karakitsios, V. (2017). Connectivity controls on the Late Miocene eastern Mediterranean fish fauna. *International Journal of Earth Sciences (geologische Rundschau)*, 106, 1147–1159.
- Agiadi, K., Giamali, C., Girone, A., Moissette, P., Koskeridou, E., & Karakitsios, V. (2019a). The Zanclean marine fish fauna and palaeoenvironmental reconstruction of a coastal marine setting in the eastern Mediterranean. *Palaeobiodiversity and Palaeoenvironments*, 100, 773–792.
- Agiadi, K., Girone, A., Koskeridou, E., Moissette, P., Cornée, J.-J., & Quillévéré, F. (2018). Pleistocene marine fish invasions and palaeoenvironmental reconstructions in the eastern Mediterranean. *Quaternary Science Reviews*, 196, 80–99.
- Agiadi, K., Vasileiou, G., Koskeridou, E., Moissette, P., & Cornée, J.-J. (2019b). Coastal fish otoliths from the Early Pleistocene of Rhodes (eastern Mediterranean). *Geobios*, 55, 1–15.
- Aguilera, O. A., Moraes-Santos, H., Costa, S., Ohe, F., Jaramillo, C., & Nogueira, A. (2013). Ariid sea catfishes from the coeval Pirabas (Northeastern Brazil), Cantaura, Castillo (Northwestern Venezuela), and Castilletes (North Colombia) formations (Early Miocene), with description of three new species. *Swiss Journal of Palaeontology*, 132, 45–68.
- Andreotto, F., Aloisi, G., Raad, F., Heida, H., Flecker, R., Agiadi, K., Lofi, J., Blondel, S., Bulian, F., Camerlenghi, A., Caruso, A., Ebner, R., Garcia-Castellanos, D., Gaullier, V., Guibordenché, L., Gvirtzman, Z., Goyle, T. M., Meijer, P. T., Moneron, J., ... Krijgsma, N. W. (2021). Freshening of the Mediterranean salt giant: controversies and certainties around the terminal (Upper Gypsum and Lago-mare) phases of the Messinian Salinity Crisis. *Earth-Science Reviews*, 216, 103577. <https://doi.org/10.1016/j.earscirev.2021.103577>
- Anfossi, G., & Mosna, S. (1979). La fauna ittologica di Monte Roero (Alba, Italia NW). *Atti Dell'Istituto Geologico della Università di Pavia*, 27, 111–132.
- Aze, T., Ezard, T. H. G., Purvis, A., Coxall, H. K., Stewart, D. R. M., Wade, B. S., & Pearson, P. N. (2011). A phylogeny of Cenozoic macroperforate planktonic foraminifera from fossil data. *Biological Reviews*, 86, 900–927.
- Avila, S. P., Melo, C., Berning, B., Cordeiro, R., Landau, B., & Marques da Silva, C. (2016). *Perististrombus coronatus* (Mollusca: Strombidae) in the lower Pliocene of Santa Maria Island (Azores, NE Atlantic): Paleoeology, paleoclimatology and paleobiogeographic implications. *Palaeogeography, Palaeoclimatology, Palaeoecology*, 441, 912–923.
- Bache, F., et al. (2012). A two-step process for the reflooding of the Mediterranean after the Messinian Salinity Crisis. *Basin Research*, 24, 125–153.
- Barbieri, R., & Ori, G. G. (1997). *Globorotalia bouregensis*, a new species of planktonic foraminifer from the latest Miocene-Early Pliocene of the Rifian Seaway (northwest Morocco). *Journal of Micropaleontology*, 16, 175–178.
- Barhoun, N., & Bachiri Taoufik, N. (2008). Événements biostratigraphiques et environnementaux enregistrés dans le corridor sud rifain (Maroc septentrional) au Miocène supérieur avant la crise de salinité messinienne. *Geodiversitas*, 30, 21–40.
- Barhoun, N., Sierro, F. J., El Hajjaji, K., & Ben Bouziane, A. (1999). Biostratigraphie et paléoenvironnement du Miocène supérieur du bassin de Zéghaghane (Rif nord-orientale, Maroc): Apport des foraminifères planctoniques. *Revista Española de Micropaleontología*, 31, 279–287.
- Bassoli, G. (1906). Otoliti fossili terziari dell' Emilia. *Rivista Italiana di Paleontologia*, 12, 36–61.
- Bauza-Rullan, J. (1955). Contribuciones al conocimiento de la fauna ictológica fossil de España. *Boletín de la Sociedad de Historia Natural de Baleares*, 1, 71–80.
- Bedini, E., Francalacci, P., & Landini, W. (1986). I pesci fossili del Miocene superiore di Montefiore Conca e Mondaino (Forlì). *Memorie del Museo Civico di Storia Naturale di Verona (II serie). Scienze della Terra*, 3, 1–66.
- Ben-Moshe, L., Ben-Avraham, Z., Enzel, Y., & Schattner, U. (2020). Estimating drawdown magnitudes of the Mediterranean Sea in the Levant basin during the Lago Mare stage of the Messinian Salinity Crisis. *Marine Geology*, 427, 106215.
- Ben Moussa, A. (1994). Les bivalves néogènes du Maroc septentrional (façades atlantique et méditerranéenne). Biostratigraphie, paléobiogéographie et paléocéologie. *Documents des Laboratoires de Géologie, Lyon*, 132, 3–281.
- Ben-Tuvia, A. (1990). Holocentridae. In: Quéro, J.C., Hureau, J.C., Karrer, C., Post, A. & Saldanha, L. (eds.). *Check-list of the fishes of the eastern tropical Atlantic* (pp. 627–628). JNICT Portugal.

- Benson, R. H., & Rakic-El Bied, K. (1991). The Messinian parastratotype at Cuevas del Almanzora, Vera Basin, Spain: Refutation of the deep-basin, shallow-water hypothesis? *Micropaleontology*, 37, 1–7.
- Blakey, R. (2020). Deep Time Maps. World Wide Web electronic service. [purchased in March 2021] <https://deeptime maps.com>
- Bourcart, J., Zbyszewski, R., & Chavan, A. (1940). La faune de Cacla en Algarve. *Comunicação Da Sociedade Geológica de Portugal*, 21, 1–106.
- Bratishko, A., Schwarzghans, W., & Vernyhorova, Y. (2023). The endemic marine fish fauna from the Eastern Paratethys reconstructed from otoliths from the middle Sarmatian s.l. (Bessarabian) of Jurkine (Kerch Peninsula, Crimea). *Rivista Italiana di Paleontologia e Stratigrafia*, 129, 111–184. <https://doi.org/10.54103/2039-4942/18877>
- Bruderer, W., & Lévy, R. G. (1954). Considerations sur la "Nappe Prerifaine" d'après les travaux de la Société Chérifienne des Pétroles. *Comptes Rendus 19 Session International Congress 1952. Alger*, 21, 277–294.
- Brzobohatý, R., & Nolf, D. (1996). Otolithes de myctophidés (poissons téléostéens) des terrains tertiaires d'Europe: Révision des genres *Benthosema*, *Hygophum*, *Lampadena*, *Notoscopelus* et *Symbolophorus*. *Bulletin de l'Institut Royal des Sciences Naturelles de Belgique, Sciences de La Terre*, 66, 151–176.
- Brzobohatý, R., & Nolf, D. (2000). *Diaphus* otoliths from the European Neogene (Myctophidae, Teleostei). *Bulletin de l'Institut Royal des Sciences Naturelles de Belgique, Sciences de La Terre*, 70, 185–206.
- Capella, W., Barhoun, N., Flecker, R., Hilgen, F. J., Kouwenhoven, T., Matenco, L. C., Sierro, F. J., Tulbure, M. A., Youfi, M. Z., & Krijgsman, W. (2018a). Data on lithofacies, sedimentology and palaeontology of South Rifian Corridor sections (Morocco). *Data in Brief*, 19, 712–736.
- Capella, W., Barhoun, N., Flecker, R., Hilgen, F. J., Kouwenhoven, T., Matenco, L. C., Sierro, F. J., Tulbure, M. A., Youfi, M. Z., & Krijgsman, W. (2018b). Palaeogeographic evaluation of the Late Miocene Rifian Corridor (Morocco): Reconstructions from surface and subsurface data. *Earth Science Reviews*, 180, 37–59.
- Capella, W., Hernández-Molina, F. J., Flecker, R., Hilgen, F. J., Hssain, M., Kouwenhoven, T. J., van Oorschot, M., Sierro, F. J., Stow, D. A. V., Trabuchio-Alexandre, J., Tulbure, M. A., de Weger, W., Youfi, M. Z., & Krijgsman, W. (2017). Sandy contourite drift in the Late Miocene Rifian Corridor (Morocco): Reconstruction of depositional environments in a foreland-basin seaway. *Sedimentary Geology*, 355, 31–57.
- Carnevale, G., & Schwarzghans, W. (2022). Marine life in the Mediterranean during the Messinian Salinity Crisis: A paleoichthyological perspective. *Rivista Italiana di Paleontologia e Stratigrafia*, 128, 283–324.
- Chaine, J., & Duvergier, J. (1934). Recherches sur les otolithes des poissons. Etude descriptive et comparative de la sagitta des Téléostéens. *Actes de la Société Linnéenne de Bordeaux*, 86, 5–256.
- Chaisson, W. P., & Pearson, P. N. (1997). Planktonic foraminifer biostratigraphy at site 925: Middle Miocene-Pleistocene. *Proceedings of the Ocean Drilling Program, Scientific Results*, 154, 3–31.
- Chavan, A. (1944). Etude complémentaire de la faune de Dar bel Hamri. *Bulletin de la Société de Géologie France*, 5(14), 155–171.
- Chiba, S. N., Iwatsuki, Y., Yoshino, T., & Hanzawa, N. (2009). Comprehensive phylogeny of the family Sparidae (Perciformes: Teleostei) inferred from mitochondrial gene analyses. *Genes and Genetic Systems*, 84, 153–170.
- Daya, D., Janin, M.-C., & Boutakiout, M. (2005). Biochronologie et corrélation des bassins néogènes du Couloir sud-rifain (Maroc) fondées sur les événements de foraminifères planctoniques et de nannofossiles calcaire. *Revue de Micropaleontologie*, 48, 141–157.
- de Weger, W., Hernández-Molina, F. J., Flecker, R., Sierro, F. J., Chiarella, D., Krijgsman, W., & Manar, M. A. (2020a). Late Miocene contourite channel system reveals intermittent overflow behavior. *Geology*, 48, 1194–1199.
- de Weger, W., Hernández-Molina, F. J., Miguez-Salas, O., de Castro, S., Bruno, M., Chiarella, D., Sierro, F. J., Blackburn, G., & Manar, M. A. (2020b). Contourite depositional system after the exit of a strait: Case study from the Late Miocene South Rifian Corridor, Morocco. *Sedimentology*, 68, 2996–3032.
- de Weger, W., Hernández-Molina, F. J., Sierro, F. J., Chiarella, D., Llave, E., Fedele, J. J., Rodrigues-Tovar, F. J., Miguez-Salas, O., & Manar, M. A. (2020c). Contourite channels—facies model and channel evolution. *Sedimentology*. <https://doi.org/10.1111/sed.13042>
- Deperet, J., & Gentil, L. (1917). Sur une faune miocène supérieure marine (Sahélienne) dans le R'arb (Maroc occidental). *Compte Rendus de l'Académie des Sciences de Paris*, 164, 21–25.
- Dieni, I. (1968). Gli otoliti del Pliocene inferiori di Orosei (Sardegna). *Memorie della Accademia Patavina di SS. LL. AA.*, 80, 243–284.
- Diester-Haass, L., & Schrader, H.-J. (1979). Neogene coastal upwelling history off northwest and southwest Africa. *Marine Geology*, 29, 39–53.
- Faure-Muret, A., & Choubert, G. (1971). Le Maroc. Domaine rifain et atlasique. *Tectonique de l'Afrique*, Unesco, Paris, 17–46.
- Feinberg, H. (1976). Mise en place au Pliocène d'une nappe de glissement à l'extrémité sud-occidentale de la chaîne du Rif (Maroc). *Compte Rendus Sommaire de la Société Géologique de France*, 6, 273–276.
- Feinberg, H. (1978). Les séries Tertiaires du Préif et des dépendances post-tectoniques du Rif (Maroc). Thèse à l'Université Paul-Sabatier de Toulouse. 1–263.
- Feinberg, H., & Lorenz, H. G. (1970). Nouvelles données stratigraphiques sur le Miocène supérieur et le Pliocène du Maroc nord-occidental. *Notes et Mémoires du Service Géologique du Maroc*, 30(225), 21–26.
- Feinberg, H., & Lorenz, H. G. (1971). Affleurements de Pliocène marin dans la Mamora centrale (Maroc septentrional). *Compte rendu Sommaire de la Société Géologique de France*, 8, 435–436.
- Flecker, R., et al. (2015). Evolution of the Late Miocene Mediterranean-Atlantic gateways and their impact on regional and global environmental change. *Earth Science Reviews*, 150, 365–392.
- Flinch, J. F. (1993). *Tectonic evolution of the Gibraltar Arc*. Thesis at Rice University, Houston, 1–381.
- Fowler, H. W. (1925). New taxonomic names of west African marine fishes. *American Museum Novitates*, 162, 1–5.
- Fricke, R., Eschmeyer, W. N., & Van der Laan, R. (eds). (2022). Eschmeyer's catalog of fishes: genera, species, references. <http://researcharchive.calacademy.org/research/ichthyology/catalog/fishcatmain.asp>. Accessed 01 Oct 2022.
- Froese, R., & Pauly, D. (2022). FishBase. *World Wide Web electronic publication*. Retrieved September 2022, from <https://www.fishbase.org/search.php>
- García-Castellanos, D., Estrada, F., Jiménez-Munt, I., Gorini, C., Fernández, M., Vergés, J., & de Vicente, R. (2009). Catastrophic flood of the Mediterranean after the Messinian salinity crisis. *Nature, Letters*, 462(10), 778–781.
- Gebhardt, H. (1993). Neogene foraminifera from the Eastern Rabat area (Morocco): Stratigraphy, palaeobathymetry and palaeoecology. *Journal of African Earth Sciences*, 16, 445–464.
- Gignoux, M. (1950). *Géologie stratigraphique* (4th ed., pp. 1–735). Masson.
- Girone, A. (2006). Emilien otolith assemblages from northern Italy (Rio Merli section, Emilia Romagna). *Bollettino della Società Paleontologica Italiana*, 45, 159–170.
- Girone, A., Nolf, D., & Cappetta, H. (2006). Pleistocene fish otoliths from the Mediterranean Basin: A synthesis. *Geobios*, 39, 651–671.
- Girone, A., Nolf, D., & Cavallo, O. (2010). Fish otoliths from the pre-evaporitic (early Messinian) sediments of northern Italy: Their stratigraphic and palaeobiogeographic significance. *Facies*, 56, 399–432.
- Golani, D., Azzurro, E., Dulčić, J., Massuti, E., & Orsi-Rellini, L. (2021). *Atlas of exotic fishes in the Mediterranean sea. 2nd, entirely revised, edition*. CIESM Publishers, 1–365.
- Gonzales Delgado, J. A., Andres, I., & Sierro, F. J. (1994). Late Neogene molluscan faunas from the northeast Atlantic (Portugal, Spain, Morocco). *Geobios*, 28, 459–471.
- Gvirtzman, Z., Heida, H., García-Castellanos, D., Bar, O., Zucker, E., & Enzel, Y. (2022). Limited Mediterranean sea-level drop during the Messinian salinity crisis inferred from the buried Nile canyon. *Communications Earth & Environment*, 3, 216. <https://doi.org/10.1038/s43247-022-00540-4>
- Haddaoui, Z., El Hatimi, N., & Hervouet, Y. (1997). Les rides sud-rifaines (Maroc septentrional): Influence de la géométrie d'un bassin jurassique sur la propagation des chevauchements néogènes. *Géologie Méditerranéenne*, 24, 51–71.
- Hilgen, F. J., Iaccarino, S., Krijgsman, W., Villa, G., Langereis, C. G., & Zachariasse, W. J. (2000). The global boundary stratotype section and point (GSSP) of the Messinian stage (uppermost Messinian). *Episodes*, 3, 172–178.
- Hodell, D. A., Benson, R. H., Kent, D. V., Boersma, A., & Rakic-El Bied, K. (1994). Magnetostratigraphic, biostratigraphic, and stable isotope stratigraphy of an Upper Miocene drill core from the Salé Briqueterie (northwestern Morocco): A high-resolution chronology for the Messinian stage. *Paleoceanography*, 9, 835–855.
- Hsü, K. J. (1972). When the Mediterranean dried up. *Scientific American*, 227(6), 26–36.

- Kennett, J. P., & Srinivasan, M. S. (1983). *Neogene planktonic foraminifera* (pp. 1–265). A phylogenetic atlas. Hutchinson Ross Publishing Company.
- Koken, E. (1884). Über Fisch-Otolithen, insbesondere über diejenigen der norddeutschen Oligocän-Ablagerungen. *Zeitschrift der Deutschen Geologischen Gesellschaft*, 36, 500–565.
- Krijgsman, W., Gaboardi, S., Hilgen, F. J., Iaccarino, S., de Kaenel, E., & van der Laan, E. (2004). Revised astrochronology for the Ain el Beida section (Atlantic Morocco): No glacio-eustatic control for the onset of the Messinian Salinity Crisis. *Stratigraphy*, 1, 87–101.
- Lanckneus, J., & Nolf, D. (1979). Les otolithes des téléostéens Redoniens de Bretagne (Néogène de l'ouest de la France). *Bulletin de l'Institut de Géologie du Bassin d'Aquitaine*, 25, 83–109.
- Landini, W., & Sorbini, L. (1992). Données récentes sur les téléostéens du Miocène et du Pliocène d'Italie. *Geobios*, 25(Suppl. 1), 151–157.
- Landini, W., & Sorbini, C. (1999). Systematic and palaeobiogeographical observations on the gadid fish *Gadiculus labiatus* (Schubert 1905). *Studi e Ricerche sui Giacimenti Terziari di Bolca*, 8, 43–58.
- Landini, W., & Sorbini, C. (2005). Evolutionary trends in the Plio-Pleistocene ichthyofauna of the Mediterranean Basin: Nature, timing and magnitude of the extinction events. *Quaternary International*, 131, 101–107.
- Lecointre, G. (1916). Sur la géologie du Djebel Outita et des environs de Dar bel Hamri (Maroc occidental). *Compte Rendus de l'Académie des Sciences de Paris*, 162, 556–559.
- Lecointre, G. (1944). Problèmes biogéographiques du Néogène et du Quaternaire marins du Maroc. *Compte rendus de Société Biogéographique de Paris*, 21, 178–181.
- Lecointre, G. (1952). Recherches sur le Néogène et le Quaternaire marin de la côte atlantique du Maroc. *Notes et Memoires du Service Géologique du Maroc*, 99, 1–198.
- Lecointre, G. (1963). Recherches sur le Néogène et le Quaternaire marin de la côte atlantique du Maroc. 3: Les acquisitions nouvelles durant la période de 1952 à 1962 (stratigraphie et paléontologie). *Notes et Memoires du Service Géologique du Maroc*, 174, 1–76.
- Lecointre, G., & Roger, J. (1943). La faune de Dar bel Hamri (Maroc) est d'âge pliocène ancien. *Bulletin Museum Histoire Naturelle*, 2(15), 359–364.
- Lin, C.-H., Brzobohaty, R., Nolf, D., & Girone, A. (2017). Tortonian teleost otoliths from northern Italy: Taxonomic synthesis and stratigraphic significance. *European Journal of Taxonomy*, 322, 1–44.
- Lin, C.-H., Girone, A., & Nolf, D. (2015). Tortonian fish otoliths from turbiditic deposits in northern Italy: Taxonomic and stratigraphic significance. *Geobios*, 48, 249–261.
- Lombarte, A., Chic, Ó., Parisi-Baradad, V., Olivella, R., Piera, J., & García-Ladona, E. (2006). A web-based environment from shape analysis of fish otoliths. The AFORO Database. *Scientia Marina*, 70, 147–152.
- Lourens, L., Hilgen, F., Chackelton, N. J., Laskar, J., & Wilson, D. (2004). The Neogene Period. In: (Gradstein, F. M., Ogg, J. G. & Smith, A. G., eds.). *A Geologic Time Scale 2004*, 409–440.
- Maniscalco, R., & Brunner, C. A. (1998). Neogene and Quaternary planktonic foraminiferal biostratigraphy of the Canary Island region. *Proceedings of the Ocean Drilling Program, Scientific Results*, 157, 115–124.
- Martin, J. M., Puga-Bernabéu, A., Aguirre, J., & Braga, C. (2014). Miocene Atlantic-Mediterranean seaways in the Betic Cordillera (southern Spain). *Revista de la Sociedad Geológica de España*, 27, 175–186.
- Matsuzaki, K. M. R., Eynaud, F., Malaizé, B., Grousset, F. E., Tisserand, A., Rossignol, L., Charlier, K., & Jullien, E. (2011). Paleooceanography of the Mauritanian margin during the last two climate cycles: From planktonic foraminifera to African climate dynamics. *Marine Micropaleontology*, 79, 67–79.
- Mendiola, C., & Martínez, J. (2003). Otolitos de la familia Sciaenidae (Osteichthys, Teleostei, Perciformes) procedentes del Plioceno inferior de Guardamar-España (Cuenca del Bajo Segura, Cordillera Bética Oriental). *Revista de la Sociedad Paleontológica D'elx*, 11, 1–57.
- Micallef, A., Camerlenghi, A., García-Castellanos, D., Otero, D. C., Gutsche, M.-A., Barreca, G., Spatola, D., Facchin, L., Geletti, R., Krastel, S., Gross, F., & Urlaub, M. (2018). Evidence of the Zanclean megaflood in the eastern Mediterranean Basin. *Scientific Reports*, 8, 1078. <https://doi.org/10.1038/s41598-018-19446-3>
- Michel, J., Westphal, H., & Von Cosel, R. (2011). The mollusk fauna of soft sediments from the tropical, upwelling-influenced shelf of Mauritania (northwest Africa). *Palaios*, 26, 447–460.
- Nelson, J. S., Grande, T. C., & Wilson, M. V. H. (2016). *Fishes of the world* (5th ed., pp. 1–707). Wiley.
- Nolf, D. (1978). Les otolithes des Téléostéens du Plio-Pleistocène Belge. *Geobios*, 11, 517–559.
- Nolf, D. (1979). Contribution à l'étude des otolithes des poissons. I Morphologie comparée des otolithes (sagittae) des Dentex de la Méditerranée et de l'Atlantique tropical africain. *Bulletin de l'Institut Royal des Sciences Naturelles de Belgique*, 51(9), 1–15.
- Nolf, D. (1980). Etude monographique des otolithes des Ophidiiformes actuels et révision des espèces fossiles (Pisces, Teleostei). *Mededelingen van de Werkgroep voor Tertiaire en Kwartaire Geologie*, 17, 71–195.
- Nolf, D. (2013). *The diversity of fish otoliths past and present* (pp. 1–584). Royal Belgian Museum of Natural History.
- Nolf, D. (2018). *Otoliths of fishes from the North Sea and the English Channel* (pp. 1–277). Royal Belgian Institute of Natural Sciences.
- Nolf, D., & Cappetta, H. (1988). Otolithes de poissons Pliocènes du Sud-Est de la France. *Bulletin de l'Institut Royal des Sciences Naturelles de Belgique*, 58, 209–271.
- Nolf, D., & Cavallo, O. (1994). Otolithes de poissons du Pliocène inférieur de Monticello d'Alba (Piemont, Italie). *Rivista Piemontese di Storia Naturale*, 15, 11–40.
- Nolf, D., & Girone, A. (2000). Otolithes de poissons du Pleistocène inférieur (Santerrien) de Morrona (sud est de Pisa). *Rivista Piemontese di Storia Naturale*, 21, 3–18.
- Nolf, D., & Girone, A. (2006). Otolithes de poissons du Pliocène inférieur (Zanclean) des environs d'Alba (Piemont) et de la côte ligure. *Rivista Piemontese di Storia Naturale*, 27, 77–114.
- Nolf, D., & Marques da Silva, C. (1997). Otolithes de poissons pliocènes (Plaisancien) de Vale de Freixo, Portugal. *Revue de Micropaléontologie*, 40, 273–282.
- Nolf, D., & Martinell, J. (1980). Otolithes de téléostéens du Pliocène des environs de Figueras (Catalogne). *Geologica et Palaeontologica*, 14, 209–234.
- Nolf, D., & Steurbaut, E. (1983). Révision des otolithes de téléostéens du Tortonien stratotypique et de Montegibbio (Miocène Supérieur de l'Italie septentrionale). *Mededelingen van de Werkgroep voor Tertiaire en Kwartaire Geologie*, 20, 143–197.
- Nolf, D., Mané, R., & Lopez, A. (1998). Otolithes de poissons du Pliocène inférieur de Papiol, près de Barcelone. *Palaeovertebrata*, 27, 1–17.
- Nolf, P., de Potter, H., & Lafond-Grellety, J. (2009). *Hommage à Joseph Chaine et Jean Duvergier. Diversité et variabilité des otolithes des poissons*. Palaeo Publishing and Library, 1–59 and 149 plates.
- Popov, S. V., Rögl, F., Rozanov, A. Y., Steininger, F. F., Shcherba, I. G., & Kovac, M. (2004). Lithological-paleogeographic maps of Paratethys. 10 maps Late Eocene to Pliocene. *Courier Forschungs-Institut Senckenberg*, 250, 1–46.
- Pérez-Asensio, J. N. (2021). Quantitative palaeobathymetric reconstructions based on foraminiferal proxies: A case study from the Neogene of South-West Spain. *Palaeontology*, 64, 475–488.
- Rakic-El Bied, K., & Benson, R. H. (1996). La stratigraphie à haute résolution: Théorie et application au Néogène supérieur du Maroc. *Notes et Memoires du Service Géologique du Maroc*, 383, 5–50.
- Reichenbacher, B., & Bannikov, A. (2021). Diversity of gobioid fishes in the late Middle Miocene of northern Moldova, Eastern Paratethys—part I: An extinct clade of *Lesueurigobius* look-alikes. *PalZ*, 96, 67–112.
- Reichenbacher, B., & Bannikov, A. (2022). Diversity of gobioid fishes in the late Middle Miocene of northern Moldova, Eastern Paratethys—part II: description of *†Moldavigobius helenae* gen. et sp. nov. *PalZ*. <https://doi.org/10.1007/s12542-022-00639-1>.
- Roldán, F. J., Galindo-Zaldívar, J., Ruano, P., Chalouan, A., Pedrera, A., Ahmamou, M., Constán, A. R., Galdeano, C. S., Benmakhlof, M., López-Garrido, A. C., Anahnah, F., & González-Castillo, L. (2014). Basin evolution associated to curved thrusts: the Prerif Ridges in the Volubilis area (Rif Cordillera, Morocco). *Journal of Geodynamics*, 77, 56–69.
- Roveri, M., Flecker, R., Krijgsman, W., Lofi, J., Lugli, S., Manzi, V., Sierro, F. J., Bertini, A., Camerlenghi, A., de Lange, G., Govers, R., Hilgen, F. J., Hübscher, C., Meijer, P. T., & Stoica, M. (2014). The Messinian Salinity Crisis: Past and future of a great challenge for marine science. *Marine Geology*, 352, 25–58.
- Roveri, M., Gennari, R., Lugli, S., Manzi, V., Minelli, N., Reghizzi, M., Riva, A., Rossi, M. E., & Schreiber, B. C. (2016). The Messinian salinity crisis: Open problems and possible implications for Mediterranean petroleum systems. *Petroleum Geoscience*, 22, 283–290.

- Saadi, S.E.M., Hilali, E.A. & Bouda, A. (1980). Carte géologique de la chaîne Rifaine. 1:500.00. *Editions du Service Géologique du Maroc, Notes et Mémoires*, 245a.
- Sani, F., Del Ventisette, C., Montanari, D., Bendkik, A., & Chenakeb, M. (2006). Structural evolution of the Rides Prerifaines (Morocco): Structural and seismic interpretation and analogue modelling experiments. *International Journal of Earth Sciences (geologische Rundschau)*, 96, 685–706.
- Santini, F., Carnevale, G., & Sorenson, L. (2014). First multi-locus timetree of seabreams and porgies (Percomorpha: Sparidae). *Italian Journal of Zoology*, 81, 55–71.
- Sasaki, K. (2022). Sciaenidae. In: Heemstra, P.C., Heemstra, E., Ebert, D.A., Holleman, W. & Randall, J.E. (eds). *Coastal fishes of the Western Indian Ocean* (pp 389–414). South African Institute for Aquatic Biodiversity.
- Sasaki, K., & Kailola, P. J. (1988). Three new Indo-Australian species of the sciaenid genus *Atrobucca*, with a reevaluation of generic limit. *Japanese Journal of Ichthyology*, 35, 261–277.
- Schwarzhans, W. (1978a). Otolithen aus dem Unter-Pliozän von Süd-Sizilien und aus der Toskana. *Berliner Geowissenschaftliche Abhandlungen*, A, 8, 1–52.
- Schwarzhans, W. (1978b). Otolith-morphology and its usage for higher systematical units with special reference to the Myctophiformes s.l. *Mededelingen Vvan de Werkgroep voor Tertiaire en Kwartaire Geologie*, 15(4), 167–185.
- Schwarzhans, W. (1981). Die Entwicklung der Familie Pterothrissidae (Elopomorpha: Pisces), rekonstruiert nach otolithen. *Senckenbergiana Lethaea*, 62, 77–91.
- Schwarzhans, W. (1986). Die Otolithen des Unter-Pliozän von Le Puget, S-Frankreich. *Senckenbergiana Lethaea*, 67, 219–273.
- Schwarzhans, W. (1993). A comparative morphological treatise of Recent and fossil otoliths of the family Sciaenidae. *Piscium Catalogus: Otolithi Piscium*, 1, 1–245.
- Schwarzhans, W. (1994). Die Fisch-Otolithen aus dem Oberoligozän der Niederrheinischen Bucht. Systematik, Palökologie, Paläobiogeographie, Biostratigraphie und Otolithen-Zonierung. *Geologisches Jahrbuch*, A, 140, 1–248.
- Schwarzhans, W. (1999). A comparative morphological treatise of Recent and fossil otoliths of the order Pleuronectiformes. *Piscium Catalogus: Otolithi Piscium*, 2, 1–391.
- Schwarzhans, W. (2008). Otolithen aus küstennahen Sedimenten des Ober-Oligozän der Niederrheinischen Bucht (Norddeutschland). *Neues Jahrbuch Geologie, Paläontologie Abhandlungen*, 248, 11–44.
- Schwarzhans, W. (2010). *The otoliths from the Miocene of the North Sea Basin* (pp. 1–352). Backhuys Publishers, Leiden & Margraf Publishers.
- Schwarzhans, W. (2013a). Otoliths from dredges in the Gulf of Guinea and off the Azores—An actuo-paleontological case study. *Palaeo Ichthyologica*, 13, 7–40.
- Schwarzhans, W. (2013b). A comparative morphological study of the Recent otoliths of the genera *Diaphus*, *Idiolychnus* and *Lobianchia* (Myctophidae). *Palaeo Ichthyologica*, 13, 41–82.
- Schwarzhans, W. (2013c). Otoliths from the Miocene of West Africa, primarily from the Mandorové Formation of Gabon. *Palaeo Ichthyologica*, 13, 151–184.
- Schwarzhans, W. (2014). Otoliths from the Middle Miocene (Serravallian) of the Karaman Basin, Turkey. *Cainozoic Research*, 14, 35–69.
- Schwarzhans, W. (2019a). Reconstruction of the fossil marine bony fish fauna (Teleostei) from the Eocene to Pleistocene of New Zealand by means of otoliths. *Memorie della Società Italiana di Scienze Naturali e del Museo di Storia Naturale di Milano*, 46, 3–326.
- Schwarzhans, W. (2019b). A comparative morphological study of Recent otoliths of the so-called Trachinoidei. *Memorie della Società Italiana di Scienze Naturali e del Museo di Storia Naturale di Milano*, 46, 327–354.
- Schwarzhans, W. (2019c). A comparative morphological study of Recent otoliths of the Congridae, Muraenesocidae, Nettastomatidae and Colocongridae (Anguilliformes). *Memorie della Società Italiana di Scienze Naturali e del Museo di Storia Naturale di Milano*, 46, 371–388.
- Schwarzhans, W., Agiadi, K., & Carnevale, G. (2020). Late Miocene-Early Pliocene evolution of Mediterranean gobies and their environmental and biogeographic significance. *Rivista Italiana di Paleontologia e Stratigrafia*, 126(3), 657–724.
- Schwarzhans, W., & Aguilera, O. (2013). Otoliths of the Myctophidae from the Neogene of tropical America. *Palaeo Ichthyologica*, 13, 83–150.
- Schwarzhans, W., & Aguilera, O. (2016). Otoliths of the Ophidiiformes from the Neogene of tropical America. *Palaeo Ichthyologica*, 14, 91–124.
- Schwarzhans, W., Ahnelt, H., Carnevale, G., Japundžić, D., Bradić, K., & Bratishko, A. (2017). Otoliths in situ from Sarma tian (Middle Miocene) fishes of the Paratethys. Part III: Tales from the cradle of the Ponto-Caspian gobies. *Swiss Journal of Palaeontology*, 136, 45–92.
- Schwarzhans, W., & Jagt, J. W. M. (2021). Silicified otoliths from the Maastrichtian type area (Netherlands, Belgium) document early gadiform and perciform fishes during the Late Cretaceous, prior to the K/Pg boundary extinction event. *Cretaceous Research*, 127(104921), 1–26.
- Schwarzhans, W., & Kovalchuk, O. (2022). New data on fish otoliths from the late Badenian (Langhian, Middle Miocene) back reef environment in the Carpathian Foredeep (Horodok, western Ukraine). *Neues Jahrbuch Geologie, Paläontologie Abhandlungen*, 303, 317–326.
- Schwarzhans, W. W., & Prokofiev, A. M. (2017). Reappraisal of *Synagrops* Günther, 1887 with rehabilitation and revision of *Parascombrops* Alcock, 1889 including description of seven new species and two new genera (Perciformes: Acropomatidae). *Zootaxa*, 4260, 1–74.
- Schwarzhans, W., & Radwańska, U. (2022). A review of lanternfish otoliths (Myctophidae, Teleostei) of the early Badenian (Langhian, Middle Miocene) from Bęczyn, southern Poland. *Cainozoic Research*, 22, 9–24.
- Smith, D.G. (1990). Congridae. In: Quéro, J.C., Hureau, J.C., Karrer, C., Post, A. & Saldanha, L. (eds.). *Check-list of the fishes of the eastern tropical Atlantic* (pp. 156–167). JNICT Portugal.
- Song, Y. S., Kim, J.-K., Kang, J.-H., & Kim, S. Y. (2017). Two new species of the genus *Atractoscion*, and resurrection of the species *Atractoscion atelodus* (Günther 1867) (Perciformes: Sciaenidae). *Zootaxa*, 4306, 223–237.
- Stainforth, R. M., Lamb, J. L., Luterbacher, H., Beard, J. H., & Jeffords, R. M. (1975). Cenozoic planktonic foraminiferal zonation and characteristics of index forms. *The University of Kansas Paleontological Contributions*, 62, 1–425.
- Steurbaut, E. (1984). Les otolithes de téléostéens de l'Oligo-Miocène d'Aquitaine (Sud-Ouest de la France). *Palaeontographica*, A, 186, 1–162.
- Tilloy, R. (1952). La vallée de l'Oued Beth et le Rharb. *Congrès Géologique International, XIX session, Algier, Série Maroc* (8), *Livret-Guide des excursions A31 et C31, Maroc septentrional*, B, 57–63.
- Tulbure, M. A., Capella, W., Barhoun, N., Flores, J. A., Hilgen, F. J., Krijgsman, W., Kouwenhoven, T., Sierro, F. J., & Yousfi, M. Z. (2017). Age refinement and basin evolution of the North Rifian Corridor (Morocco): No evidence for a marine connection during the Messinian Salinity Crisis. *Palaeogeography, Palaeoclimatology, Palaeoecology*, 485, 416–432.
- Tuset, V. M., Lombarte, A., & Assis, C. A. (2008). Otolith atlas for the western Mediterranean, north and central Atlantic. *Scientia Marina*, 72(S1), 7–198.
- Van Hinsbergh, V., & Hoedemakers, K. (2022). Zanclean and Piacenzian otolith-based fish faunas of Estepona (Málaga, Spain). *Cainozoic Research*, 22, 241–352.
- Veen, J. & Hoedemakers, K. (2005). *Synopsis iconographique des otolithes de quelques espèces de poissons des côtes ouest Africaines*. Wetlands International, 1–40.
- Wade, B. S., Pearson, P. N., Berggren, W. A., & Pälike, H. (2011). Review and revision of Cenozoic tropical planktonic foraminiferal biostratigraphy and calibration to the geomagnetic polarity and astronomical time scale. *Earth-Science Reviews*, 104, 111–142.
- Weiler, W. (1971). Fisch-Otolithen aus dem Jungtertiär Süd-Siziliens. *Senckenbergiana Lethaea*, 52, 5–37.
- Wernli, R. (1978). La base du Moghrebien est d'âge Pliocène moyen (zone à *G. crassaformis*) dans la Mamora. *Archives des Sciences, Genève*, 31, 129–132.
- Wernli, R. (1988). Micropaléontologie du Néogène post-nappes du Maroc septentrional et description systématique des foraminifères planctoniques. *Notes et Mémoires du Service Géologique du Maroc*, 331, 1–270.
- Young, J.R., Wade, B.S., & Huber, B.T. (eds) (2022). pforams@mikrotax website. accessed June 2022. <http://www.mikrotax.org/pforams>
- Yousfi, M. Z., Barhoun, N., Essamoud, R., & Kouwenhoven, T. J. (2013). Biostratigraphie et paléoenvironnements du forage DRJ-6 (Bassin du Gharb-Maroc) au Miocène supérieur et au Pliocène. *Sciencelab Mersenne*, 5(131104), 1–21.
- Zizi, M. (1996). *Triassic-Jurassic extensional systems and their Neogene reactivation in northern Morocco (the Rides Prerifaines and GuerCIF Basin)*. Thesis at Rice University, Houston, 1–230.

- Zouhri, L., Lamouroux, C., & Buret, C. (2001). La Mamora, charnière entre la Meseta et le Rif: Son importance dans l'évolution géodynamique post-paléozoïque du Maroc. *Geodinamica Acta*, 14, 361–372.
- Zouhri, L., Lamouroux, C., Vachard, D., & Pique, A. (2002). Evidence of flexural extension of the Rif foreland: The Rharrb-Mamora basin (northern Morocco). *Bulletin de la Société Géologique de France*, 173, 509–514.

Publisher's Note

Springer Nature remains neutral with regard to jurisdictional claims in published maps and institutional affiliations.

Submit your manuscript to a SpringerOpen[®] journal and benefit from:

- Convenient online submission
- Rigorous peer review
- Open access: articles freely available online
- High visibility within the field
- Retaining the copyright to your article

Submit your next manuscript at ► [springeropen.com](https://www.springeropen.com)
